SYNTHESIS, CHARACTERIZATION AND ANTIBACTERIAL PROPERTIES OF COPPER (II) COMPLEXES OF SCHIFF BASES DERIVED FROM BENZOPHENONE DERIVATIVES AND SELECTED ANILINES

FESTUS KIMUTAI KOSGEI

A Thesis Submitted to the Graduate School in Partial Fulfilment of the Requirements for the Award of the Degree of Master in Chemistry of Chuka University

CHUKA UNIVERSITY

OCTOBER, 2024

DECLARATION AND RECOMMENDATION

Declaration

This thesis is my original work and has not been presented for examination in any institution for the award of any degree.

Signature.....Date.....14/10/2024.....

Festus Kimutai Kosgei
SM11/57727/22

Recommendation

This thesis has been examined, passed and submitted with our approval as the university supervisors.

Signature.....Date.....

Prof. Joel Mwangi Gichumbi
Chuka University

Signature.....Date.....14/10/24.....

Prof. Eric Chomba Njagi
Chuka University

DEDICATION

I dedicate this work to my father, Willson Tonui and my mother, Valentine Tonui, for their motivations concerning success and education. They instilled in me a positive attitude and determination towards schooling at a very tender age. Through their love, advice and consistent support, I have been motivated to work smart and never give up on this level.

ACKNOWLEDGEMENT

Philippians 4 vs 13 “I can do all things through Christ who strengthens me” with those words I would like to thank the Lord, God for his everlasting love, His love and protection through this journey till today He has been faithful to me. Dear Lord, I am grateful for all your blessings without Him, this work wouldn’t have been possible. Secondly, I am grateful to my supervisors, Prof. Joel Gichumbi and Prof. Eric Njagi, for providing invaluable guidance in achieving the objectives of this project. My special thanks go to both supervisors for their goodwill in assisting me whenever I needed them and for sharing knowledge and ideas throughout my studies. I sincerely appreciate your encouragement and willingness when I call and respond to my messages when I need assistance. For your guidance and your teachings, I lack words of how to thank them, May God bless them for everything.

I also appreciate the effort and skills of chemistry lab technologists Chrisphine, Eric and Juliet. I worked under their instructions when synthesizing and characterizing Schiff base ligands and their Copper (II) complexes. Their social nature, willingness and collaborative skills encouraged me to continue my lab work smoothly and successfully. I want to thank Prof. Abiy Yenesew of the University of Nairobi for his assistance in assessing the NMR spectrometer and obtaining NMR spectra. Many thanks go to Amos Mbabu and Geoffrey Langat of microbiology for their kind heart and willingness to assist me when conducting an antibacterial bioassay of the synthesized compounds.

Lastly, I am grateful to my parents for their financial and moral support, as well as postgraduate colleagues Geoffrey Kiprono, Shem Ong’echi, Kelvin Otao and Joseph Karithi; I thank them for their share of knowledge, fun and encouragement in one way or another for completing this research work.

ABSTRACT

In every region of the world, antibiotic resistance is increasing to dangerously high levels. The emergence and global dissemination of new bacterial resistance threaten human beings' capacity to cure widespread infectious diseases. As antibiotics lose their effectiveness, many infections, including blood poisoning, pneumonia, and tuberculosis, become difficult to cure and occasionally incurable. Therefore, there is a pressing need to develop new antibacterial agents to address this resistance. Thus, this study entailed synthesizing, characterizing, and determining the antibacterial activities of the Schiff base and its copper (II) complexes. The Schiff base ligands were synthesized by mixing 2-hydroxy-4-methoxybenzophenone with selected anilines in a 1:1 ratio, followed by refluxing for 3-4 hours. The precipitate obtained was filtered and dried at room temperature. The Cu (II) complexes were prepared in a 2:1 ratio by treating a hot solution of Schiff base ligands dissolved ethanol with an aqueous Cu (II) chloride under 4 hours of refluxing. The synthesized compounds melted at a constant temperature, confirming that they were pure. The Schiff base ligands and their Cu (II) complexes were characterized using various analytical techniques such as Fourier Transform-Infrared (FT-IR), Ultra Violet-Visible (UV-VIS) and Proton Nuclear Magnetic Resonance (^{1}H-NMR) spectroscopy and molar conductance measurements. The FT-IR data of the Schiff base ligands displayed the absence of NH_2 and C=O, confirming the formation of azomethine group (-HC=N-) at region 1610-1631.78cm^{-1} which shifted to lower wavelengths upon complexation with Cu (II) ions. The peak due to OH appeared at 3420-3450 cm-1 but later disappeared due to formation Cu (II) complex. The appearance of two new peaks 475.46-480.28 and 523.68-581.55cm^{-1} in the Cu (II) complex spectra attributed to Cu-O and Cu-N, respectively. UV-vis spectra of the free ligands appeared at 40322.58-41580cm^{-1} due to the transition of non-bonding electrons of azomethine nitrogen. Molar conductance measurements of Cu (II) complexes range from 13.34-22.208(Scm^2mol^{-1}), while that of free ligands range from 4.86-12.58 (Scm^2mol^{-1}), confirming they were non-ionic. ^{1}H NMR analysis of free ligands in deuterated DMSO-d_6 revealed the presence of the presence of OH group at δ 11.81-12.65 ppm, which disappear upon complexing with Cu (II) ions. The antibacterial sensitivity levels of the Schiff base ligands and their Cu (II) complexes were determined using the disk diffusion method. The synthesized compounds tested for antibacterial bioassay against two gram-negative bacteria, *Pseudomonas aeruginosa* and *Escherichia coli* and one gram-positive bacterium, *Staphylococcus aureus,* at 4 different concentrations. All synthesized compounds show antibacterial activities against all bacteria strains. The zones of inhibition ranged from 6.00- 21.00 mm. However, no test compound showed higher inhibition zones than gentamycin and amoxiclav (positive controls). Data was analyzed using Two-Way ANOVA. The results showed a significant difference ($p \leq 0.05$) between the means, indicating that methyl, nitro and carboxyl groups and coordination of the ligands to Cu (II) affected antibacterial activity. Cu (II) complexes displayed higher antibacterial activity than their free ligands. It was concluded that the substituted ligands with methyl, carboxyl and nitro groups and Cu (II) complexes have promising antibacterial activity. The results suggest potential applications of Schiff base ligands obtained from benzophenone derivatives and their Cu (II) complexes as antibacterial agents.

TABLE OF CONTENTS

LIST OF TABLES

LIST OF FIGURES

LIST OF PLATES

LISTS OF SCHEMES

ABBREVIATIONS AND ACRONYMS

^{13}C NMR	Carbon Nuclear Magnetic Resonance
^{1}H NMR	Proton Nuclear Magnetic Resonance
ANOVA	Analysis of variance
CAUTIs	Catheter-associated urinary infections
CDC	Centre for Disease Control
CFU	Colony Forming Unit
DMSO	Dimethyl sulfoxide
DNA	Deoxyribonucleic acid
ESBLS	Extended Spectrum-Lactamases
FT-IR	Fourier Transformation infrared
ILCT	Intra-Ligand Charge Transfer
KEMRI	Kenya Medical Research Institute
LMCT	Ligand-Metal Charge Transfer
MHA	Muller -Hinton Agar
MIC	Minimum Inhibitory Concentration
MLCT	Metal-Ligand Charge Transfer
SAR	Selective Activity Relationship
TMS	Tetramethyl Silane
UTIs	Urinary tract infections
UV/Vis	Ultra-violet /Visible
WHO	World Health Organization
δ	Chemical shift
λ	Lambda
Λ_m	Molar conductivity
υ	Frequency
μ	Spin only magnetic moment

CHAPTER ONE
INTRODUCTION

1.1 Background Information

Emerging infectious diseases and the growing number of multidrug-resistant microbial pathogens continue to make treating infectious diseases a significant and challenging problem worldwide (Paul *et al.,* 2022). Infections produced by multidrug-resistant strains are now linked to a significant increase in morbidity, mortality, and healthcare expenditures worldwide (Abushaheen *et al.,* 2020). Multidrug resistance associated with a significant number of clinically important pathogenic bacteria such as *Staphylococcus aureus*, *Escherichia coli*, *Salmonella typhi*, *Bacillus cereus* and *Pseudomonas aeruginosa* has been reported (Teng *et al*., 2023). Bacterial resistance is growing and poses a severe hazard in hospitals and the community (Karam *et al.,* 2016).

The dramatic rise in the incidence of multidrug-resistant bacteria nosocomial and community-acquired infections has prompted an urgent need for novel and more effective antibacterial agents capable of combating multidrug-resistant strains (Khan *et al.,* 2016). In recent years, there has been a lot of interest in finding new bioactive compounds with antibacterial capabilities. Benzophenone derivatives are compounds with remarkable biological properties. The benzophenone scaffold is a structure in medicinal chemistry present in various synthesized or naturally occurring compounds that demonstrated various biological activities (Marinov *et al*., 2023; Lei *et al*., 2024). Thus, the study focused on the class of bioactive compounds known as Schiff base, obtained through condensation of benzophenone derivatives with selected anilines.

Hugo Schiff, one of the fathers of modern chemistry, discovered Schiff base ligands, compounds with an alkyl or aryl group and a double bond between nitrogen and carbon (Raczuk *et al*., 2022). These compounds are commonly known to have an azomethine function group with a generic formula (R-CH=NR), where R is an alkyl or aryl substituent and contains an azomethine functional group (Kanwal *et al*., 2022). The azomethine group in such compounds has been critical to their biological activities, such as antifungal, antibacterial, antimalarial, antiproliferative, anti-inflammatory and antiviral (Saeed *et al*., 2020; Nath *et al*., 2022). Due to their vast applicability in numerous biological functions, transition metal complexes of Schiff base are one of the

most investigated systems (Abubakar *et al*., 2024). The lone pair of electrons in the nitrogen atom's 2p orbitals of the azomethine group has a significant chemical significance and provides good chelating capacity, especially when combined with one or more donor atoms near the azomethine group (Yimer, 2014). This chelating ability of the Schiff bases, combined with the ease of preparation and flexibility in varying the chemical environment of the C=N group, makes it an interesting ligand in coordination chemistry (More *et al.,* 2019).

Transition metal complexes obtained from Schiff base form another class of bioactive compounds that are shown to exhibit promising antibacterial activities. Significant progress has been made in the use of transition metal complexes as drugs to treat a variety of human diseases. Transition metals have different oxidation states and can interact with a variety of negatively charged molecules, resulting in the development of metal-based drugs with promising pharmacological applications and the potential for novel therapeutic opportunities (Rafique *et al.,* 2010).

Many researchers have recently investigated the use of transition metal ions to enhance the activity of antibacterial drugs through chelation (Al-Radadi *et al*., 2020). In many investigations, metal complexes have been found to exhibit more promising antibacterial properties than their corresponding free ligands (Gupta *et al*., 2024). This observation has been explained using Overtone's cell permeability notion and Tweedy's chelation chelating theory. According to Overtone's theory, the lipid membrane surrounding the cell allows only lipid-soluble molecules to pass through (Abu-Dief *et al*., 2024). Therefore, liposolubility plays a crucial role in controlling the antimicrobial activity of bioactive compounds (Jose *et al.,* 2018). Tweedy's chelation theory, on the other hand, suggests that during chelation, the polarity of the metal ion is lowered to a greater extent due to ligand orbital overlap and partial sharing of the metal ion's positive with donor groups (Mounika *et al.,* 2010).

Moreover, the chelation increases the delocalization of the metal chelates. Better lipophilicity enhances metal chelates' permeation through microbial cell lipoid membranes (Abousaty *et al*., 2024). A postulation has also been put forward suggesting that inside the microbial cell, the metal chelates disturb the cell's respiration, thereby

blocking the synthesis of proteins and further restricting the growth of the bacteria (Raman *et al*., 2009). Schiff base metal complexes have received significant attention because of their biological activities, essentially due to their ability to form a tetradentate or bidentate chelate with metal ions, bonding through sulphur, oxygen, and nitrogen (Maher *et al.,* 2015).

In recent studies, numerous Schiff base ligands and their metal complexes have been found to have promising antibacterial activities. The Schiff base metal complexes of Cr (II), Co (II), Ni (II), and Cu (II) derived from 2,6-pyrine carboxaldehyde-thiosemicarbazone demonstrated better activity than Schiff base against Gram-positive bacterium *Staphylococcus aureus* and Gram-negative bacterium *Escherichia coli*. The antibacterial studies also revealed that the metal complexes outperformed the Schiff bases ligand in terms of antimicrobial activity (Ali & Yunus, 2014).

According to Spînu *et al*. (2008), a novel bidentate Schiff base and its metal complexes of Fe (II), Co (II), Ni (II) and Cu (II) were prepared, isolated, and characterized. The condensation of 2-thiophene carboxaldehyde and 2-aminopyridine produced the Schiff base ligand. Disk diffusion was used to test the metal complexes' antibacterial properties against various bacterial species, including *Escherichia coli, Pseudomonas aeruginosa* and *Staphylococcus aureus*. The metal chelates outperformed the free Schiff base ligand regarding their antibacterial activity. The Co (II) and Fe (II) complexes significantly inhibited the growth of *Escherichia coli*. These findings on the antibacterial activities of Schiff base and their metal complexes suggest that this class of compounds could form valuable leads in developing new antibacterial agents.

Structural modification is a frequent strategy used in drug design initiatives to produce novel antibacterial medication candidates. The logic adopted in this technique is to begin with some bioactive compounds and generate new molecules that may then be exposed to bioassay screening (Nassar, 2022). Aromatic rings are found in the structural frameworks of several bioactive compounds, including the Schiff base. Variations in the substituent groups attached to these rings have been used as a powerful tool to modify their structures and tune the various physicochemical properties that affect biological activities, such as lipophilicity, membrane permeability, and binding

interactions with biological receptors (Parekh *et al.,* 2017). Substituent groups significantly impact bioactive compounds' electronic properties and binding interactions (Zafar *et al.,* 2021). A bioactive molecule's electronic properties may be altered by incorporating suitable electron-withdrawing or electron-donating groups (Elangovan *et al*., 2022).

Several researchers have applied the method of substituent variation in designing novel Schiff base ligands for antibacterial efficacy testing. Maddela *et al.* (2015) synthesized Schiff base N-substituted 2-methylquinoline-3-carbohydrazide derivatives (Figure 1) by varying the substituents on the phenyl ring.

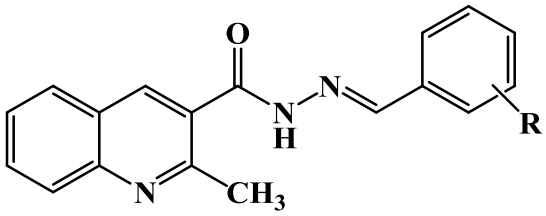

R=(a) H; (b)4-CH_3; (c)4-OCH_3; (d)4-F;(e) 4-Cl;(f) 2-Cl;(g) 3-Cl
(h) 4-OH,3-OCH_3

Figure 1: N'-substituted 2-methylquinoline-3-carbohydrazide derivatives

The compounds were screened for antimicrobial activities against gram-positive *Staphylococcus aureus*, *Bacillus substilis* and *Streptococcus pyogenes* and gram-negative bacteria *Klebsiella pneumoniae, Enterococcus aerogenes* and *Escherichia coli* and also fungal strains *Candida albicians* and *Fusarium oxysporium* using two-fold serial dilution. Compound b (4-CH_3) showed pronounced activity against *Klebsiella pneumoniae, Escherichia coli* and *Enterococcus aerogenes*. Compound d (4-F) displayed promising activity against *Escherichia coli* and *Enterococcus aerogenes.* Compound g (3-Cl) and h (OH), OCH_3 showed better activity against *Escherichia coli.* Also, compound f (2-Cl) displayed good activity against *Candida albicians,* while Compound b (4-CH_3) and h (4-OH, 3-OCH_3) had better activity against *Fusarium oxysporium.* Incorporation of electron-donating groups such as OH, OCH_3 and CH_3 and electron-withdrawing groups such as Cl and F onto the phenyl ring is linked to enhancing the lipophilicity of synthesized compounds, thus improving the antimicrobial activities of synthesized compounds.

Singh *et al*. (2010) designed and synthesized 2-[4-(substituted-benziminomethyl)-phenoxy]-3-methyl quinoxalines analogs with the general structure in Figure 2.

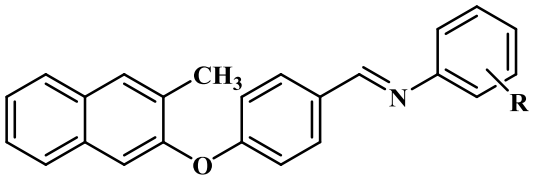

(R=H, 4=Cl, 4=CH_3, 4-COOH , 2,6-CH_3

Figure 2: 2-[4-(substituted-benziminomethyl)-phenoxy]-3-methyl quinoxalines

Different analogs were employed by varying the substituent R on the phenyl ring. The synthesized Schiff base ligands were evaluated for antimicrobial activities against bacterial strains such as *Pseudomonas aeruginosa*, *Escherichia coli*, *Bacillus substilis* and *Staphylococcus aureus.* The antibacterial study revealed that Schiff base ligands having methyl and chloro substituent groups displayed high antibacterial activity against the tested bacterial strains. This observation was explained based on the lipophilic nature of these substituents. Since they are naturally lipophilic, the methyl and chloro substituents considerably impacted the synthesized Schiff base ligand's lipophilicity, which helped improve its bioactivity. The compounds' mild activity with carboxyl groups correlated with the group's acidity. According to antibacterial study findings, substituents such as methyl, chloro, methoxy and carboxyl may help increase the antibacterial activity of Schiff base ligands with similar structural.

Condensation of anilines substituted with carboxylic (-COOH) nitro (-NO_2) and methyl (-CH_3) to 2 -hydroxy -4-methoxybenzophenone are essential since they result in the formation of imine (-RC=N) in which nitrogen is used in the coordination of copper (II) ions to Schiff base ligands to form complexes. Moreover, the azomethine (-RC=N-) forms hydrogen bonds at a few corresponding places in the cell structure, impacting cells (Omoruyi *et al.,* 2016). The substitution of electrons donating group (-CH_3) in aniline affects the reactivity of the complexes; this led to an increase in electron density at the ortho and para positions. The methyl group has an essential contribution to the antibacterial activity of bioactive compounds (Bazzini & Wermuth, 2008). Usually, introducing a methyl group into the structure of a bioactive compound increases its lipophilicity, which improves cell membrane permeability (Bockus *et al*., 2015). This,

in turn, enhances the permeation of the molecule into the microbial cell via lipoid membranes (More *et al*., 2019).

On the other hand, COOH is electron-withdrawing and an essential active ingredient in many drugs such as Statins, nonsteroidal anti-inflammatory drugs (NSAIDs) and β-Lactam contain the carboxylic groups in their structures (Lima *et al.,* 2020; Bredael *et al.,* 2022). The Carboxyl group has an impact on antibacterial activity since it enhances the hydrophilicity of bioactive compounds by increasing solubility through the biological membranes (Ballatore *et al*., 2013). Also, the acidity of this group and its ability to establish strong electrostatic interactions and hydrogen bonds make it an apt choice in many drug designs (Kariuki and Njagi, 2018). Lastly, the NO_2 group is a strong electron-withdrawing group showing a broad spectrum of activities, including antineoplastic, antibiotic, and antimicrobial. Additionally, the nitro group causes redox in the cells, which is poisonous to bacteria and eventually leads to their death, as well as multicellular organisms like parasites (Noriega *et al*., 2022).

Copper is an essential trace metal element for various biological activities. It is a metal with an excellent biocidal effect on bacteria (Bharadishettar *et al.,* 2021). In a recent investigation, copper was found to successfully suppress a panel of bacterial species associated with human diseases, including pathogenic *Escherichia coli, Staphylococcus aureus, Bacillus subtilis, Pseudomonas aeruginosa,* and *Mycobacterium tuberculosis* (Evans & Kavanagh 2021). Furthermore, numerous copper (II) complexes have been reported to have antibacterial properties against pathogenic bacteria (Claudel *et al*., 2020). As a result, copper is now generating a lot of attention in research investigations to develop possible metal-based antibacterial agents

1.2 Statement of the Problem

Pathogenic bacteria such as *Vibrio cholerae, pseudomonas aeruginosa, staphylococcus aureus* and *Escherichia coli* are developing resistance to antibacterial agents at a very high rate and the current effective antibacterial agents are likely to become resistant in the future. The emergence and global dissemination of new bacterial resistance mechanisms threaten human beings' capacity to cure widespread infectious diseases. As antibiotics lose effectiveness, many infections, including food-borne diseases, blood

poisoning, urinary tract infections (UTIs), pneumonia, and tuberculosis, become difficult to cure and occasionally incurable. A severe lack of potent medications for treating bacterial illnesses has resulted from the rapid emergence and dissemination of multidrug-resistant bacteria. Multidrug-resistant pathogenic microorganisms also contribute significantly to increased morbidity and mortality from infections. Schiff bases are promising antibacterial agents that can be used against these drug-resistant microbes. Schiff bases obtained from benzophenone derivatives with selected anilines and their metal complexes represent a bioactive compound whose antibacterial capacities have not been exhaustively explored. Therefore, the search for novel benzophenone-based compounds endowed with better antibacterial efficacies must be pursued.

1.3 Objectives of the Study

1.3.1 General Objective

To synthesize, characterize and determine antibacterial properties of Schiff bases derived from benzophenone derivatives and selected anilines and their copper (II) complexes.

1.3.2 Specific Objectives

i. To synthesize Schiff bases derived from benzophenone derivatives and selected anilines.
ii. To characterize synthesized Schiff base derived from benzophenone derivatives and selected anilines and their copper (II) complexes.
iii. To determine the antibacterial properties of synthesized Schiff bases derived from benzophenone derivatives and selected anilines and their copper (II) complexes.

1.4 Research Questions

i. Is it possible to synthesize Schiff bases derived from benzophenone derivatives and selected anilines and their copper (II) complexes?
ii. Is it possible to characterize Schiff bases derived from benzophenone derivatives and selected anilines and their copper (II) complexes using various analytical techniques?

iii. Do Schiff bases from benzophenone derivatives and selected anilines and their copper (II) complexes possess antibacterial properties?

1.5 Justification

Antibacterial resistance has arisen as one of the twenty-first century's most serious public health challenges due to emerging infectious diseases directly associated with increasing multidrug-resistant microbial pathogens to antibiotics (WHO, 2014). As a result, the only alternative for humanity is to look for new and strategic treatment options that could circumvent the problem of multidrug resistance. Therefore, it is necessary to look for novel drug analogs or active agents with better action and structural activity modes than traditional antibacterial organic compounds to treat infectious diseases. As a result, efforts are being focused on developing Schiff base and their metal complexes, active agents with greater efficacy, increased selectivity for disease-causing organisms, lower toxicity, and a broader range of activity. Thus, Schiff base ligands and their metal ion complexes have been identified as possible antibacterial agents. Hence, the availability of potent antibacterial drugs at all times will enhance the growth of the global economy by reducing morbidity and mortality. Sophisticated medical operations like surgeries that rely on antibacterial medications to treat opportunistic bacterial infections that emerge from such operations are likewise threatened by an expanding spectrum of bacterial diseases resistant to routinely used and available antibiotics. The scarcity of antibacterial drugs caused by bacterial infections' extensive resistance to existing drugs justifies the search for more effective antibacterial agents.

CHAPTER TWO
LITERATURE REVIEW

2.1 Schiff Bases

Schiff base is the compound with imine group (-HC=N-). They are the condensation of carbonyl groups, which are ketones or aldehydes with primary amines, first observed by Hugo Schiff in 1864 (Abu-Yamin *et al*., 2022). The Schiff base has the general formula RN = CR'R'' where R, R', and R'' could be substituted with alkyl, aryl, heteroaryl and cycloalkyl (Hameed *et al.,* 2017). The -C = N- imine bond in Schiff bases is vital in conferring broader spectrum pharmacological applications to these compounds. The -C=N- imine bond's electrophilic carbon and nucleophilic nitrogen give great binding chances with many nucleophiles and electrophiles, suppressing targeted illnesses, enzymes, or DNA replication. These compounds are helpful in the pharmaceutical and medical industries due to their various biological activities (Raju *et al.,* 2022). Numerous studies have been conducted on the transitional complexes produced by Schiff base ligands that exhibited various biological activities (Venkatesh *et al*., 2024).

2.2 Synthesis of Schiff Base Ligands.

The synthesis of Schiff base was first observed by Hugo Schiff in the 19th century (Mahmood, 2022). Aldehydes or ketones can be condensed to Schiff bases in a reversible process that often occurs when an acid or base catalyzes the reaction or when the compound is heated. In most cases, the product is separated from the formation, the water is removed, or both are done. Aqueous acid or base can hydrolyze several Schiff bases back to their respective aldehydes, ketones, and amines (Solankee *et al*., 2010). The formation of a Schiff base follows the mechanism in Scheme 1 (Dehghanpour *et al.* 2007).

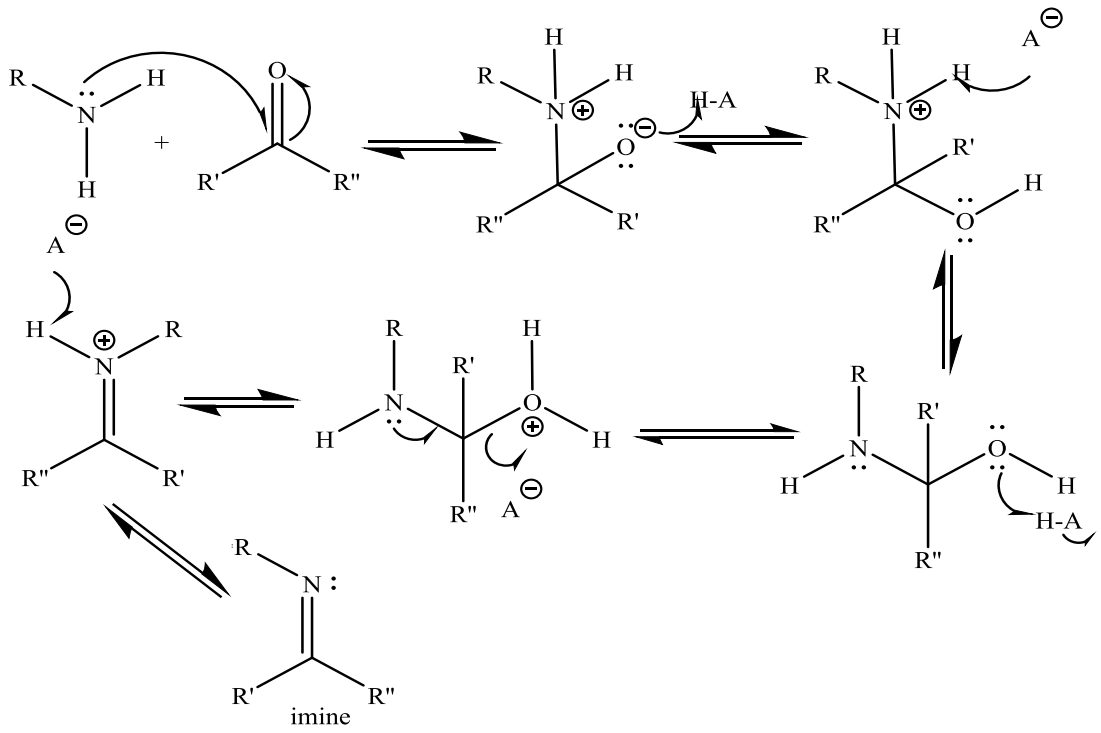

Scheme 1: Mechanism for the formation of a Schiff base

2.2.1 Methods of Synthesizing Schiff Bases

Several research groups have developed different methods to synthesize Schiff bases, but these methods have experienced drawbacks, such as long reaction times and small yields (Rao *et al.,* 2010). In line with this, other researchers considered ways to reduce the reaction time and obtained very high yields for Schiff-based syntheses (Verma *et al*., 2022). The methods of synthesizing Schiff base ligands include microwave irradiation, grinding, classical, and water base, while the refluxing method synthesizes both Schiff base ligands and Schiff base metal complexes. These methods are discussed below:

2.2.1.1 Microwaves Irradiation Method

Microwave synthesis of Schiff bases has been performed using microwave irradiation. The Schiff bases were prepared with aromatic aldehyde and aromatic amine using cashew shell extract as a catalyst under microwave irradiation. This reaction is rapid, efficient, and solvent-free and involves the one-pot synthesis of Schiff bases under microwave irradiation. Scheme 2 illustrates the synthesis of Schiff base ligand using the microwave irradiation method according to Kulshrestha *et al.* (2010).

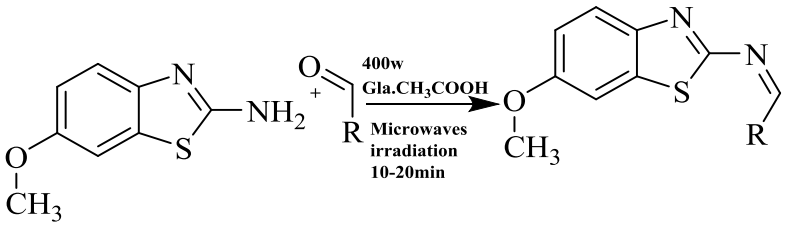

R= 2-NO_2-C_6H_4,-CH=CH-C_6H_5; 4-F-C_6H_4
1-Napthalene, 2-Anthracene

Scheme 2: Synthesis of Schiff base using microwave irradiation method

Any substance with mobile electric charges, such as polar molecules in a solvent or conducting ions in a solid, will typically be heated by microwave radiation because it has high-energy electric fields. The synthesis of Schiff bases under the effect of microwave irradiation was discovered to be considerably more straightforward and quicker than conventional heating in recent years. The synthesis using microwave radiation under solvent-free or low-solvent conditions is an effective way to decrease pollution, lower costs, and enhance output while also making the process and handling easier (Shntaif & Rashid, 2016)

2.2.1.2 Grinding Method

The grinding method is another method for synthesizing Schiff base ligands with solvent and refluxing-free conditions; it has a higher yield, and the reactions are faster. The procedure involves grinding aldehyde or ketone in a motor for several minutes at room temperature. The yielded water is removed under vacuum at about 70℃. The method is quick and economical; the reaction occurs at room temperature without adding a base (Zarei & Jarrahpour, 2011). Scheme 3 illustrates the synthesis of Schiff base ligands using the grindstone method, according to Sachdeva *et al.* (2012).

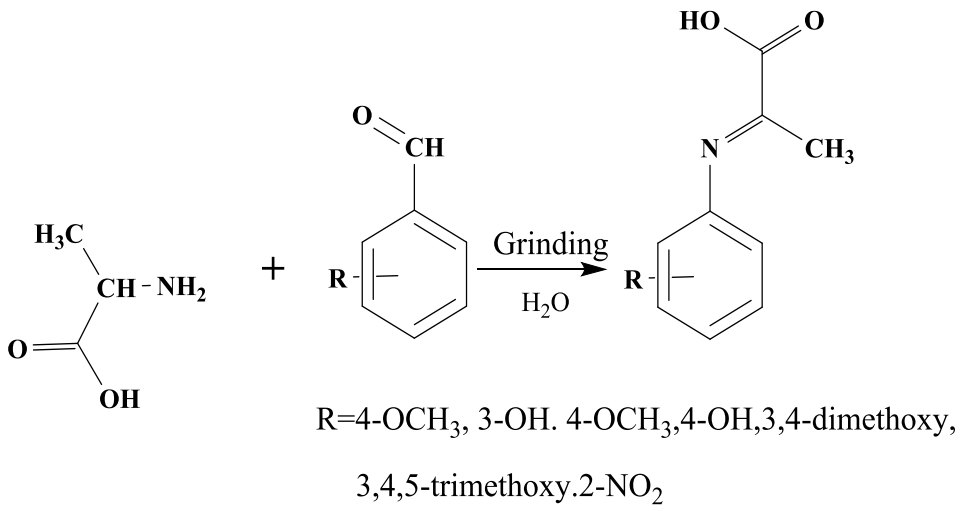

Scheme 3: Synthesis Schiff base using grindstone method

The use of grindstone has replaced the use of heat and solvent in the synthesis of Schiff bases. On a larger scale, this can be accomplished by using extremely high grinding in a ball mill. Improved conversion resulting from using a cylinder reactor without additional purifying processes. Although this method has a high yield and is environmentally friendly, the reaction to the product can take some time. The approach, however, cannot be applied to both liquid reactants (Banerjee *et al*., 2022).

2.2.1.3 Classical Method

The classical method for synthesizing imines is the initial reaction reported by Hugo Schiff (Qin *et al.,* 2013). Essentially, it involves the removal of water molecules and the reaction of an aldehyde or ketone with a primary amine. Acid catalysis can speed up this reaction, often carried out by refluxing a mixture of an amine and a carbonyl molecule in a Dean-Stark apparatus to get rid of the water. This removal is crucial because (Scheme 3) the transformation of hemiketal (3) into imine (4) is reversible (Yaseen *et al*., 2021). Several dehydrating agents have been successfully employed, including sodium sulphate and molecular sieves (Westheimer *et al.*,1971). As an alternative, various *in situ* techniques have also been documented that use dehydrating solvents such as tetramethyl orthosilicate or trimethyl orthoformate (Love *et al.*, 1993). As far as the use of an acid catalyst is concerned, it has been observed that Lewis's acids like $ZnCl_2$, $TiCl_4$, $SnCl_4$, BF_3, Et_2O, $MgSO_4$, $Mg(ClO_4)_2$, etc., as well as mineral

acids like H_2SO_4 or HCl, organic acids like p-toluene sulphonic acids or pyridinium *p*-toluene sulphonate, acid resin, and montmorillonite. Scheme 4 illustrates the synthesis of Schiff base using the classical method according to Yaseen *et al*. (2021).

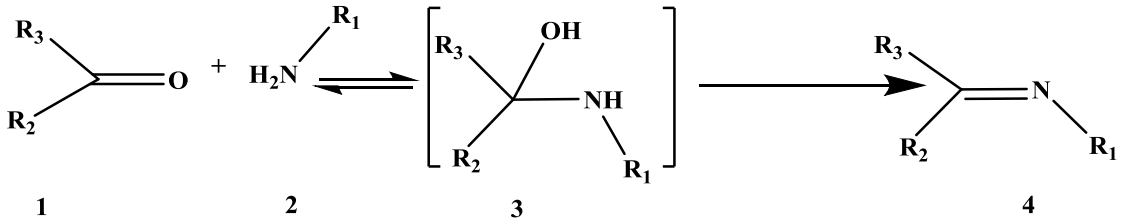

Scheme 4:Synthesis of Schiff base ligand using the classical method.

2.2.1.4 Water Base Method

Water base synthesis involves the use of water in the synthesis of Schiff base. Aldehyde or ketone with primary amine is stirred in water for several minutes at room temperature; the reaction raises temperature since the reaction is exothermic. The product is obtained by filtering, washing it with water, and drying it (Arshi *et al*. 2009). Scheme 5 shows the synthesis of Schiff base using the water base method, as reported by Bhagat *et al.* (2013).

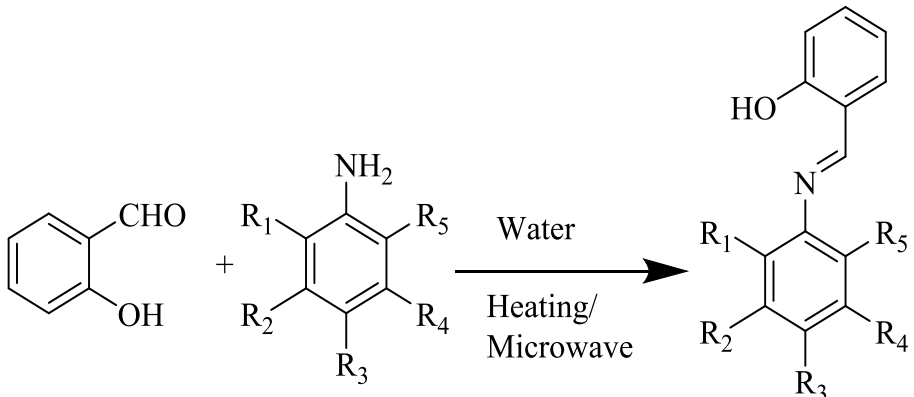

a) R_1=F; R_2=H; R_3=F; R_4=H; R_5=H
b) R_1=H; R_2=H; R_3=Cl; R_4=H; R_5=H
c) R_1=F; R_2=F; R_3=F; R_4=F; R_5=H
d) R_1=H; R_2=H; R_3=F; R_4=H; R_5=H

Scheme 5: Synthesis of Schiff base ligand using water base method

Water, an abundantly available affordable reaction solvent, is environmentally beneficial and encourages green chemistry synthesis. However, the approach has limited use because most organic molecules are insoluble in water and Schiff bases can also be hydrolyzed in water (Moreno *et al.,* 2010).

2.2.1.5 Reflux method

The reflux method is a commonly used method for synthesizing Schiff base ligands. The pH of an ethanolic solution of the aldehyde or ketone and the primary amine in a round-bottomed flask is adjusted by adding a few drops of basic or acidic solution. The reaction mixture is then refluxed with controlled heating for two to three hours, and then cold water is added to precipitate the product. The precipitate is collected by filtration, dried, recrystallized from ethanol and dried at room temperature (Saikumari, 2021. Scheme 6 illustrates the synthesis of Schiff base ligand using the reflux method according to Sujarani & Ramu (2013).

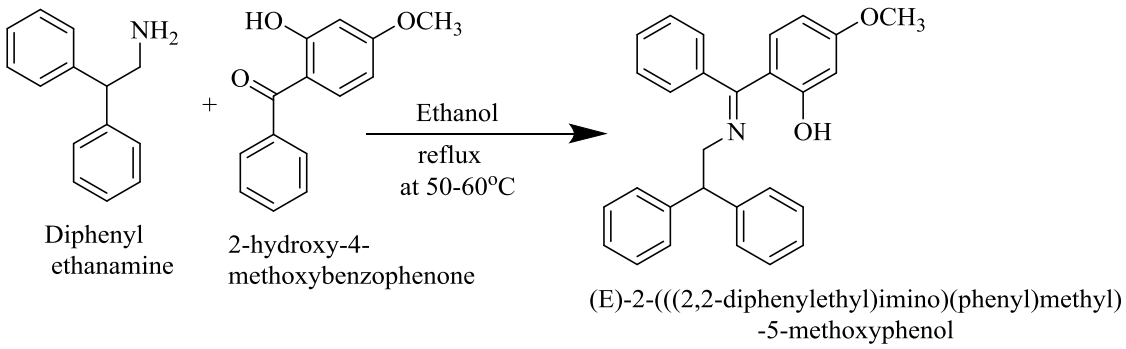

Scheme 6: Synthesis of Schiff base ligand using reflux method

2.3 Schiff Base Metal Complexes

Schiff base metal complexes are formed when the Schiff base ligand reacts with transition metal ions. The high affinity of Schiff bases for chelation with transition metal ions is used to prepare their complexes. Metal complexes have been shown to have promising antimicrobial activities. Such metal complexes metals include copper (Dinku *et al.,* 2024), cobalt (Ghanghas & Poonia, 2024)., silver (Liang *et al.,* 2018), gold (Lu *et al*., 2022) zinc (Abendrot *et al*., 2020) and ruthenium (Es-Sounni *et al*., 2024). The development of bioinorganic chemistry has increased the interest in Schiff base since it has been recognized that many of these complexes may serve biologically essential species. Coordination compounds have been reported to act as enzyme

inhibitors and are helpful due to their pharmacological application (Ghanghas *et al*., 2021). The advances in inorganic chemistry enable great options to use metal complexes as antibacterial agents, which have become increasingly pronounced (Liang *et al*., 2021). Schiff base metal complexes are bioinorganic chemistry's most versatile and widely researched systems (Uddin *et al*., 2020). According to reports, the occurrence of coordination molecules in living systems is crucial to the fast-emerging discipline of bioinorganic chemistry. As a result, Schiff base metal complexes could serve as models for physiologically significant entities (Hameed *et al*., 2017; Khan *et al.*, 2022).

2.3.1 Methods of Synthesizing Schiff Bases Metal Complexes

The reflux method is also used to synthesize numerous Schiff metal complexes. A solution of the requisite metal salts is treated with a Schiff base ligand dissolved in hot ethanol. The solutions are usually mixed and refluxed with magnetically stirring at a constant temperature maintained upon which the complex is precipitated. The precipitate is filtered under reduced pressure and washed with organic solvents to remove the unreacted Schiff base. Finally, purification is done by recrystallization (Iftikhar *et al*., 2018). Scheme 7 illustrates the synthesis of Schiff base metal complexes according to Ommenya *et al*. (2020).

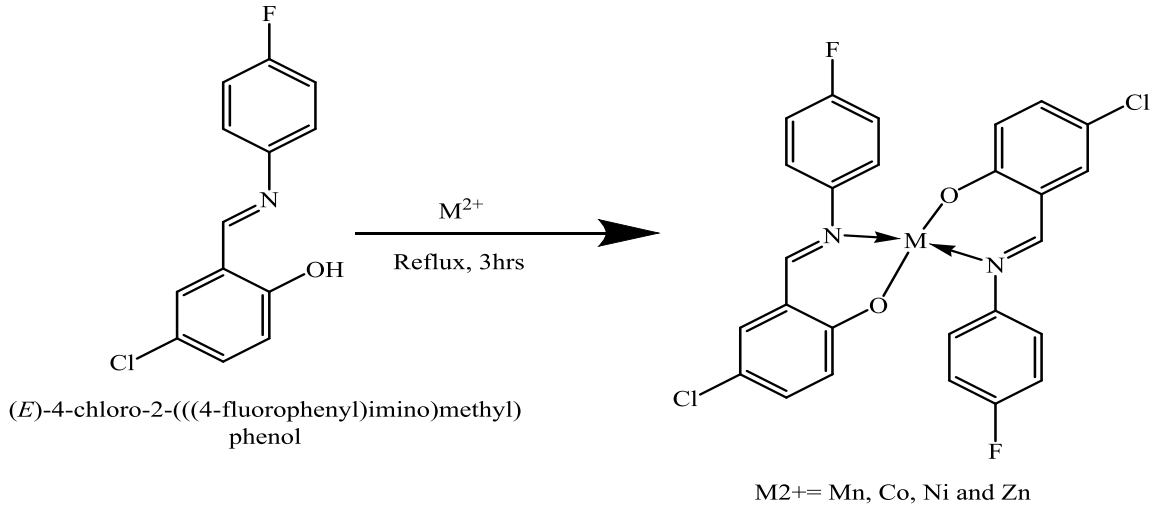

(*E*)-4-chloro-2-(((4-fluorophenyl)imino)methyl) phenol

Scheme 7: Synthesis of Schiff base metal complexes using the reflux method

2.4 Characterization of Schiff Base Ligand and their Copper (II) Complexes

2.4.1 Analytical Methods: Theoretical Basis

Several analytical methods are used to characterize the Schiff base ligands and their copper (II) complexes. These analytical techniques include nuclear magnetic resonance, Fourier transform infrared, ultra-violet/visible, and molar conductivity. The methods for characterizing Schiff base and copper (II) complexes are discussed below:

2.4.1.1 Determination of melting point

The melting point is the temperature at which solid substances change to liquid substances upon heating. Pure substances melt at constant temperatures, while impure substances melt at various temperatures. Therefore, melting point is used in characterization to check the purity of Schiff base ligands and Schiff base metal complexes (Mohamed *et al.,* 2009).

2.4.1.2 Elemental Analysis

Carbon (C) and a few other light elements like hydrogen (H), nitrogen (N), and oxygen (O) are present in a wide variety of organic and inorganic compounds. These elements are found in several compounds, which has made it necessary to test them for various academic and research applications. Elemental analysis determines the molecular formula of unknown compounds (Gabbaï *et al*., 2016). The sample is heated to about 900℃ in oxygen during the elemental analysis, producing a mixture of carbon (IV) oxide, carbon (II) oxide, water, nitrogen, and nitrogen (II) oxide. The products are swept into a tube furnace at 750℃ by a stream of helium, where copper is reduced to nitrogen (II) oxide and oxygen is eliminated. Copper (II) oxide transforms carbon (II) oxide into carbon (IV) oxide (Atkins *et al*., 2010). The resulting mixture is analyzed by running it through three thermal conductivity detectors. The first detector measures hydrogen, and water is subsequently captured in a trap. The third detector measures the remaining nitrogen. The information collected using this method is presented as mass percentages of C, H, and N. Elements analysis helps confirm a compound's purity. It offers data that helps elucidate a compound's molecular formula (Fadeeva *et al.*, 2008).

2.4.1.3 FT-IR Spectroscopy

FT-IR Spectroscopy is a technique used for the identification and structural analysis of molecules. IR spectroscopy measures the vibrational of atoms. It involves various molecules' atomic groups, which lead to twisting, bending, rotational, and vibrational motions. Additionally, while IR radiation cannot excite electrons from lower to higher energy states, it does generate vibrations in covalent bonds between individuals or groups of atoms (Tasumi, 2014). Strong bonds and light atoms typically experience higher wave numbers. The functional groups contained in a molecule can be identified using information from the I.R. spectra. The near, mid, and far infrared regions of the infrared spectrum of a molecule are used to interpret the spectrum using known group frequencies (Stuart *et al*., 2004). The near I.R. regions join the visible region at about 12,500 cm^{-1} and extend to approximately 4,000 cm^{-1}. This region is present in numerous absorption bands resulting from harmonic overtones of fundamental bands and combination bands frequently linked to hydrogens. These include the first overtones of O-H and N-H stretching vibrations at about 7140 cm^{-1} and 6667 $cm^{-1,}$ respectively. Bands resulting from C-H stretching and deformation vibration of alkyl groups are detected at 4548cm^{-1} and 3850 $^{-1,}$ respectively. The middle infrared region is divided into the "group frequency" region at 4000 cm-1, extending to approximately 1300 cm^{-1}, and the "fingerprint" region at 1300 cm^{-1}, extending to about 650 cm^{-1}. Far–I.R. region is between 667 cm^{-1} to 10 cm^{-1} and contains the bending vibrations of Carbon, Nitrogen, Oxygen, and Fluorine with atoms heavier than mass 19 and 26 additional bending motions in cyclic or unsaturated systems (Alpertet *et al*., 2012).

2.4.1.4 Nuclear Magnetic Resonance

NMR is a technique used to study the nuclei in a molecule when exposed to an external magnetic field (Hore *et al*., 2015). Nuclei have angular momentum because they spin around the axis of the externally provided magnetic field. Chemical structure and molecular dynamics are just two examples of the many physical and chemical aspects that NMR spectroscopy may investigate (Mitchell *et al*., 2008). Characterizing Schiff base ligands and their metal complexes frequently uses proton NMR. Proton NMR provides information such as chemical shift, signal intensity, and splitting pattern or multiplicity. Chemical shift is the resonance frequency of a nucleus in a magnetic field relative to a standard (Keeler, 2010).

Tetramethylsilane (TMS) is the standard reference compound that is typically employed. This compound was selected because, compared to most known compounds, its methyl groups' protons are better protected. The protons' resonances in a different compound are reported in terms of displacement from those TMS, expressed in Hertz. The location and quantity of chemical shifts can frequently be used to diagnose a molecule's structural issues (Hoffman, 2006). A proton NMR spectrum may or may not show many peaks for each signal. The Signal multiplicity results from this produces singlet, doublet, triplet, quartet, and multiplicity (Lambert *et al.*, 2019). The integral area of a peak represents the signal's intensity. The combined NMR signal intensities should ideally match the number of nuclei in a molecule. Together, the chemical shifts, multiplicity (coupling constants), and integrated intensities enable the protons in a molecule to be structurally assigned (Richards & Hollerton, 2023).

2.4.1.5 UV -Vis Spectroscopy

The UV -VIS spectroscopy is a technique that uses lights in visible and adjacent ranges. Since molecules and atoms exhibit electronic transitions, it examines how a sample reacts to electromagnetic radiation in the ultraviolet and visible ranges (Perkampus & Heinz-Helmut, 2013). This technique is beneficial for identifying and clarifying the nature of conjugated systems in molecules containing aromatic rings (Yadav & Las Dhar, 2013). Sigma, Pi, and nonbonding electron transitions are among the electronic transitions occurring in organic compounds; complexes contain d-d transitions. Ultraviolet light energy can be absorbed by molecules with electrons in both bonding and nonbonding orbitals to excite them to the higher anti-bonding molecular orbital. The longer the wavelength of light it absorbs, the more readily excited the electrons are. Identifying the functional groups within molecules by correlating the absorption wavelength with the type of bonds in a specific molecule is helpful (Rocha *et al.*, 2018).

The molecular orbital theory mainly describes the electronic structure of coordination compounds (Bersuker, 2010). Transition metal complexes primarily exhibit three broad wavelength-spanning electronic excitation band types: d-d (ligand) transitions (300–1500 nm), metal-to-ligand charge transfer (MLCT) and ligand–to–metal charge transfer (LMCT) transitions (200–500 nm); and localized transitions on the ligands that are frequently referred to as intra-ligand charge transfer (ILCT) transitions. An electron in

a metal's d-orbit gets stimulated to a higher-energy d-orbital during a d-d transition (Nkungli *et al*., 2015). The impact of ligands on the energy of the d-orbitals of metal ions affects these transitions. Since d-orbital spitting is caused differently by octahedral, square-planar, and tetrahedral fields, the geometry will be a prominent factor during d-d transitions in a metal complex. (Power, 2012; Deeth *et al*., 2009).

Charge-transfer transitions in transition metal complexes are responsible for some of the bright colours seen in them. The charge-transfer transitions typically have molar absorption coefficients of 10^3 to 10^5 $Lmol^{-1}cm^{-1}$ and are quite strong (Pashanova *et al*., 2022). Charge-transfer transitions are stronger than d-d transitions, often prohibited by the Laporte rule. Charge-transfer transitions may obscure the former when strong and ligand-transfer transitions occur in the same electronic spectrum (Dorenbos, 2017). The absence of d-d transitions in the electronic spectrum results from such a circumstance. The charge-transfer transitions at the middle of a charge-transfer transition typically obscure the former. The absence of d-d transitions in the electronic spectrum results from such a circumstance. A charge-transfer transition's peak centre usually lies at a shorter wavelength (higher wavenumber) than the centre of d-d transitions of the same complexes (Bysewski *et al*., 2024). The ligand may consist of reducing and oxidizing parts, which is the occurrence of ILCT transitions. The latter are in $n \rightarrow \pi^*$ and $\pi \rightarrow \pi^*$ type transitions, which are localized within the organic moiety of the metal complex.

2.4.1.6 Molar Conductance

Studies on the electrolytic behaviour of metal complexes reveal information on their nature and makeup. To a certain extent, the electrolytic and non-electrolytic character of metal complexes is revealed by molar conductance measurements. For the benefit of academics and researchers, an attempt has been made to summarize the molar conductance ranges of metal complexes in various solvents. Additionally, data on molar conductance has been used to predict the geometries of metal complexes (Ali *et al*., 2013).

Additionally, efforts have been made to discuss how conductance data can be used to estimate the size of complexes with structural relevance. Molar conductance has also been used to calculate the stoichiometry of metals and ligands. Finally, molar

conductance measurements highlight the structural variability of metal complexes in various solvents (Al-Qahtani *et al*., 2021).

2.4.2 Analytical Methods: Practical Applications

Hemalatha *et al*. (2020) designed and characterized Schiff base (E)-2-((2-hydroxy-4-methoxyphenyl)(phenyl)methyleneamino)benzoic acid derived from 2-hydroxy-4-methoxybenzophenone and 2-aminobenzoic acid and bidentate N_2 type 1,10-phenanthroline and their metal complexes of Mn (II), Co (II), Cu (II) and Zn (II) complexes as illustrate in scheme 8 below.

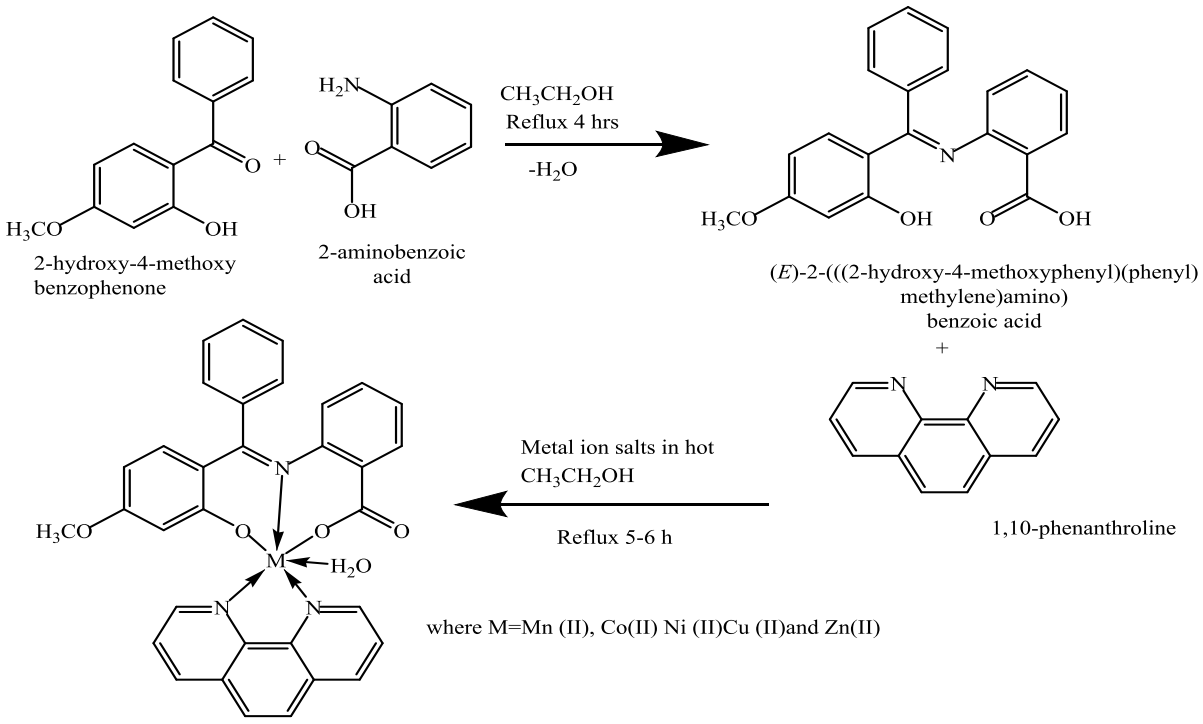

Scheme 8: Synthesis of Schiff base derived from 2-hydroxy-4-methoxybenzophenone and 2-aminobenzoic acid and 1,10-phenanthroline and their metal (II) complexes

The compounds obtained were in crystalline form with different colours. For instance, the Schiff base had yellowish orange while Mn (II), Co (II), Ni (II), Cu (II) and Zn (II) complexes had reddish brown, pink, pale green, brown and pale yellow in that order. The melting point of the parent ligand was 142^{o}C while Mn (II) and Co (II) complexes were 272 and 276℃, respectively. The remaining complexes had a melting point greater than 280℃. The techniques used to characterize the compounds included IR, NMR and electronic spectra. IR spectra of the ligands with that of their complexes confirmed the

formation of the complexes. The Schiff base acts as a tridentate ligand (NO_2 type), binding to metal (II) ions through azomethane-N, carboxylate-O and deprotonated phenolic-O atoms. All the complexes showed a moderately intense band, which appeared in the regions of 1105–1085 and 748–717 cm^{-1} and was assigned to be –C–H and –C,N stretching vibrations of ligand 1,10-phenanthroline respectively; this indicates that the binding mode of 1,10-phenanthroline ligand with the metal (II) ions is in a bidentate (N2 type) manner utilizing two phenyl ring N atom. The kind of coordination was further confirmed in the far IR region, and the appearance of two new peaks of low intensity were observed at 465–480 and 555–585 cm^{-1} for υ (M–O) and υ (M–N) binding modes respectively. Further coordination type confirms in the far IR spectra show two low-intensity peaks observed at 465–480 and 555–585 cm^{-1} for binding modes of υ (M–O) and υ (M–N), respectively. Broad bands were observed in the spectra at regions of 3475– 3380 cm^{-1} for υ (OH) stretching, 852–835 cm^{-1} for υ (OH) rocking and 725–712 cm^{-1} for υ (OH) wagging, which indicates coordination of H_2O molecule.

Electronic spectra of parent ligand with metal (II) complexes show that Schiff base displays three absorption peaks at 44,643 cm-1 (for benzene π– π *), 37,878 cm-1 (for imino π – π *) and 25,773 cm (for LMCT n– π *). The last band appears at 25773 cm^{-1} and shifts to a long wavelength region through an increase in the intensity of absorption for the metal complexes, which is due to the transfer of lone pairs from the Schiff base ligand towards the M(II) ion (N→M) of the complexes. The ^1H NMR spectra of the free ligand and Zn (II) complex showed the disappearance of phenolic-O (at 10.42 ppm) and carboxylate-O (at 3.62 ppm) proton peaks. Furthermore, NMR spectra demonstrated that the Schiff base and 1,10-phenanthroline ligands, which act as tri and bidentate through azomethine-N, deprotonated phenolic-O, carboxylate-O and two phenyl ring-N atoms, respectively around Zn (II) ion to frame a stable structure.

Endale *et al*. (2018) reported the synthesis and characterization of copper (II) and cobalt (II) vanillin-aniline Schiff base complexes, as illustrated in scheme 9 below.

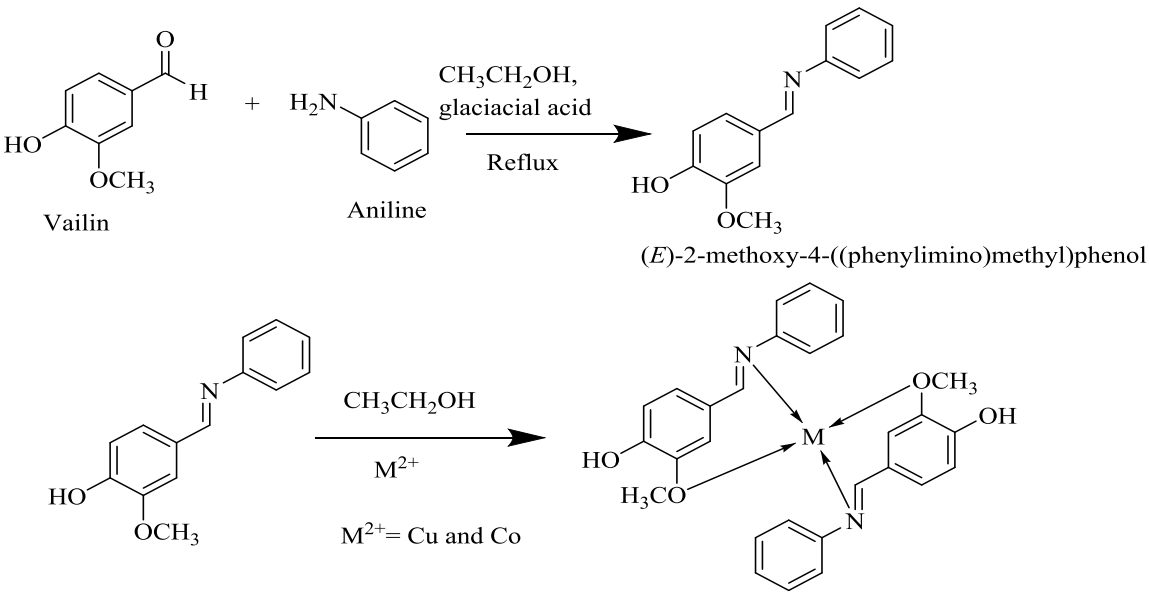

Scheme 9: Synthesis of copper (II) and cobalt (II) vanillin-aniline Schiff base complexes

The synthesized Schiff base and its metal complexes had melting points ranging from 134- 280℃. Elemental analysis of free ligands and their complexes revealed that both observed and calculated H, C and N values agreed. The techniques used to characterize Schiff base and their metal complexes were CHN analysis, IR, ^{1}H and ^{13}C NMR. The ^{1}H NMR spectra of free ligands display singlet peaks at δ H 3.8, 9.8 and δ H 8.5, indicating the presence of OCH_3, OH moiety and proton of CH=N group, respectively. The presence of aromatic protons at δ H 7.3 indicates a monosubstituted phenyl ring and the presence of ABX spin patterns at δ H 7.1, 7.65 and 6.95 suggests a trisubstituted phenyl ring. ^{13}C NMR spectrum of the Schiff base ligand confirms peaks at δ C 160.5, and C 152.4 and 150.7, respectively attributed to the carbon atom of imine (N=CH) group and sp^2 oxygenated quaternary aromatic carbons where an OH and OCH_3 groups are attached. The IR spectrum of Schiff base ligand observed bands at 3050-3090 cm^{-1} and 2953-2935 cm^{-1} in the spectra of both Schiff bases and Co (II) and Cu (II) complexes confirm OH group and aliphatic sp^3 C-H vibrations, respectively. The broad peak at 3600-3200cm^{-1} and 3421-3176 cm^{-1} for Co (II) and Cu (II) complexes, respectively, confirms a significant shift for vibrations of an OH group. This peak reveal that the oxygen atom containing the OH group does not participate in the bonding. Strong bands appear at 1585 cm^{-1} in the spectra of free ligands, which confirms imine *υ* (C=N) stretching vibration. The magnetic moment reveals that Co (II) complexes of high spin and Cu (II) complexes should have a value of 3.88 BM and 1.73 BM,

respectively. The magnetic moment's results reveal that the Co (II) complex has a high spin with three unpaired electrons with μ of 4.83BM, while the Cu (II) complex has a low spin with one unpaired electron with μ of 1.69 BM.

Zafar *et al*. (2015) prepared Schiff base complexes of Fe (II), CO (II), Cu (II) and Zn (II) from Schiff base obtained from 2-acetylpyrrole and 1,3-diaminopropane. The complexes were characterized using various analytical techniques such as elemental analyses, NMR (^{1} H and ^{13}C), IR, electronic spectra magnetic susceptibility, and molar conductance measurement.

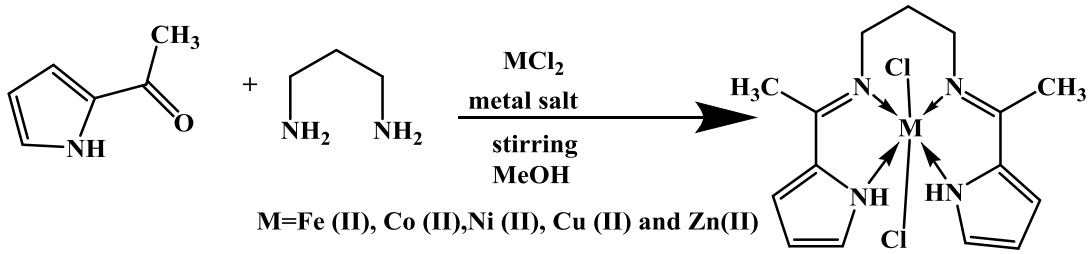

Scheme 10: Synthesis of Schiff base complexes of Fe (II), Co (II), Cu (II) and Zn (II)

The colours of complexes for Fe (II), Co (II), Ni (II), Cu (II), and Zn (II) complexes were brown, light green, pink, dark green and off-white. The IR spectra for all complexes showed a medium intensity band in the regions 1500-1530 $cm^{-1,}$ which were assigned to be coordinated via imine υ(C=N) stretching vibration. Another band also appeared in the 3210-3220 cm-1 region, which was designated to be coordinated through the N-H stretching vibration of the pyrrole ring. Weak absorption appeared in the region 2810-2815 cm^{-1} and was assigned to be CH_3 stretching vibration. The bands shown to appear in the regions 2910–2920 cm^{-1} and 1440–1465 cm^{-1} in all complexes may be because of υ(C-H) and υ(C-H), respectively.

^{1}H NMR spectra for the Zn (II) complex display a sharp signal at δ 2.37 ppm, which was assigned to CH_3. Also, another chemical shift appeared at the region of δ 1.93-1.99 ppm, which was assigned to be (N-CH_2-C) of 1,3-diaminopropane moiety. A multiplet peak was shown in the range δ 5.025-5.351ppm, attributed to pyrrole protons. ^{13}C NMR spectra of Zn (II) complex showed signals of C=N, CH_3, CH_2, CH at δ 170.10, 30.21, 60.20 and 70.19 ppm in that order. At the same time, pyrrole ring carbon showed a

multiple signal at 108.1, 113.0, 127.1 and 125.80 ppm. The molar conductivity measurements of Fe (II), Co (II), Ni (II) and Cu (II) complexes were in the range 20.20-27.5 $ohm^{-1}cm^2mol^{-1}$.

The electronic spectrum of the Fe (II) complex showed weak intensity at 18200cm^{-1}, which was assigned to be $^5T_{2g} \rightarrow {}^5E_g$ transitions in an octahedral geometry in the Fe (II) ion. For Co (II), electronic spectra display two bands at 17400cm^{-1} and 19100cm^{-1}, which were assigned to be $^4T_{1g}$ (F)$\rightarrow {}^4T_{1g}$(P) and $^4T_{1g}$(F) $\rightarrow {}^4A_{2g}$ transitions, respectively, which corresponds to an octahedral geometry complex in Co (II) ion. Furthermore, the Ni (II) complex shows two bands at 21800cm^{-1} and 20200cm^{-1}, which corresponds to $^3A_{2g}$(F) $\rightarrow {}^3T_{1g}$(P) transitions, respectively, in the octahedral geometry of the Co (II) ion. Finally, Cu (II) exhibited a wide band at 19200cm^{-1}, which had a shoulder at 1600cm^{-1} assigned to be $^2B_{1g} \rightarrow {}^2E_{1g}$ and $^2B_{1g} \rightarrow {}^2B_{2g}$ transitions respectively, corresponding to a distorted octahedral geometry of Cu (II) ion.

2.5 Application of Schiff Base and their Complexes

Schiff bases and their metal complexes are widely used in various industries and applications, including food, agrochemicals, dyes, analytical chemistry, catalysis, energy storage, environmental, chemo sensing, bio-sensing, nanotechnology, and biomedical applications.

2.5.1 Catalysis

Schiff base metal complexes promote catalytic activity in homogenous and heterogeneous reactions (Mondal & Mistri, 2023). The type of ligand, coordination sites and central metal ion usually determine the catalytic activity of a compound (Zaera, 2022). Different reactions, such as polymerization, ring-opening polymerization, oxidation, epoxidation, allylic alkylation, reduction of ketones, hydrazination of acetophenones, Michael addition reaction, decomposition of hydrogen peroxide, annulation reaction, Heck reaction, carbonylation reaction, the Diels-Alder reaction, have been employed to investigate the catalytic activity of Schiff base metal complexes (Alshaheri *et al.,* 2017). Because of their straightforward synthesis and heat stability, Schiff base ligands have great potential for usage as metal complexes in

catalysis. The sort and structure of ligands employed in Schiff base complexes significantly impact their catalytic activity (Gupta & Sutar, 2008).

2.5.2 Dye industry

Many Schiff bases and complexes, which have been synthesized, studied, and used as mordants, are used in the dyeing process (Abuamer *et al*., 2014). Transition metal complexes have been generated from various Schiff bases and used as a dye to create a range of transition metal complexes, including iron (III), nickel (II), cobalt (II), and copper (II) complexes. It is known that many azomethine linkages containing azo dyes are generated by aldehyde groups that include azo dyes as a result of condensation with primer amines (Singha *et al*., 2019; Kazemnejadi *et al*., 2017). The textile industry uses these dyes to colour a range of textiles. Azo dyes with the amine group are highly valued in photochemistry, even beyond the textile industry (Bafana *et al*., 2011).

2.5.3 Biomedical applications

The biomedical pharmaceutical industries use Schiff bases and their metal complexes in various applications, including bioprinting), tissue regeneration (Xu *et al*., 2019), antibacterial (El-Gammal *et al*., 2021), antifungal (Wei *et al*., 2021), antimalarial, anticancer (Daravath *et al*., 2022), antiviral, anti-inflammatory (Hamid, & Salih, 2022), antioxidant (Ali *et al*., 2022) and antileukaemia (Iraji *et al*., 2022). The azomethine nitrogen found in Schiff bases functions as a binding site in biological systems, allowing metal ions to bind to various biomolecules for antimicrobial activity, including proteins and amino acids. The Schiff bases in our bodies catalyzed many metabolic processes by activating enzymes against specific bacteria. Numerous investigations have been carried out to enhance the bio-functions of Schiff bases and their metal complexes. Schiff bases can combat viruses, bacteria, fungi, cancer, and ulcers depending on which transition metal ions they contain (de Fátim *et al*., 2018).

2.5.3.1 Chemistry of 2-hydroxy-4-methoxybenzophenone

Previous reported publication shows that 2-hydroxy-4-methoxybenzophenone moiety has remarkable biological and pharmaceutical properties (Marinov *et al*., 2023). Substitution of 2-hydroxy-4-methoxybenzophenone at position 4 shows better antimicrobial activity than substitution at any other position. This was because OCH_3

contained 2-hydroxy-4-methoxybenzophenone in an electron-donating group. It increases electron density at the ortho and para position; hence, 2-hydroxy-4-methoxybenzophenone shows meta-position electrophilic attack is comparatively electron poorer than ortho/para (El-Asmy & Al-Hazmi, 2009).

Sujarani and Ramu. (2013) synthesized bidentate Schiff base and their complexes of Cu (II), Co (II), Mn (II), and Ni (II) from 2,2-diphenyl ethanamine and 2-hydroxy-4-methoxybenzophenone. The free ligands and their complexes were screened for antibacterial activity against the gram-positive bacterium *Staphylococcus aureus* and gram-negative bacterium *E. coli.* Additionally, the study examined DNA interaction, showing that metal complexes had a high binding content. This finding may be explained by the extra oxygen atoms in the ligand skeleton, which validates a groove binding with CT-DNA.

Hemalatha *et al*. (2020) reported novel hetero complexes of Mn (II), Co (II), Cu (II) and (E)-2-((2-hydroxy-4-methoxyphenyl)(phenyl)methyleneamino)benzoic acid; derived from 2-hydroxy-4-methoxybenzophenone and 2-aminobenzoic acid and bidentate N_2 type 1,10-phenanthroline ligands. The novel Schiff base and its metal complexes were determined for antimicrobial activities against two gram-positive *Staphylococcus saphyphiticus and Staphylococcus aureus* and gram-negative bacterial strains *Escherichia coli and Pseudomonas aeruginosa,* respectively with Muller Hinton agar nutrient and the fungal strains namely *Aspergillus niger*, *Candida albicans* and *Enterobacter species* using modified well diffusion technique in potato dextrose agar (PDA) medium. The results of antibacterial and antifungal activities showed that metal complexes had higher antibacterial activity than their corresponding free Schiff base.

2.6 Bacteria Resistance to Antibacterial Agent

Antibacterial agents inhibit microorganism growth and survival without severe toxicity to the host. The life-threatening infectious diseases caused by multidrug-resistant bacteria have increased daily worldwide (Sousa *et al*., 2021). The spread of antibiotic resistance has become a significant problem for managing infectious diseases. However, resistance was reported for at least one bacterial pathogen for most antibacterial agents in clinical practice (Urban-Chmiel *et al*., 2022). Resistance to

antibiotics is an important and timely problem of contemporary medicine. The rapid evolution of resistant bacteria calls for new preventive measures to slow down this process, and longer-term progress cannot be achieved without a good understanding of the mechanisms through which drug resistance is acquired and spreads in microbial populations (Waclaw, 2016).

Bacterial evolution toward drug resistance, particularly multidrug resistance, is inevitable since it is a specific manifestation of the inexorable evolution of bacteria as a whole (Pang *et al*., 2020). Delaying the appearance and subsequent spread of resistant bacteria or resistance genes is the only way to cope with this predicament. Bacterial mutations in housekeeping structural or regulatory genes can cause resistance to antimicrobial medicines (Osterman *et al*., 2020). Bacteria adopt various successful tactics to counteract the effects of antibiotics, frequently leaving no other alternatives for treating infectious diseases they cause. Bacteria use physiological and biochemical pathways to build tolerance or resistance (Kohanski *et al*., 2010).

2.6.1 Classes of Antibacterial Drugs

Tetracycline, developed in the 1940s, is a class of antibiotics that inhibit protein synthesis by blocking aminoacyl-tRNA from attaching to the ribosomal acceptor (A) site. Tetracyclines are broad-spectrum antibiotics with activity against gram-positive and gram-negative bacteria atypical organisms such as chlamydia, mycoplasmas, rickettsaiae and protozoan parasites. These medicines are widely used to treat human illnesses because of their excellent antibacterial capabilities and lack of substantial unfavourable side effects (Chopra *et al*., 2001). Tetracycline antibiotics that are commonly used clinically include 7-chlorotetracycline, 5-hdrotetracycline, 2-N-pydrinmethyltetracycline, 2-hydromethyltetracycline, 6-Deoxy-5-hydrotetracyline and minocycline (Ahmad *et al*., 2021). Figure 3 below illustrates the structures of tetracycline.

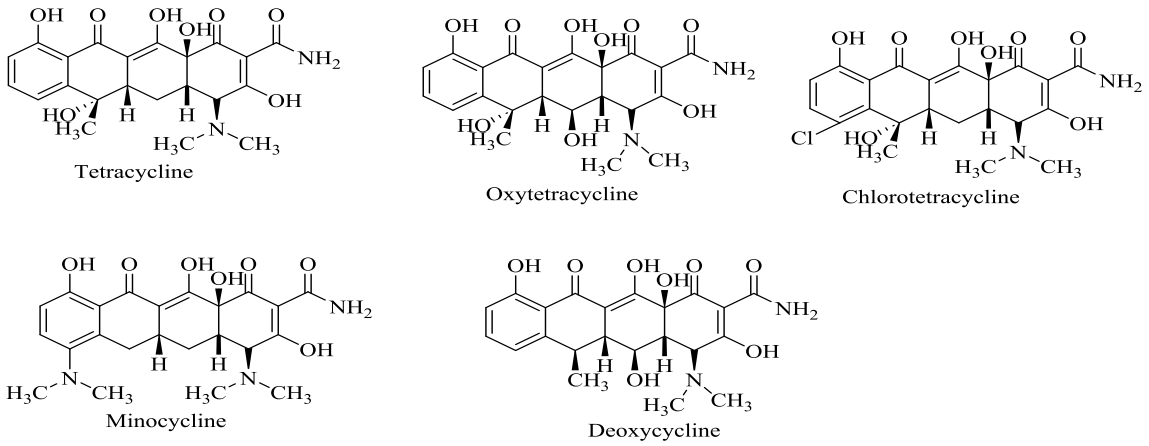

Figure 3: Structures of various examples of tetracycline

The quinolone class of antibiotics inhibits bacterial DNA synthesis by interrupting bacterial topoisomerase type II and decreasing the catalytic activity of DNA gyrase and topoisomerase IV (Collins & Osheroff, 2024). These two essential bacterial enzymes regulate the chromosomal supercoiling required for DNA synthesis. Quinolone resistance has become a significant issue among many developing resistant microorganisms. Bacterial mutations against quinolones are frequently found at target enzyme binding sites in DNA gyrase and topoisomerase IV. Furthermore, resistance to this class of antibiotics can be developed through the horizontal transfer of a resistant plasmid from other sources in the environment, resulting in the rapid spread of resistance (Hooper & Jacoby, 2015). Quinolone antibiotics used in clinical practice include nalidixic acid, ciprofloxacin, levofloxacin, and norfloxacin (Oliphant & Green, 2002). Figure 4 below illustrates various examples of structures of quinolone.

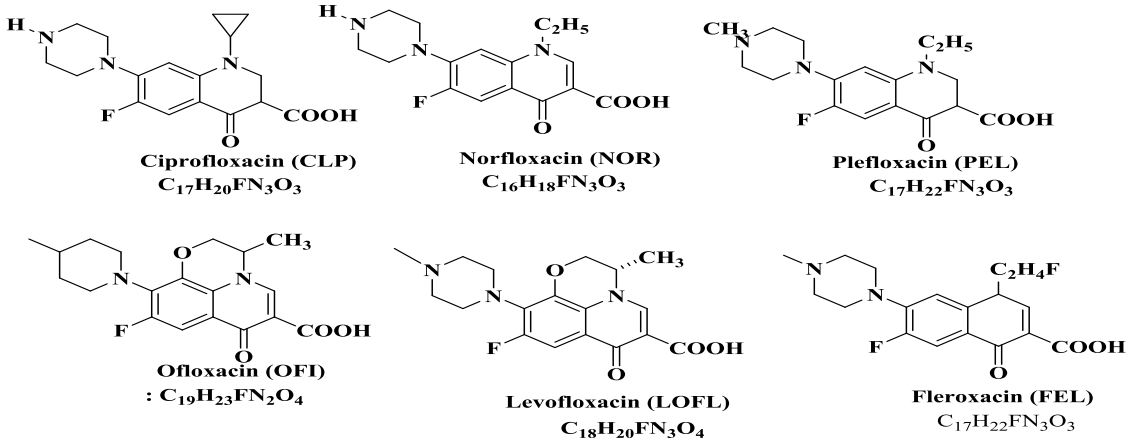

Figure 4: Structures of various examples of quinolone

Macrolide antibiotics are protein synthesis inhibitors that act by targeting the bacterial ribosome. A macrocyclic lactone ring with one or more deoxy sugars attached is the common structural element of macrolide antibiotics. The reversible binding of the macrolide antibiotics to the 50S ribosomal subunits of susceptible microorganisms prevents the synthesis of bacterial proteins. They attach to the nascent peptide exit tunnel and partially occlude it. As a result, macrolides have been viewed as 'tunnel plugs' that block the creation of every protein (Schroeder & Stephens, 2016). Recent research shows that macrolides selectively impede the translation of a subset of cellular proteins. Their activity depends on the developing protein sequence and the antibiotic structure. As a result, macrolides appear as translational regulators rather than worldwide inhibitors of protein synthesis. The context-specific effect of macrolides serves as the foundation for regulating the expression of resistance genes (Vázquez-Laslop & Mankin, 2018). Erythromycin is the model macrolide; other therapeutically significant macrolides include clarithromycin and azithromycin (Tenson *et al*., 2003).

Aminoglycoside antibiotics work by inhibiting protein synthesis, and they are used to treat illnesses primarily caused by aerobic Gram-negative bacteria (Trylska & Kulik, 2016). They function by attaching to the bacterial 30s ribosomal subunit, which results in the misreading of tRNA and prevents the bacterium from synthesizing proteins necessary for growth. Aminoglycoside antibiotics commonly used clinically include streptomycin, amikacin, neomycin and gentamicin (Dowling, 2013). Figure 5 below illustrates the of structures of various examples of aminoglycoside.

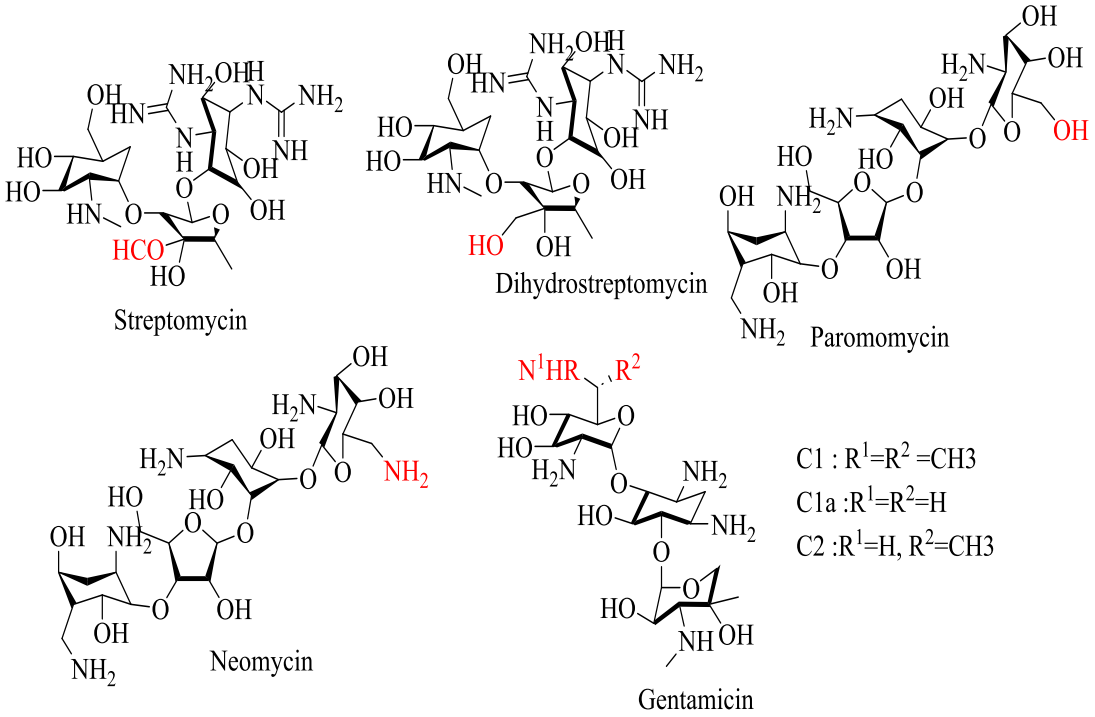

Figure 5: Structures of various examples of aminoglycoside

Oxazolidinones, a new chemical class of synthetic antibacterial drugs, offer a distinct method for combating bacterial protein synthesis. Linezolid, the first oxazolidinone licensed for therapeutic use, exhibits in-vitro activity (usually bacteriostatic) against a wide range of significant resistant bacteria, including methicillin-resistant Staphylococcus aureus, vancomycin-resistant enterococci, and penicillin-resistant *Streptococcus pneumoniae* (Diekema *et al*., 2001). Linezolid is a parenteral drug with near-complete oral bioavailability and favorable pharmacokinetic and toxic effect profiles. Clinical trials have confirmed linezolid's activity in treating pneumonia, skin and soft-tissue infections, and vancomycin-resistant enterococci infections. Linezolid shows potential as an alternative to glycopeptides and streptogramins in treating severe infections caused by resistant gram-positive pathogens (Yuan *et al*., 2023).

Cephalosporin antibiotics are categorized according to their generation. Cephalosporins of the first generation include cefalexin, cefaclor, and cefadroxil. Cefoxitin, cefaclor, and cefuroxime are cephalosporins from the second generation. Cefotaxime, cefodizime, ceftriaxone, and cefixime are examples of third-generation cephalosporins, whereas cefepime, cefozapran, and cefquinome are examples of fourth-generation cephalosporins (Harrison & Bratcher, 2008). Impenem, meropenem, ertapenem, and

doripenem are examples of carbapenem antibiotics used in clinical practice (Mehta & Sharma, 2016). Aztreonam is the only monobactam antibiotic available commercially. Chloramphenicol hinders protein synthesis by attaching to the 50S subunit of the 70S ribosome, resulting in a static action against the most susceptible bacteria (Stratton, 2002). Although chloramphenicol is one of the most effective antibiotics against anaerobic bacteria, such as Bacteroides fragilis, clindamycin, metronidazole, and imipenem are more commonly used to treat infections caused by these bacteria (Dubreuil, 2024). Chloramphenicol is effective against many bacteria, including spirochetes, rickettsiae, chlamydiae, and mycoplasmas. Most gram-positive and gram-negative aerobic bacteria are inhibited by chloramphenicol, although other therapeutic agents are available against most pathogens (Balbi, 2004).

β-Lactam antibiotics are one of the world's most crucial antibacterial agent medication classes. The development and commercialization of the first β-lactam antibiotic (Penicillin G) is regarded as a watershed moment in modern chemotherapy (Lima *et al*., 2020). The bactericidal medications known as β-lactam antibiotics are structurally related and include the β-lactam ring in their chemical structure (Kim *et al*., 2023). Penicillins, cephalosporins, carbapenems, penems (also known as thiopenems), and monobactams are the categories they fall into. This categorization is based on the chemical composition of the ring fused to the pharmacophore unit of the -lactam, producing a noncoplanar bicyclic scaffold. The penam framework is created when the β-lactam system in penicillin antibiotics is joined to a five-membered ring that contains sulphur (1). A six-membered sulphur-containing ring is bonded to the β -lactam to create the cephem scaffold in cephalosporins (2). The lactam unit is fused to cyclopentene and 2,3-dihydrothiophene rings in carbapenem (5) and penem (4). Antibiotics called monobactam (3) don't have any rings fused to the β-lactam system (Lima *et al*., 2020). β. Figure 6 below illustrates the structures of the β-lactam ring.

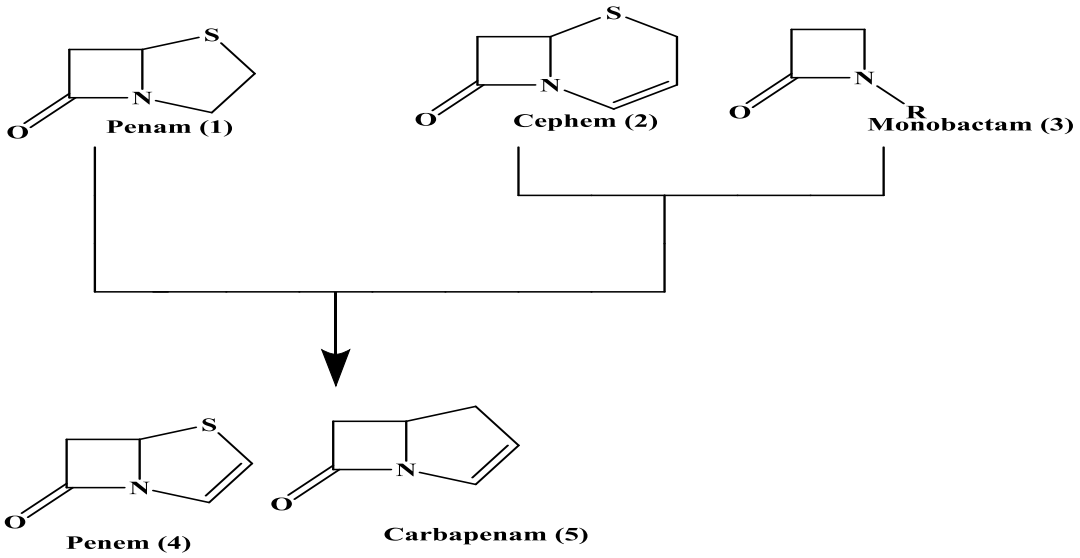

Figure 6: Structures of β-lactam ring.

In bacterial cells, sulfonamides act as competitive inhibitors of the dihydropteroate synthase (DHPS), an enzyme involved in folate synthesis (Bourne, 2014). These antibacterial agents are bacteriostatic; they inhibit the growth and multiplication of the bacteria but do not kill them. Examples of sulfonamide antibiotics used in clinical settings include sulfadiazine, sulfamethoxazole, trimethoprim, and co-trimoxazole (Dorn *et al*., 2018).

2.6.2 Multidrug-Resistant Bacterial Pathogens

Pathogenic bacteria are now posing a severe threat to worldwide public health due to their development of resistance to various antimicrobial drugs. Rising antibiotic resistance poses a danger to the enormous medical gains made possible by antibiotics over the past 70 years, and drug-resistant bacterial infections significantly increase patient mortality and morbidity (Worthington *et al*.,2013). Multidrug-resistant pathogenic bacteria that are now of clinical concern include *Staphylococcus aureus, Proteus mirabilis, Vibrio cholerae, Shigella ssp., Klebsiella pneumoniae,* pathogenic *Escherichia coli strains, Salmonella spp.,* and *Pseudomonas putida*. The following section briefly overviews the bacterial pathogen's resistant trends.

Staphylococcus aureus is a Gram-positive bacterium that forms irregular grape-like clusters. It is non-motile, non-sporing, and catalases positive. It develops quickly and

abundantly in aerobic circumstances. Its genomic DNA has a G + C composition of 36%. Lysine is the diamino acid in the cell wall peptidoglycan, and the cross-bridge is made from five glycine residues. It usually forms glistering, smooth, whole, elevated, translucent, and often golden colonies (Plata *et al*., 2009). Staphylococcus aureus is a pathogen that causes severe infections such as pneumonia, endocarditis, and bacteraemia once in the host's bloodstream (Chang *et al*., 2020).

Proteus mirabilis, a Gram-negative rod-shaped bacterium known for its swarming motility and urease activity, is a common cause of polymicrobial catheter-associated urinary tract infections (CAUTIs). Urolithiasis, the formation of bladder or kidney stones due to urease-catalyzed urea hydrolysis, can accompany these illnesses (Armbruster *et al*., 2018). *Proteus mirabilis* is a member of the class Gammaproteobacteria and the order Enterobacteriales, family Enterobacteriaceae. It is also a member of the class Gammaproteobacteria. The order Enterobacteriales, however, has recently been reclassified according to a group's reconstruction of a phylogenetic tree based on shared core proteins, ribosomal proteins, and four multilocus sequence analysis proteins, with Proteus being included in a new Morganellaceae family (Adeolu *et al*., 2016).

Increased reports of *proteus mirabilis* resistance to ciprofloxacin due to the formation of the extended spectrum-lactamases (ESBLS) have been made (Sohn *et al*., 2011). It has been observed that fluoroquinolone resistance is sharply increasing (Saito *et al*., 2007). There have also been reports of proteus mirabilis strains being resistant to cefotaxime, nitrofurantoin, ampicillin, co-trimoxazole, gentamicin, piperacillin, nalidixic acid, and aztreonam, among other antibiotics. (Luzzaro *et al*., 2001).

Vibrio cholerae, a Gram-negative bacterium belonging to the family Proteobacteriaceae's γ-subdivision, is the causative agent of cholera, a deadly diarrheal disease that frequently arises in epidemics. The *Vibro cholerae* genome, which comprises two distinct circular mega-replicons, contains the genetic markers that allow the bacterium to live in water and the human intestine (Faruque *et al.*, 2004). Cholera is a deadly epidemic disease that has killed millions of people and is a significant public health concern around the world (Wai *et al*., 1999). The management of cholera

infections has been significantly hampered in recent years due to reports of an increase in the vibrio cholerae strain's resistance to routinely used antibacterial medications (Vila and Pal., 2010). There have been reports of resistance to antibiotics such as sulfamethoxazole, co-trimoxazole, trimethoprim, chloramphenicol, tetracycline, nalidixic acid, and gentamicin (Rahmani *et al*., 2012; Okoh and Igbinosa, 2010).

Klebsiella pneumoniae is a Gram-negative bacterium with a large accessory genome of plasmids and chromosomal gene loci. *K. pneumoniae* is a common cause of healthcare-associated infections, including pneumonia, urinary tract infections (UTIs), and bloodstream infections. *K. variicola* and *K. quasipneumoniae* are often clinically indistinguishable from opportunistic *K. Pneumoniae* (Martin *et al*., 2018). *Klebsiella* species with the ability to produce extended-spectrum beta-lactamases (ESBL) have increasingly been reported to show resistance against many antibiotics such as aminoglycosides, cephalosporins, fluoroquinolone, tetracyclines and chloramphenicol, and co-trimoxazole (Riwu *et al.,* 2020).

Escherichia coli are Gram-negative and have a rod-shaped bacterium in the Enterobacteriaceae family. The bacterium lives primarily in the lower intestine tracts of warm-blooded animals, including humans, and is frequently released into the environment via faeces or wastewater effluent (Jang *et al*., 2017). The translocation of gut bacteria into other bodily regions and the environmental spread in hospitals and long-term care facilities are the two causes of extraintestinal sickness brought on by *E. coli*. The most common gram-negative bacterium that causes extraintestinal sickness in people is *E. coli,* which can also cause pneumonia, bacteraemia, meningitis, abdominal and pelvic infections, and meningitis (Sora *et al*., 2021). The development of antibiotic resistance has jeopardized the therapeutic management of *E. coli* infections. The most significant mediator of resistance to a wide range of β-lactams in *E. coli* is β-lactamase synthesis. Most Enterobacteriaceae, specifically *E. coli*, produce β-lactamases, a large class of enzymes frequently encoded on plasmids. In Gram-negative bacteria, β-lactamases are an emerging source of multidrug resistance that confers resistance to penicillins and cephalosporins (De Angelis *et* al., 2020).

Pseudomonas aeruginosa is a Gram-negative and rod-shaped faculture anaerobe, usually part of normal flora (Urgancı *et al.*, 2022). *Pseudomonas aeruginosa* is a ubiquitous microorganism that can survive under various environmental conditions. It not only causes disease in plants and animals but also in humans, causing serious infections in immunocompromised patients with cancer and patients suffering from severe burns and cystic fibrosis (CF) (Crone *et al*., 2020; Kovács & Jakab, 2020). Many *Pseudomonades aeruginosa* strains show an intrinsic reduced susceptibility to several antibacterial agents and a propensity to develop resistance during therapy, especially in carbapenem-resistant (chiefly imipenem) strains (Somily *et al*., 2012).

2.6.3 Schiff Base Ligands and their Metal Complexes as Antibacterial Agents

Schiff base ligands and their metal complexes have been found to show antibacterial activities against both gram-negative and gram-positive bacteria (Hasan *et al*., 2024). In recent decades, many Schiff base ligands and their metal complexes have been determined for antimicrobial activities against bacteria strains and fungi (Ibrahim & Abdalhadi, 2021). Due to their biological activities, the transition metal complexes obtained from Schiff base ligands are one the most researched areas (Sinicropi *et al*., 2022). According to earlier research, certain medications displayed more fantastic action when supplied as metal complexes than organic substances (Frei, 2020).

The Schiff base ligands were synthesized and evaluated for antibacterial activities against two gram-positive bacteria, *Staphylococcus aureus Staphylococcus epidermidis* and two gram-negative bacteria, *Escherichia coli*, *Pseudomonas aeruginosa,* using ciprofloxacin as standard drug. Figure 7 illustrates Schiff base ligands derived from benzamide derivatives.

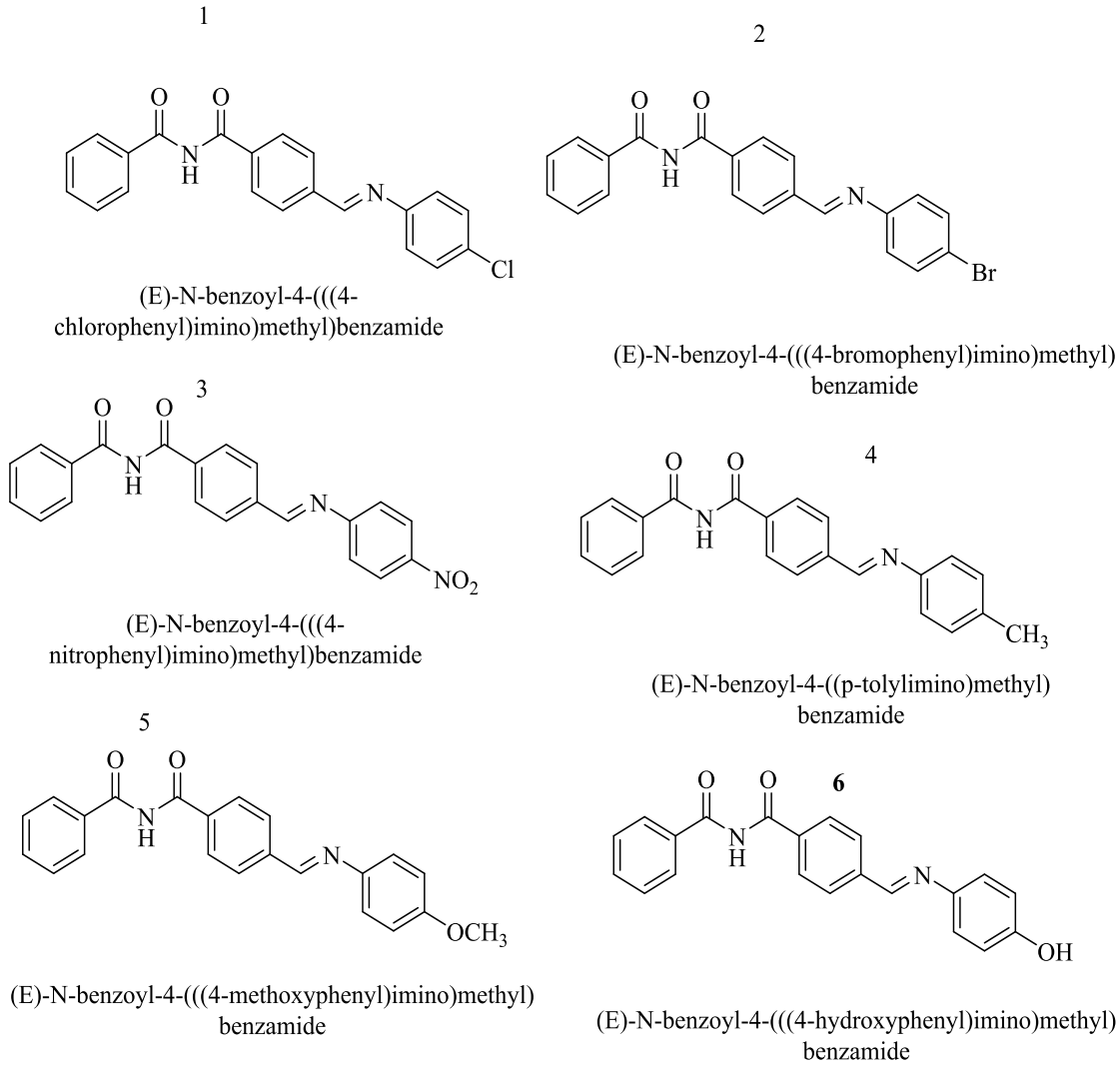

Figure 7: Schiff base ligands derived from benzamide derivatives

The synthesized Schiff base ligands show antibacterial activities against tested bacteria strains with a range of MIC values of 7.4 -11.8 µg/mL for *S. aureus*, 8.6-12.3 µg/mL for *S. epidermis*, 9.7-13.6µg/ml for *E. coli* and 6.9-13.2 µg/mL for *P. aeruginosa.* Schiff base containing chloro substituent displays potent antimicrobial agents with MICs of 7.4, 8.6, 10.4 and 6.9 µg/mL against *S. aureus*, *S. epidermidis*, *E. coli* and *P. aeruginosa*. All the synthesized Schiff bases had higher antibacterial activities than the standard drug ciprofloxin. Incorporation of electron withdrawing and electron donating groups such as -Cl, Br, NO_2, CH_3, OCH_3 and OH as substituents onto phenyl rings of Schiff base proved to be essential in enhancing the antibacterial activities of the result compounds. The contribution of these substituent groups helps improve bioactive compounds' activities due to their ability to amend fundamental physiochemical

properties such as lipophilicity, binding interactions and hydrophilicity (Naganagowda *et al*., 2014).

Azo Schiff base ligands and their metal complexes were synthesized. Chloramphenicol was used as a standard reference drug, and its antibacterial activities were determined against gram-positive *(S. aureus* and *B. subtilis*) and gram-negative bacteria (*E. coli* and *Salmonella typhi*). Scheme 11 illustrates azo Schiff base ligand synthesis and their metal (II) complexes.

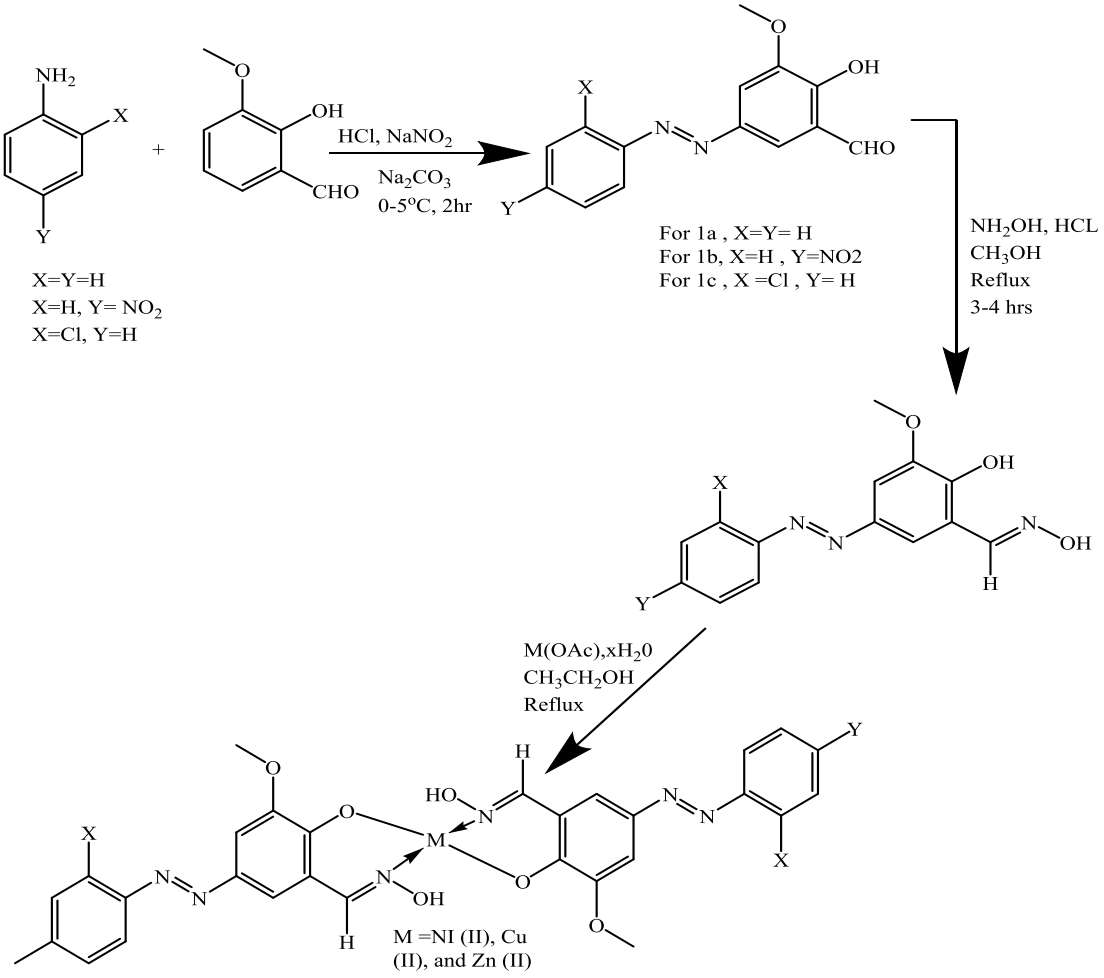

Scheme 11: Synthesis of azo Schiff base ligand and their metal (II) complexes

The minimum inhibitory concentration results revealed that free Azo Schiff base ligands and their metal complexes had better antibacterial activities than chloramphenicol. *S. aureus* shows 3.90 µg/mL, followed by *B. subtilis* with 7.80 µg/mL, *E. coli* with 62.5 µg/mL and S. typhi with 125 µg /mL. Metal complexes of Zn

(II) complexes display better antibacterial activities against all isolated bacteria than chloramphenicol. In comparison, metal complexes of Ni (II) and Cu (II) complexes show lower antibacterial activities in all isolated bacteria (Kasare *et al*., 2019).

2.7 Structure-Activity Relationship of Antimicrobial Compounds

A strategy intended to establish the relationship between the chemical structure and the biological activity of the researched system is known as the "structure-activity relationship." The structure-activity relationship (SAR) has been used as a critical tool to link the activity of these compounds with their molecular structures. SAR analysis helps identify the functional groups that are important for the activity of a given compound and makes it possible to determine the chemical groups on the substance that trigger an organism's biological target (Silverman *et al.,* 2014).

SAR analysis makes it possible to pinpoint the functional groups on the compound that cause the organism to behave in a way that is intended biologically. This makes it possible to alter the chemical structure of a bioactive substance to alter its action or potency. To add new functional groups to a product and evaluate the change's biological impact, medicinal chemists employ a method called chemical synthesis. A substance's biological activity is influenced by a variety of factors, including its affinity for the target site, ability to survive in the application medium, ability to survive inside a biological system, transport properties, target organism condition, and distribution of electronic charge density (Zhao *et al.,* 2020).

The electronic property of the compounds has close relations with biological activity. If the drug's charge density distribution is just suited to the specific receptor, the interaction between the drug and the receptor would increase (Persch *et al*., 2015). Then, the drug and receptor then form complexes and increase the activity. The antibacterial structure-activity relationship of Schiff base derivatives shows that the degree of delocalization of the unshared electron pairs of a sulphur atom is more significant than that of an oxygen atom. Hence, compounds' electronic charge density distribution differs (Nath *et al*., 2022). This section looks at the SAR studies of a few compounds that have been synthesized and evaluated activities in the recent past.

Fonkui *et al*. (2019) synthesized a series of benzimidazole Schiff base derivatives (Scheme 11) by varying the substituent (R) and replacing X on the phenyl ring. The synthesized benzimidazole Schiff base derivatives were screened for antimicrobial activities against gram-positive bacteria (*Bacillus cereus*; *Bacillus subtilis*, *Enterococcus faecalis*, *Mycobacterium smegmatis*, Staphylococcus *epidermidis*, *Staphylococcus aureus*) and gram-negative bacteria (*Enterobacter cloacae*; EC, *Escherichia coli*, *Enterobacter aerogenes*, *Proteus vulgaris*, *Klebsiella oxytoca*, *Klebsiella* pneumonia, *Proteus mirabilis*; *Pseudomonas aeruginosa*). Antimicrobial studies were performed using the broth microdilution method using streptomycin and nalidixic acid as standard reference drugs.

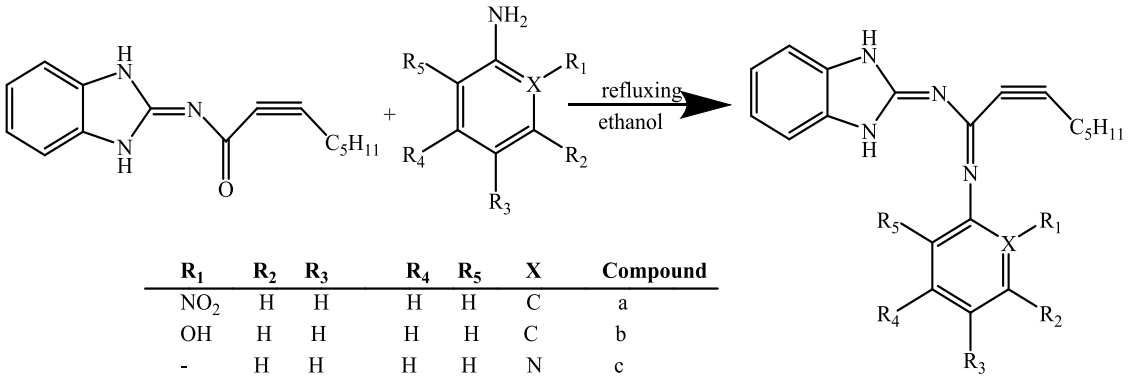

R_1	R_2	R_3	R_4	R_5	X	Compound
NO_2	H	H	H	H	C	a
OH	H	H	H	H	C	b
-	H	H	H	H	N	c
H	H	COOH	H	H	C	d
OH	H	SO_3H	H	H	C	e
OCF_3	H	H	H	H	C	f

Scheme 12: Synthesis of benzimidazole Schiff base derivatives

The synthesized compounds were demonstrated by varying degrees of activity against different bacteria strains. Compounds that demonstrated significant activities against *Enterococcus faecalis, Bacillus cereus, Enterobacter aerogenes, Proteus mirabilis* and *Pseudomonas aeruginosa* included **a (**MIC= 250µg/mL), both **b** and **c** (MIC = 125µg/mL) respectively. Compounds that display better activities against *Bacillus subtilis* included **a**, **c**, **d**, **e**, and **f** (MICs = 125µg/mL) each and **b** (MIC = 62.5µg/mL). Compounds **d** and **e** were also active against *Enterococcus faecalis, S. aureus, Bacillus cereus*, *Enterobacter cloacae*, *Enterobacter aerogenes* and *Proteus mirabilis* with MICs= 250µg/mL. The synthesized compounds also demonstrated antifungal activities. They were active against *F. verticillioides*, including a, b, c, d, e and f (MIC = 62.5µg/ML). Compounds **a, b, e** and **f** were against *Spergillus carbonarius*, *Aspergillus favus*, *A. niger* and *F. proliferatum* with MIC values of 32.5 µg/mL each.

Based on SAR studies, the results revealed that the antimicrobial activities of the synthesized benzimidazole Schiff base derivatives were significantly influenced by the substituent groups' variation on the phenyl ring. The incorporation of the electron-withdrawing indicated significant improvement in antimicrobial activities. Compounds **a** and **d,** which had NO_2 and COOH groups on the phenyl ring, respectively, showed higher antimicrobial activities against all the evaluated microbial strains. It suggests that for such bioactive compounds, an optimum electron density (for example, the presence of the electron-withdrawing groups) is favourable to achieving substantial antimicrobial activities. Electron withdrawing groups reduce electron density at the *ortho* and *para* positions; thus, they will have a bearing on the electronic properties of the resultant compounds. Also, the incorporation of the electron-donating groups showed higher antimicrobial activities. Compounds **e** and **f,** possessing OH and OCF_3 groups on the phenyl ring, show better antimicrobial activities against bacteria strains tested. Compound **c** shows a broad-spectrum activity due to a heterocyclic ring of the amine. The results obtained from the above study revealed that both electron-withdrawing and donating groups are helpful substituents in improving the activities of antibacterial compounds.

The use of transitional metal ions improves the antimicrobial activities of a compound through chelation, which has also been explored in various studies in recent decades (Nasiri Sovari & Zobi, 2020). In many cases, better antimicrobial activities have been observed for transitional Schiff base complexes than their corresponding Schiff base ligands. Overtones' concept of cell permeability and Tweedy chelation have been used to explain such observation. Overtone's cell permeability theory explains the enhanced action of metal chelates (Sujarani & Ramu, 2013). One key element that regulates the antibacterial action is liposoluble. The polarity of the ligand orbital and the partial sharing of the metal ion's positive charge with donor groups during chelation lead to an increase in the lipophilicity of the complex and the delocalization of π-electrons throughout the whole chelates ring. This elevated lipophilicity facilitates the complexes' entry into lipid membranes and restricts the metal-binding sites on microorganism enzymes (Mounika *et al.,* 2010; Jose *et al.,* 2018).

Numerous transitional metal complexes of bioactive Schiff base ligands have been evaluated for antimicrobial activities. Sunitha *et al.* (2012) synthesized the Schiff base ligand, 2-[2]-{[2-1-Benzimidazol-2yl}phenyl]imino}methyl}-6ethoxyphenol (figure 8) and its Ni (II), Co (II), Cu (II), Zn (II), Mn (II) and V (IV) complexes. The Schiff base ligand and their metal complexes were investigated for antimicrobial activity against pathogenic bacteria strains such as *Escherichia coli, Staphylococcus aureus, Bacillus subtilis* and *Pseudomonas fluorescence* using diffusion. Streptomycin was used as a standard reference, while DMSO was used as a solvent control.

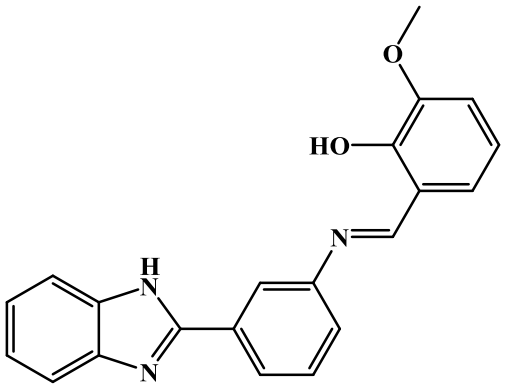

Figure 8: Synthesized Schiff base of 2-[2]-{[2-1-Benzimidazol-2yl}phenyl]imino}methyl}-6 ethoxy phenol

The study revealed that metal complexes possess higher antibacterial activities than the parent ligand. Zinc (II) complexes was active against *Escherischia coli* (MIC = 17 mm), *Staphylococcus aureus* (MIC= 20mm), *Bacillus subtilis* (MIC= 17 mm) and *Pseudomonas fluorescence* (MIC = 18 mm). Ni (II) complexes displayed a moderated activity range of 8-11mm against all bacteria strains. Mn (II) and Ni (II) complexes demonstrated low activity against *P. fluorescence* and *E. Coli* with MIC values of 8mm and 5mm, respectively. The order of antimicrobial of the synthesized Schiff base and their metal complexes were as follows: Zn (II) >Cu (II)> Co (II) >Vo (IV) >Ni (II) >Mn (II)> Schiff base ligand. This study underscores the importance of transitional metal ions in modifying synthesized compounds' antibacterial activities. The study also displayed that metal complexes are bioactive compounds with better antibacterial properties. Furthermore, the study revealed that the Zn (II) complex exhibited better antibacterial activities among the other five metal complexes studied.

The following observations are made from the studies reviewed above: Substitute groups attached to the phenyl rings of synthesized compounds tested for antimicrobial activities have a pronounced influence on their bioactivity. By altering the physicochemical characteristics linked to bioactivity, appropriate substituents can be employed to fine-tune the activities of antimicrobial compounds. Additionally, chelation can help modify the antibacterial activity of bioactive compounds and metal ions. The antibacterial activity of bioactive Schiff base ligands' Schiff base metal complexes has frequently been reported to be higher than that of the free ligands in the same combination. As a result, the hunt for new antimicrobial agents must include novel bioactive compounds and their metal complexes.

2.8 Chemistry of Copper

Copper is a transitional metal usually found in the first row of the d-block series. It has the electronic configuration of $1s^2 2s^2 2p^6 3s^2 3p^6 3d^{10} 4s^1$ when in zero oxidation (Fukuzumi *et al.*, 2019). It usually has oxidation states of +1 and +2. These two oxidations are relatively stable. The electron configuration of copper (I) is $1s^2 2s^2 2p^6 3s^2 3p^6 3d^{10}$. This means that the d orbitals of copper are fully filled. Copper (II) has the electronic configuration of $1s^2 2s^2 2p^6 3s^2 3p^6 3d^9$. This implies that the partially filled Copper (II) ion d-orbitals and the ligand field (d-d) transition are expected. With the d^9 electronic configuration, the Cu (II) ion has the spectroscopic ground state term symbol of ^2D. The ^2D is usually split in an octahedral field into ^2Eg and $^2T_{2g}$ (Reddy *et al.*, 2012). Therefore, the d-d electronic configuration transition $\{^2T_{2g} \leftarrow {}^2E_g\}$ is possible expected copper (II) complexes. Thus, for many of the copper (II) complexes, the energy involved in the transition corresponds to wavelength in the visible region of the electromagnetic spectrum (600-900 nm) and accounts for the green/blue coloration often observed with copper (II) complexes. For the d^9 system in the tetrahedral field, the ^2D orbitals are split into $^2T_2$ and ^2E; thus, the d-d transition is expected for $^2T_{2g} \leftarrow {}^2E_g$ (Solomon & Bell, 2010).

Cu (II) ions with their d^9 configuration in octahedral or tetrahedral environments usually undergo Jahn-Teller distortion (Judd, 1988). Thus, regular octahedral or tetrahedral geometries occur rarely. In the absence of distortion, regular octahedral Cu (II) complexes are expected to have one d-d absorption band corresponding to $^2T_{2g} \leftarrow$

^{2} E_g transitions. However, octahedral complexes of Cu (II) are almost invariably distorted. Due to the Jahn-Teller effect, the ground ^2E_g state usually splits in the lowering of symmetry of the Cu (II) ion. This state splits into $^2B_{1g}$ ($d_{x^2-y^2}$) and $^2A_{1g}$ (d_{z^2}) in tetragonal symmetry. Similarly, the excited $^2T_{2g}$ state splits into $^2B_{2g}$ (d_{xy}) and 2Eg (d_{xz}, d_{yz}) levels. Thus, for six coordinated Cu (II) complexes with D_{2h} symmetry, three spin-allowed ligand field (d-d) transitions are expected in near IR and visible regions (). These bands are resolved by Gaussian analysis and assigned to $^2A_{1g}$←$^2B_{1g}$ (d_{z^2}←$d_{x^2-y^2}$), $^2B_{2g}$←$^2B_{1g}$ (dxy←$d_{x^2-y^2}$) and ^2E_g←$^2B_{1g}$ (d_{xz}, d_{yz}←$d_{x^2-y^2}$) transitions in the order of increasing energy. The sequence of the energy levels depends on the amount of distortion due to the ligand field and the Jahn-Teller effect (Reddy *et al*., 2012).

2.8.1 Toxicity of Copper

Copper is an essential trace mineral that is vitally crucial for physical and mental health. Copper is a potent inhibitor of enzymes. It is needed by the body for many functions, predominantly as a cofactor for several enzymes such as ceruloplasmin, cytochrome oxidase, dopamine β-hydroxylase, superoxide dismutase and tyrosinase. It is present in several haematinics, and its salts are also used therapeutically for their astringent and antiseptic properties. Still, copper salts are sometimes poisonous to the human organ system (Ashish *et al*., 2013).

2.8.2 Biological Application of Copper

Copper is an essential component and catalytic agent of many enzymes and proteins in the body, so it can influence human health through multiple mechanisms (Wei *et al*., 2021). Copper-based metalloenzymes can reactions catalyzed such as electron transfer, dioxygen transport, substrate oxygenation /oxidation coupled to O_2 reduction to H_2O_2 or water and nitrogen oxide reduction (Quist *et al*., 2017). Copper is also one of the metals well known for their oligodynamic action. Oligodynamic action refers to the ability of some metals to have a lethal effect on microorganisms (Varkey, 2010). Some studies have shown that copper and copper-based alloys inhibit several pathogenic bacteria, including *vibrio cholerae*, *pseudomonas aeruginosa*, *staphylococcus aureus* and *Escherichia coli* (Evans & Kavanagh 2021). Copper-based complexes have also demonstrated encouraging antimicrobial activities of various microbial pathogens, including gram-positive bacteria, gram-negative bacteria and fungi (Arendsen *et al.*,

2019; Govind *et al*., 2021). Thus, copper and copper-based compounds are receiving significant attention in the search for new metal antimicrobial agents.

2.9 Antimicrobial Susceptibility Testing Methods

Antimicrobial susceptibility tests (AST) are used to evaluate the efficacy of the potential antimicrobial against different bacterial strains. AST standard test method may be divided into major categories, namely disk diffusion methods and dilutions methods.

2.9.1 Disk Diffusion Method

The disk diffusion method is based on the principle that an antibiotic-impregnated disk, placed on agar previously inoculated with the test bacterium, picks up moisture, and the antibiotic diffuses radially outward through the agar medium, producing an antibiotic concentration gradient. The antibiotic concentration at the edge of the disk is high. It gradually diminishes as the distance from the disk increases to a point where it is no longer inhibitory for the organism, which then grows freely. A clear zone or ring is formed around an antibiotic disk after incubation if the agent inhibits bacterial growth **(**Jorgensen & Turnidge, 2015). The techniques most often used in determining disk diffusion tests are paper disk diffusion and agar well diffusion.

2.9.1.1 Paper disk diffusion test

Agar plates are inoculated with a standard inoculum of the test microorganism for this test. After that, filter paper disks with the tested substance at the correct concentration are deposited on the agar surface. These disks, typically 6mm in diameter, are used in this procedure. Under ideal circumstances, the plates are incubated. The antibacterial agent spreads throughout the agar. If it is effective against the test microbe, the bacterium's development is inhibited, causing a zone of inhibition around the paper disk (Balouiri *et al*., 2016). The diameter of this zone of inhibition is measured in millimetres.

2.9.1.2 Agar well diffusion test

This technique uses a similar strategy to the paper disk diffusion test, inoculating the agar plate surface by evenly dispersing a volume of the microbial inoculum throughout

the surface. The agar well method differs from the disk diffusion approach in that a well with a diameter of 6 to 8 mm is created on the agar medium aseptically using a sterile corn borer, and a volume (20 to 100 ml) of the test antimicrobial agent at a predetermined concentration is then added to the well. Agar plates are then incubated under the proper circumstances. A zone of inhibition forms around the well, as the antimicrobial drug diffuses in the agar media, preventing the bacteria strain from growing. The diameter of the inhibitory zone is usually measured in millimetres (Boyanova *et al*., 2005); Missoun *et al*., 2020).

2.9.2 Dilutions methods

Dilution testing establishes the lowest concentration (in mg/ml) of antimicrobial agent required to inhibit or kill bacteria. This is accomplished by immediately adding two-fold dilutions of the antimicrobial agent to an agar pour, a broth tube, or a micro-broth panel (Lalitha, 2004); Tomar *et al*., 2015). The Minimum Inhibitory Concentration (MIC) is defined as the lowest level that inhibits the observable growth of the organism (Vassallo *et al*., 2018). A gar method and broth dilution are the most often used to evaluate the MIC of antibacterial agents that suppress the microorganisms. These techniques are usually used when quantitative methods are needed for microorganisms with variable growth rates and microaerophilic microorganisms (Chiu *et al*., 2021).

2.9.2.1 Agar dilution test

The agar dilution method creates a series of agar plates with increasing concentrations of the antimicrobial drug to be evaluated, typically in doubling dilutions (i.e., 1, 2, 4, 8, 16, 32 g mL, etc.) (Yalew, 2020). Using a replicator device, 1–5 l of a suspension of the organism to be tested is applied to each plate with varying concentrations of the antimicrobial agent (final inoculum is 5–10^4 CFU/spot). This suspension equals the turbidity of a 0.5 McFarland standard (1–10^8 colony forming units (CFU) mL^{-1}). Thirty distinct bacterial isolates (plus quality control organisms) can be evaluated simultaneously on each agar plate (Stavropoulou *et al.,* 2022).

Even though it is time-consuming to prepare each batch of agar plates for each antimicrobial drug to be tested, the agar dilution approach is frequently less expensive for labs that test a lot of bacterial isolates against a small number of antimicrobial

agents. When determining MICs, agar dilutions are commonly preferred to broth dilution because they yield results faster. The MIC endpoint is defined as the lowest concentration of antibacterial agent that completely inhibits the growth of the pathogenic microorganism under a single compound (López-Malo *et al*., 2020).

2.9.2.2 Broth dilution test

This method entails either broth micro-dilution or macro-dilution test. The procedure involves preparing two-fold dilutions of the antimicrobial agents, for example, 1, 2, 4, 8, 16 and 32 mg/mL in a liquid growth medium dispensed in tubes containing a minimum volume of 2mL (macro-dilution) or with smaller volumes using 96-well micro-titrations plate (micro-dilution) (Balouiri *et al*., 2016). Then, each tube or well is inoculated with a microbial inoculum prepared in the same medium after dilution of standardized microbial suspension adjusted to 0.5 McFarland scale. After thorough mixing, the inoculated tubes or the 96-well micro-titration plate are incubated under suitable conditions depending on the test microorganisms. The MIC is recorded as the lowest concentration of the test compound that completely inhibits the growth of the microorganisms in the tubes or micro-dilutions as detected by the unaided eye (Ferraz *et al*., 2020).

CHAPTER THREE
MATERIALS AND METHODS

3.1 Experimental Sites

Schiff base ligands and their respective copper (II) complexes were synthesized at the Chuka University Chemistry Laboratory. Characterization of new Schiff base ligands and their copper (II) complexes was carried out using various techniques such as Ultraviolet-Visible (UV-Vis) spectroscopy, Fourier Transform Infrared Spectroscopy (FT-IR) and molar conductivity measurements were carried in the same laboratory except for Proton Nuclear Magnetic Resonance (^{1}H NMR) that was done in University of Nairobi. Antibacterial activities of synthesized compounds were determined at Chuka University's Microbiology Laboratory.

3.2 Experimental Design

A complete factorial randomized design with 8x3x4 factors for three bacterial strains was used, where eight synthesized compounds were tested, three replications and four different concentrations were used. Factor A was assigned tested compounds: positive control (Gentamycin and Amoxiclav as standard drugs) and the negative control (DMSO), while factor B was assigned bacteria strains with three different strains. Factor C was the concentration of each test compound, which had four levels. Each experimental unit was done in triplicate, and the average diameter of inhibition zones was obtained. A series of synthesized Schiff ligands and copper (II) complexes dilutions was taken to 4 different concentrations to determine the minimum inhibitory concentration.

3.3 Chemicals and Reagents

Chemicals and solvents of analytical grade were used in the study without further purification. Aniline (98%), 2-hydroxy-4-methoxybenzephenone (98%), 4-dimethylaniline (99.6%), 2,4-dinitroaniline (98%), Mueller Hinton Agar (98%), Nutrient Agar (98%), sodium sulphate (98%), acetone (98%), acetonitrile (98%) and 4-aminobenzoic acid (98%) were purchased from Sigma Aldrich. Dimethyl sulfoxide (99.9%), copper chloride dihydrate (98%), absolute ethanol (95%), potassium bromide (99%) and anhydrous calcium chloride (97%) were obtained from Protist Lab Africa Ltd.

3.4 Synthesis of Schiff Base Ligands

Schiff base ligands were synthesized using the procedures according to Sujarani & Ramu (2013) with slight modification. The selected anilines and 2-hydroxy-4-methoxy benzophenone were dissolved in 30 mL ethanol, and the reaction mixture was refluxed in a water bath (plate 1) at 40℃ for 4 hours under constant stirring with the addition of drops of HCl until the coloured homogeneous liquid solution was obtained. The precipitate was separated by filtration and purified in ethanol. The crystals were washed 2 to 3 times with diethyl ether to remove unreacted selected anilines and 2-hydroxy-4-methoxybenzephenone. The solid formed was dried in air at room temperature and stored in a calcium chloride desiccator.

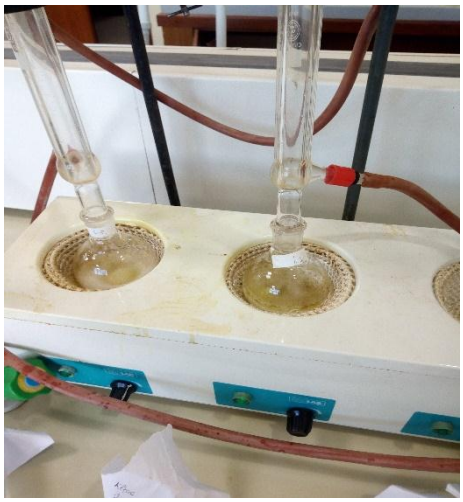

Plate 1: Reflux apparatus used to synthesize Schiff bases

3.4.1. Synthesis of *(E)*-5-methoxy-2-(phenyl(phenylimino)methyl)phenol (L_1)

2.28 g (0.01moles) of 2-hydroxy-4-methoxybenzophenone was dissolved in 30 mL ethanol. Then 0.9 cm3 (0.01 moles) of aniline was added to 30 mL of 2-hydroxy-4-methoxybenzophenone ethanol solution in a reaction flask. This reaction flask was then fixed with a refluxing column, placed in a laboratory heating mantle, and refluxed for three hours. A yellow solution was obtained, and sharp needle-like crystals were observed on cooling. The yellow solid crystals were obtained through vacuum filtration and washed with cold ethanol, followed by diethyl ether to remove unreacted aniline and 2-hydro-4-methoxybenzophenone. The product was then dried at room temperature. The dried solids were transferred into glass sample vials for storage,

awaiting characterization and antibacterial testing (Ommenya *et al*., 2020). Scheme 13 shows the reaction for the synthesis of Schiff base ligand L1.

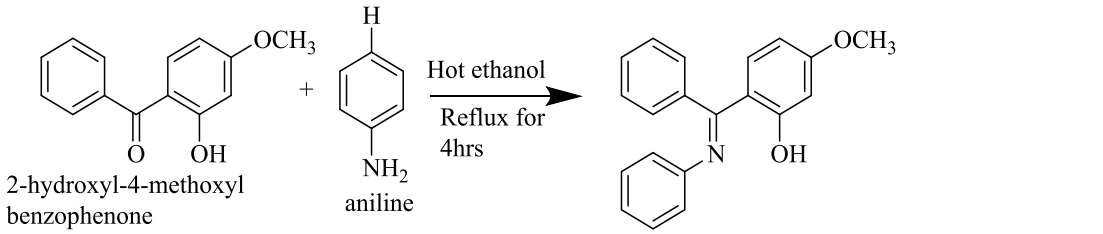

Scheme 13: The reaction for the synthesis of ligand L_1

3.4.2 Synthesis of *(E)*-5-methoxy-2-(phenyl(*p*-tolylimino)methyl)phenol (L_2)

2.28 g (0.01moles) 2-hydroxy-4-methoxybenzophenone was dissolved in 30 mL ethanol. A reaction flask added 1.07 g (0.01 moles) of 4-methylaniline to 30 mL of 2-hydroxy-4-methoxybenzophenone ethanol solution. This reaction flask was then fixed with a refluxing column, placed in a laboratory heating mantle, and refluxed for four hours. A pale-yellow solution was obtained, and sharp needle-like crystals were observed on cooling. The pale-yellow crystals were obtained through vacuum filtration and washed with cold ethanol, followed by diethyl ether to remove unreacted aniline and 2-hydro-4-methoxybenzophenone. The product was then dried at room temperature. The dried solids were transferred and stored in a glass sample vial, awaiting characterization and antibacterial testing (Ommenya *et al*., 2020). Scheme 14 illustrates the synthesis of ligand L_2.

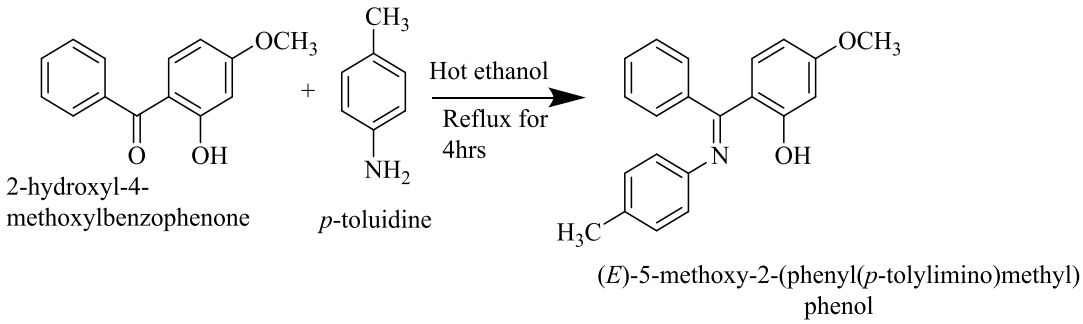

Scheme 14:The reaction for the synthesis of ligand L_2

3.4.3 Synthesis of (*E*)-2-(((2,4-dinitrophenyl)imino)(phenyl)methyl)-5-methoxy phenol (L_3)

2.28 g (0.01moles) 2-hydroxy-4-methoxybenzophenone was dissolved in 30 mL ethanol. 1.83 g (0.01moles) of 2,4-dintroaniline to 30 mL of 2-hydroxy-4-methoxybenzophenone ethanol solution. This reaction flask was then fixed with a refluxing column, placed in a laboratory heating mantle and refluxed for four hours. A yellowish solution was obtained, and shiny needle-like crystals were observed on cooling. The yellowish shiny crystals were obtained through vacuum filtration and washed with cold ethanol, followed by diethyl ether to remove unreacted aniline and 2-hydro-4-methoxybenzophenone. The product was then dried at room temperature. The dried solids were transferred into a glass sample vial for storage, waiting for, characterization, synthesis of copper (II) complexes and antibacterial testing (Ommenya *et al*., 2020). Scheme 15 illustrates the synthesis of ligand L_3.

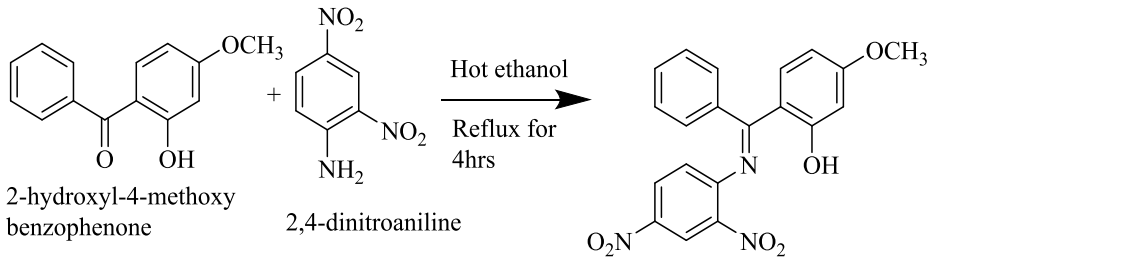

Scheme 15: The reaction for synthesis of ligand L_3

3.4.4 Synthesis of ((*E*)-4-(((2-hydroxy-4-methoxyphenyl) (phenyl)methylene) amino) benzoic acid (L_4)

2.28 g (0.01moles) 2-hydroxy-4-methoxybenzophenone was dissolved in 30 mL ethanol. 1.37 g (0.01moles) of 4-aminobenzoic acid to 30 mL of 2-hydroxy-4-methoxybenzophenone ethanol solution. This reaction flask was then fixed with a refluxing column, placed in a laboratory heating mantle, and refluxed for four hours. An orange solution was obtained, and sharp needle-like crystals were observed on cooling. The solid crystals were obtained through vacuum filtration washed with cold ethanol followed by diethyl ether to remove unreacted aniline and 2-hydro-4-methoxybenzophenone. The product was then dried at room temperature. The dried

solids were transferred into a glass sample vial for storage, awaiting characterization and antibacterial testing (Ommenya *et al*., 2020). Scheme 16 shows the reaction for the synthesis of ligand L_4.

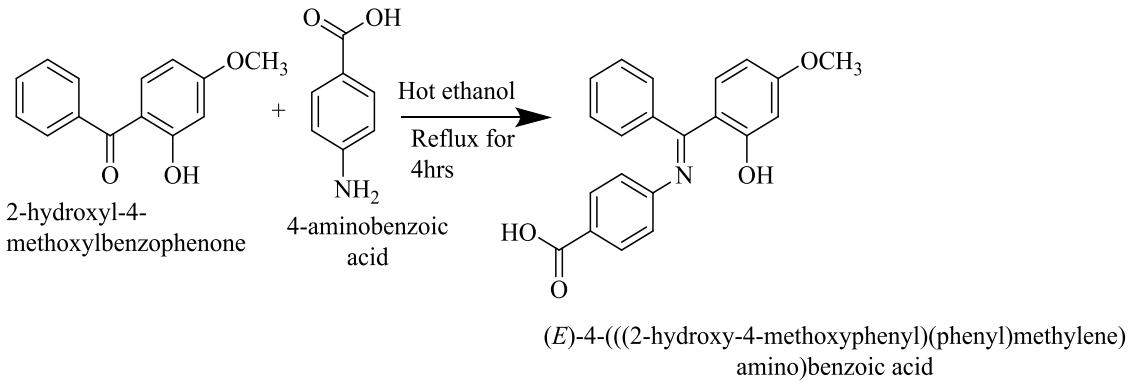

Scheme 16: The reaction for synthesis of ligand L_4

3.5 Synthesis of Copper (II) Complex from Schiff base ligand

Synthesis of Cu (II) complexes, Cu-L_1-Cu-L_4, was done using the method described by Iftikhar *et al*. (2018) with some slight modifications. Schiff base copper (II) complexes were synthesized from Schiff base ligands with hydrated copper (II) chloride in ethanolic solution. The resulting mixture was magnetically stirred and refluxed in a water bath at 60ºC for 5–6 hours. The precipitate was separated by filtration, followed by washing with water, ethanol and diethyl ether to remove unreacted Schiff base and copper (II) chloride. The Schiff base copper (II) complex was then dried in an electric oven at 50 to 60℃ and stored under anhydrous calcium chloride (Kargar *et al.,* 2021).

3.5.1 Synthesis of Cu-L_1 Complex

0.3 g (0.000989 moles) of L_1 was carefully put into a 100 ml reaction flask. 30 mL of absolute ethanol was then transferred into the flask containing the Schiff base. The flask was placed in the laboratory heating mantle and then heated to dissolve the Schiff base. After that, 0.0842 g (0.0004945 moles) hydrated copper (II) chloride was added carefully into the round botted flask containing the Schiff base solution. The refluxing column was fitted over the round-bottomed flask and refluxed for five hours. Dark green crystals were obtained through vacuum filtration and purified by washing with cold ethanol followed by diethyl ether to eliminate any unreacted Schiff base or copper (II) chloride. The product was then dried at room temperature then transferred into a

glass sample vial for storage, awaiting characterization and antibacterial testing (Kargar *et al.,* 2021). The scheme for the reaction is shown in Scheme 17.

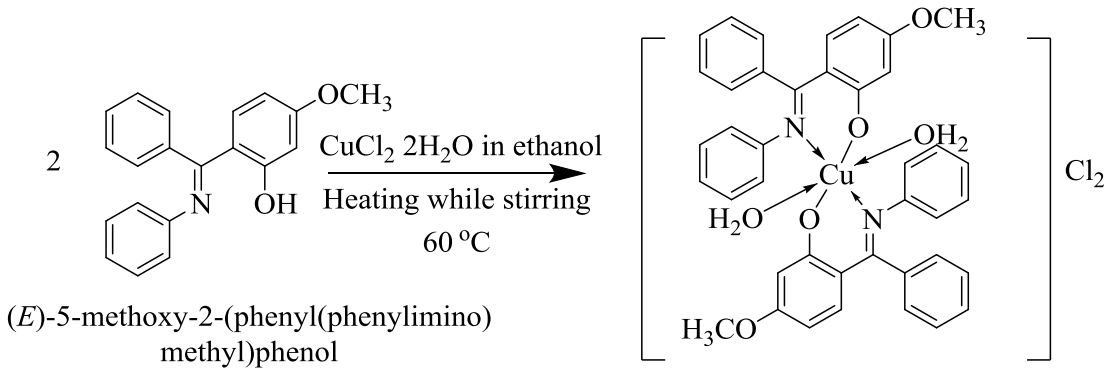

Scheme 17: The reaction for the synthesis of Cu-L_1 complex

3.5.2 Synthesis of Cu-L_2 complex

0.3 g (0.00094521 moles) of the L_2 ligand was carefully put into a 100 mL reaction flask. 30 mL of absolute ethanol was then transferred into the flask containing the Schiff base. The flask was placed in the laboratory heating mantle and then heated to dissolve the Schiff base. Thereafter, 0.0806 g (0.0004726 moles) of hydrated copper (II) chloride was added carefully into the round botted flask containing Schiff base solution. The refluxing column was fitted over the round-bottomed flask and refluxed for five hours. The crystals were obtained through vacuum filtration and purified by washing with cold ethanol followed by diethyl ether to eliminate any unreacted Schiff base or copper (II) chloride. The product was then dried at room temperature and the solids were then transferred into a glass sample vial for storage, awaiting characterization and antibacterial testing (Kargar *et al.,* 2021). Scheme 18 shows the reaction for the formation of the Cu-L_2 complex.

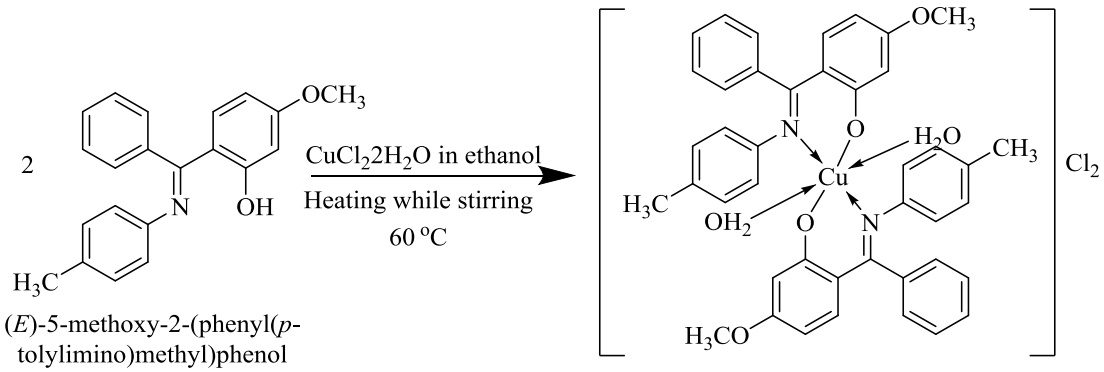

Scheme 18: The reaction for the synthesis of Cu-L_2 complex

3.5.3 Synthesis of Cu-L_3 Complex

0.3 g (0.0007627 moles) of the L_3 ligand was carefully put into a 100 mL reaction flask. 30 mL absolute ethanol was then transferred into the flask containing the Schiff base. The flask was placed in the laboratory heating mantle and then heated to dissolve the Schiff base. Thereafter, 0.0650 g (0.0003813 moles) hydrated copper (II) chloride was added carefully into the round botted flask containing Schiff base solution. The refluxing column was fitted over the round-bottomed flask and refluxed for five hours. The greenish-yellow crystals were obtained through vacuum filtration and purified by washing using cold ethanol followed by diethyl ether to eliminate any unreacted Schiff base or copper (II) chloride. The product was then dried at room temperature. The dried solids were transferred into a glass sample vial for storage, awaiting characterization and antibacterial testing (Kargar *et al.,* 2021). Scheme 19 shows the reaction for the formation of Cu-L_3 complex.

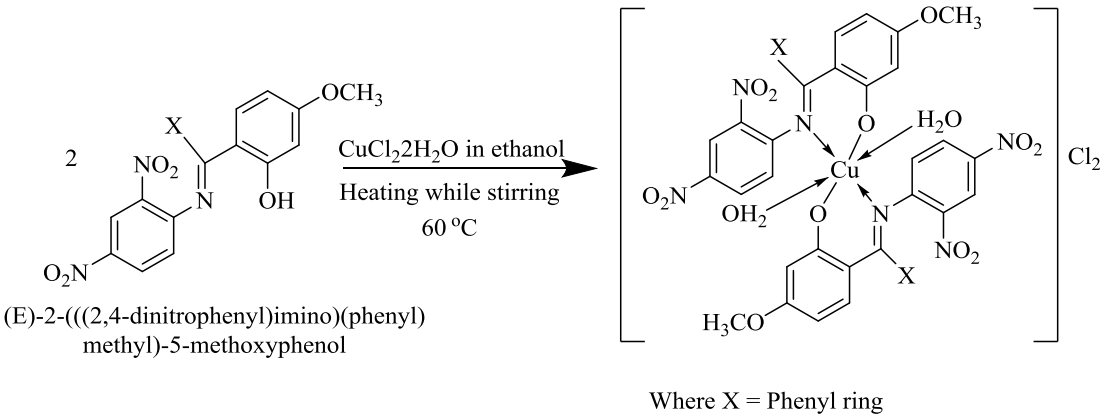

Scheme 19: The reaction for the synthesis of Cu-L_3 complex

3.5.4: Synthesis of Cu-L_4 Complex

0.2 g (0.0005758 moles) of L4 was carefully put into a 100 mL reaction flask. 30 mL of absolute ethanol was then transferred into the flask containing the Schiff base. The flask was placed in the laboratory heating mantle and then heated to dissolve the Schiff base. Thereafter, 0.0491 g (0.0002879 moles) hydrated copper (II) chloride was added carefully into the round botted flask containing the Schiff base solution. The refluxing column was fitted over the round-bottomed flask and refluxed for five hours. The dark green crystals were obtained through vacuum filtration and purified by washing with cold ethanol followed by diethyl ether to eliminate any unreacted Schiff base or copper (II) chloride. The product was then dried at room temperature. The dried solids were transferred into a glass sample vial for storage, awaiting characterization and antibacterial testing (Kargar *et al.,* 2021). Scheme 20 shows the reaction for the formation of the Cu-L_4 complex.

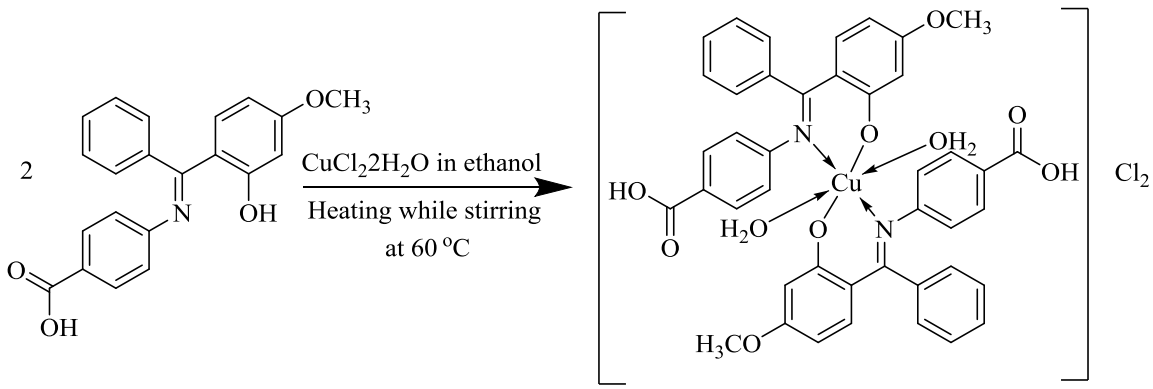

Scheme 20: The reaction for the synthesis of Cu-L_4 complex

3.6 Characterization of the Synthesized Schiff Bases and their Copper (II) Complexes

The new Schiff base ligands and their copper (II) complexes were characterized to obtain information that establishes their purity and homogeneity in composition and structure. The following analytical techniques were used to characterize the synthesized compounds.

3.6.1 Determination of the Melting Point

The melting point of Schiff base ligands and their Cu (II) complexes was determined by the open capillary method, according to Iftikhar et al. (2018). The capillary tube was closed in one of its open ends by heating it in the non-luminous flame for about 3 minutes. The Schiff base and their Cu (II) complexes, whose melting points were to be determined, were placed on a tile and then crushed into a fine powder. The capillary tube with a closed-end was held steadfastly by hands. Then, the open end of the capillary tube was carefully dipped into finely powdered solid samples to pick them. It was then gently tapped to fill the compound to about a length of 1-2 cm. With the help of a thread, the capillary tube was attached to the thermometer and then dipped into a beaker containing liquid paraffin such that the bulbs of the thermometer and the closed-end capillary tubes were on the same label and they were both dipped into liquid paraffin up to a length of around 2cm. The thermometer was then held using a stand and clamps. The liquid paraffin was heated using non-luminous flames of a Bunsen burner, as shown in plate 2.

Plate 2: The setup of apparatus for determining the melting point of free ligands and their Cu (II) complexes

The temperature of the liquid was observed as it rose continuously, and the temperature at which the compound began to melt was noted immediately and recorded as T_1. The

temperature at which the compound had melted completely was indicated as T_2. T_1 and T_2 values were averaged to determine the melting point of the synthesized compounds.

3.6.2 UV -Vis Spectra

UV-Vis spectra of new Schiff base ligands and their Cu (II) complexes were obtained using a Shimadzu UV-Vis spectrometer with quartz cuvettes of 1 cm path length, according to Rocha (2018). Samples of ligands L_1, L_2, L_3 and L_4 and their copper (II) complexes were dissolved in acetonitrile. 1 ml of each solution was placed in a UV-Vis spectrophotometer cell and the sample's absorbance was scanned from 200 nm to 800 nm.

3.6.3 Molar Conductivity

The molar conductance measurement of the synthesized Schiff base ligands and their copper (II) complexes was done in acetonitrile using the HANNA Instrument EC 214 conductivity meter following the procedure according to Ommenya *et al*. (2020). The conductivities of synthesized compounds were measured at 25℃. The conductivity cell used in the determination had a cell constant of 0.99. The conductivity meter was calibrated using 0.01 M KCl solution. Molar conductivity measurements were recorded by immersing the electrode into the sample solutions. The electrode was rinsed with double distilled water before the molar conductivity measurements of the subsequent solutions were determined. The molar conductivity measurements were recorded in triplicates.

3.6.4 FT -IR Spectra

FT-IR spectra of the synthesized Schiff base ligands and their copper (II) complex were determined using a Shimadzu Fourier Transform Infrared spectrometer. Powdered samples were analyzed using the potassium bromide pellet method (Abdel- Rahman *et al*., 2017). The 0.001 g sample was mixed with 0.1 g of potassium bromide in mortar and ground to a fine powder. A disk-molding apparatus was used to make a disk from the homogenous mixture by applying pressure to form a disk. The disk was then transferred to the spectrometer and scanned from 4000 to 200 cm^{-1}.

3.6.5 NMR Spectra

The ^{1}H NMR analysis of the free ligands and their copper (II) complexes determined using Bruker Avance III HD Nanobay NMR spectrometer was according to Hore (2015). 6 mg of each solid synthesized compound was measured. DMSO-d_6 was used as a deuterated solvent, while tetramethyl silane (TMS) was used as an internal standard for chemical shift calibration. All the chemical shifts (δ) values of Schiff base ligands and their copper (II) complexes were recorded in part per million (ppm) downfield to TMS.

3.7 Determination of Antibacterial Properties of Synthesized Schiff Base Ligands and their Copper (II) Complexes

The synthesized Schiff base ligands and their copper (II) complexes were tested for their *in vitro* antibacterial against the three bacteria strains where *Escrischeria coli and Pseudomonas aeruginosa* were gram-negative. At the same time, *Staphylococcus aureus* was a gram-positive bacterium. These three bacteria strains were bought from KEMRI. Three bacteria strains were gram-stained to confirm their identity before an antibacterial susceptibility test was conducted. The bacteria strains were first sub-cultured from freezer stocks onto Muller Hinton agar plates and incubated at 37℃ for 24 hours. Antibacterial activities of synthesized compounds were determined using the disk diffusion method according to El-Gammal *et al*. (2021).

3.7.1 Preparation of Media

Muller Hinton Agar (MHA) medium was used. The media was prepared by dissolving 38 g of dehydrated MHA in 1000 mL of distilled water. The dissolved media was autoclaved at 121℃ and 15 pounds pressure for 15 minutes, then cooled at 40℃. 15 mL of agar, dispensed to sterile Petri dishes under sterile conditions and allowed to solidify as shown in Plate 3.

Plate 3: Petri dishes containing MHA media

3.7.2 Preparation of Solution for Antibacterial Screening

The stock solution of a concentration of 1000ppm was prepared by dissolving 20mg of test compounds into 20 mL dimethyl sulfoxide (DMSO). 500 ppm, 250 ppm and 125 ppm were prepared by serial dilutions with DMSO (Plate 4).

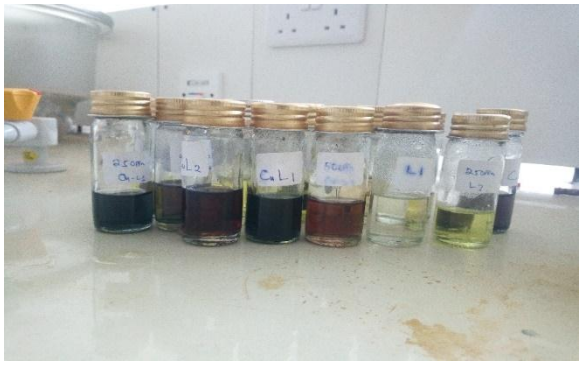

Plate 4: Prepared solutions using serial dilutions

3.7.3 Disk Diffusion Method

Test bacteria were inoculated onto the solid MHA by streaking with a spreader. Whatman filter papers (6 mm diameter) were sterilized in an autoclave and then soaked into the solution of 1000, 500, 250 and 125 ppm of the test compounds and allowed to dry for some time before application on the bacteria-grown agar plates. The dry paper disks containing the tested compounds were placed on the inoculated MHA at equidistant positions from each other. A paper disk impregnated with DMSO was placed in each plate to serve control, while impregnated with gentamicin and

amoxicillin served as positive control. The plates were incubated at 37℃ for 24 hours. The diameters of inhibition zones were measured using a millimeter ruler in triplicate sets and recorded at the end of the incubation period.

3.7.4 Data Collection

After the paper disc containing the test compounds was placed in Petri dishes containing nutrients, ager seeded with the test bacteria strains and incubated for 24 hours at 37℃. The diameter of inhibition zones was measured separately using a millimeter ruler, and the values was recorded.

3.7.5 Data analysis

Data collected experimentally was analyzed by using descriptive and inferential statistics. Two-way ANOVA was used with two independent variables: bacteria strain and the test compounds. Analysis of variable (ANOVA) was used to test the significant differences of the inhibition zones of test compounds and the means were separated using least significance differences (LSD) at $\alpha \leq 0.05$. ANOVA enables the comparison effects of antibacterial activity (by comparing the means diameter of zones of growth inhibition) against the test compound against each concentration on the specific bacteria strain to show if the dependent variable changes according to the levels of the independent variables (Connelly *et al.,* 2021).

3.8 Ethical Consideration

The research permit (Appendix XV) was be obtained from the National Commission for Science Technology and Innovation (NACOSTI) before the research begins). The integrity of the research was upheld by avoiding plagiarism and acknowledging the work done by others through citations and references. The study's outcome was carefully and critically reviewed so that the results are credible and was reported with honesty, integrity, and confidentially

CHAPTER FOUR

RESULTS AND DISCUSSIONS

4.1 Physical Properties and Percentage Yield of the Synthesized Compounds

The melting points, percentage yields and physical properties of synthesized Schiff base ligands and their Copper (II) complexes are provided in Table 4.1. Schiff base ligands are assigned as **L_1-L_4**. The Cu (II) complexes synthesized from Schiff base ligands (**L_1-L_4**) were designated **Cu-L_1-Cu-L_4.**

Table 4.1: Physical properties of the free ligands and their Cu (II) complexes

Compound	Melting point (℃)	Mass Obtained (g)	% Yield	Colour	Calculated molecular formulae	Calculated molecular Weight
L_1	188	3.512	92	Yellow	$C_{20}H_{17}NO_2$	303.361
L_2	180	2.915	87	Pale yellow	$C_{21}H_{19}NO_2$	317.388
L_3	178	3.740	91	Shiny yellow	$C_{20}H_{15}N3O_6$	393.355
L_4	230	3.430	94	Brown	$C_{21}H_{17}NO_4$	347.370
Cu-L_1	191	0.278	72.3	Dark yellow	$C_{40}H_{36}CuN_2O_6$	704.282
Cu-L_2	201	0.381	77.6	Brown	$C_{42}H_{40}CuN_2O_6$	732.336
Cu-L_3	181	0.272	74.6	Pale yellow	$C_{40}H_{32}CuN_6O_{14}$	884.270
Cu-L_4	246	0.249	78.6	Greenish yellow	$C_{42}H_{36}CuN_2O_{10}$	792.300

The melting point of Schiff base ligands ranged from 176 to 230℃ while those for Cu (II) complexes ranged from 181 and 246℃ (Table 4.1). The melting point of *(E)*-5-methoxy-2-(phenyl(phenylimino)methyl) phenol (**L_1**) was 188℃. It formed yellow crystals and its percentage yield was 92% (3.51 g). It was insoluble in water and cold ethanol but soluble in organic compounds like acetone, acetonitrile, dimethyl sulfoxide and hot ethanol.

The melting point of *(E)*-5-methoxy-2-(phenyl(*p*-tolylimino) methyl)phenol **(L_2)** was 180℃ while the percentage yield was 87 % (2.915 g). The compound was obtained in form of pale-yellow crystals. Additionally, the compound was insoluble in water and cold ethanol but was soluble in acetone, acetonitrile, dimethyl sulfoxide and hot ethanol.

The melting point of *(E)*-2-(((2,4-dinitrophenyl)imino)(phenyl)methyl)-5-methoxyphenol (**L_3**) was 178℃. The percentage yield was 91 % (3.740 g). The compound was obtained in form of yellow shiny microcrystals. It was insoluble in water and cold ethanol but soluble in acetone, acetonitrile, dimethyl sulfoxide and hot ethanol.

The melting point of (*E*)-4-(((2-hydroxy-4-methoxyphenyl)(phenyl)methylene) amino benzoic acid (**L_4**) was 230℃. The compound obtained had a percentage yield of 94 % (3.430 g) and formed brown crystals. It was insoluble in water but soluble in acetone, acetonitrile, dimethyl sulfoxide and hot ethanol.

The melting points of the synthesized Cu (II) complexes, **CuL_1** – **CuL_4**, were 191, 201, 181 and 246℃, respectively. Their percentage yields were 72.3 (0.278 g), 77.6 (0.381 g), 74.6(0.272 g) and 78.6 % (0.249 g), respectively. The colours of Cu (II) complexes of L_1-L_4 were dark green, brown, pale yellow and greenish-yellow, respectively. The synthesized Schiff base ligands and their Cu (II) complexes generally show different colours upon changing substituent groups (Amer *et al.*, 2013). All the Cu (II) complexes were insoluble in water and cold ethanol but slightly soluble in diethyl ether. They were soluble in acetone, acetonitrile, dimethyl sulfoxide and hot ethanol.

The calculated molecular formulae and their molecular weight of free ligands and Cu (II) complexes are as follows: **L_1** $C_{20}H_{17}NO_2$, 303.361: **L_2** $C_{21}H_{19}NO_2$, 317.388: **L_3** $C_{20}H_{15}N_3O_6$, 393.355: **L_4** $C_{21}H_{17}NO_4$, 347.370: **Cu-L_1** $C_{40}H_{36}CuN_2O_6$, 704.282: **Cu-L_2** $C_{42}H_{40}CuN_2O_6$, 732.336: **Cu-L_3** $C_{40}H_{32}CuN_6O_{14}$, 884.27and **Cu-L_4** $C_{42}H_{36}CuN_2O_{10}$, 792.3 g/mol.

4.2 Spectroscopic Characterization of Synthesized Compounds

4.2.1 FT-IR Analysis

Figure 9 shows a representative of the FT-IR spectrum of compound **L_1**. The FT-IR spectra of compounds L_2-L_4 and Cu-L_1-Cu-L_4 are in Appendix I. The significant bands of vibrational frequencies in the FT-IR spectra of L_1-L_4 are shown as follows **L_1**: 741.5, 1105.25, 1270 *υ* (C–O), 1525.72 υ(C=O), 1610 υ(C=N), 2950 υ(C-H) and 3450 υ(OH): **L_2** 810.10, 1114.86, 1267.23 υ(C-O), 1568.13 υ(C=C), 1625 υ(C=N), 2920 υ(C-H) and 3425 υ(OH): **L_3** 698.23, 1116.78, 1502.55 υ(C=C), 1631.78 υ(C=N), 2950 υ(C-H) and

3450 υ(OH): **L_4** 754.17, 1109.07, 1250 υ(C-O), 1502.55 υ(C=C),1630 υ(C=N), 2925 υ(C-H) and 3445 υ(OH) cm^{-1}. The vibrational frequencies of Cu-L_1 -Cu-L_4 complexes were as follows **Cu-L_1** 474.46 υ(Cu-O), 523.68 υ(Cu-N), 683.78 υ(OH), 1250 (υ(C-O)), 1520.90 υ(C=C), 1600 υ(C=N), 2900 υ(C-H) and 3430 υ(OH): **Cu-L_2** 486.07 υ(Cu-O), 523.68 υ(Cu-N), 683.78 υ(OH), 1250 υ(C-O), 1529.32 υ(C=O), 1615 (υ(C=N), 2910 υ(C-H) and 3400 υ(OH): **Cu-L_3** 480.25 (υ(Cu-O), 581.55 υ(Cu-N), 680 υ(OH), 1250 υ(C-O), 1500 υ(C=C), 1620 υ(C=N), 2900 υ(C-H) and 3500 υ(OH): **Cu-L_4** 480.25 υ(Cu-O)), 530 υ(Cu-N), 685.71 υ(OH), 1244.11 υ(C-O), 1500 υ(C-O), 1611.55 υ(C=N), 2925 (υ(C-H) and 3425 υ(OH) cm^{-1}.

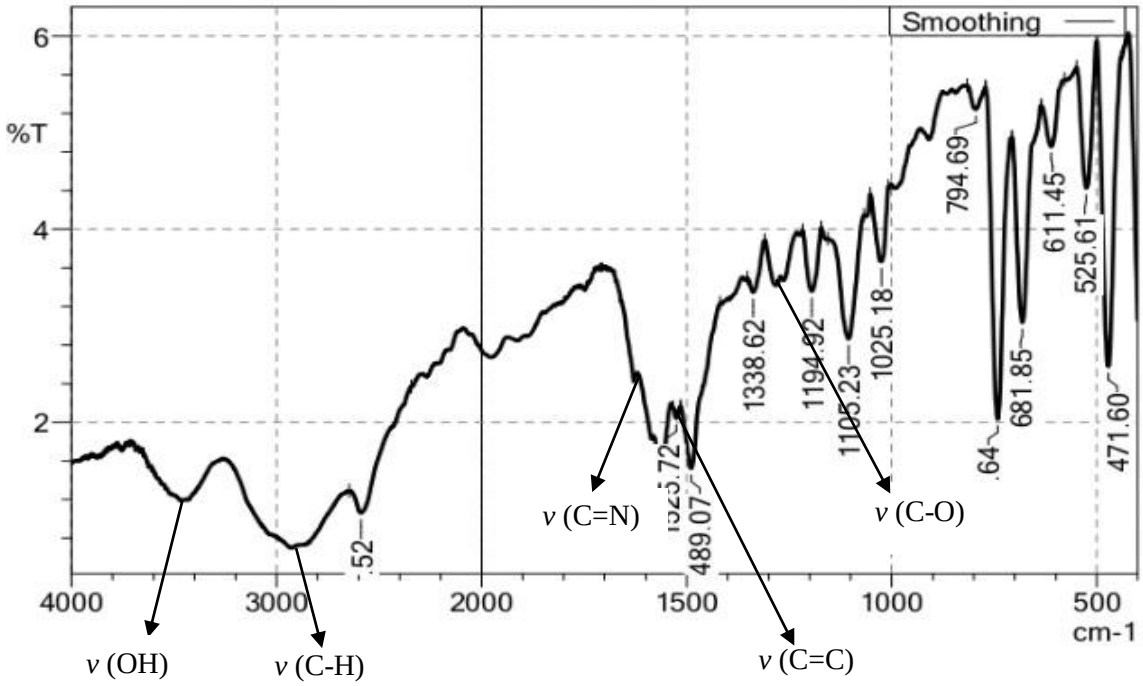

Figure 9: FT-IR spectrum of ligand L_1

The establishment of the Schiff base through azomethine (-HC=N-) was confirmed by the absence of weak bands at 3280 cm^{-1} and 1664 cm^{-1} for the NH_2 and C=O function groups. This was in agreement with previous publications by Rezaei *et al*. (2023), who indicated that the formation of imine bonds was confirmed by the absence of NH_2 and C=O at 3280 cm^{-1} and 1664 cm^{-1}, respectively. This was confirmed by the appearance of bands at 1610, 1625, 1631.7 and 16310cm^{-1} (figure 9, 20, 21 and 22) due to the formation of imine bond (-C=N-) stretching vibration for L_1, L_2, L_3 and L_4, respectively. This was agreement with the results obtained from other Schiff base ligands described previously reported by Kakanejadifard *et al*. (2013). Azomethine vibrations were

shifted to a lower wave number after complexation of Cu (II) ions, for instance, 1600, 1615, 1620 and 1611 for Cu-L_1- Cu-L_4 (figure 23, 24, 25 and 26), respectively illustrated in Table 4.2. This negative shift υ(C=N) can be attributed to the electron-withdrawing effect of the coordinated Cu (II) ions, which decreases electron density in the azomethine bond and leads to a lower υ(C=N) frequency. Such an observation was reported by Es-Sounni *et al*. (2023). This suggests the involvement of the nitrogen atom of the imine group in complexation with Cu (II) ions. Further, it confirms the coordination of Schiff base ligand via nitrogen in imine bond (-C=N-) (Almáši *et al*., 2021).

The FT-IR spectra of Cu (II) complexes (figure 23, 24, 25 and 26) also displayed a strong band in the region of 3420-3450cm^{-1} (Table 4.2), suggesting the presence of coordinated water in the Cu (II) complexes (Hemalatha *et al*., 2020). This was further confirmed by the appearance of bands in the region 683.78-690cm^{-1}, which was attributed to the rocking mode of water (Ommenya *et al.*, 2020).

Table 4.2: Selected FT-IR absorption bands cm^{-1} of Schiff base ligands and their Cu (II) complexes

Compound	υ(OH)	υ(C=N)	υ(C-O)	υ(H_20)	υ (C=C)	υ (C-H)	υ(M-N)	υ(M-O)
L_1	3450	1610	1270	-	1525.23	2950	-	-
L_2	3425	1625	1267.23	-	1568.13	2920	-	-
L_3	3450	1631.7	1267.23	-	1502.55	2950	-	-
L_4	3445	1631.7	1250	-	1502.55	2925	-	-
Cu-L1	3430	1600	1250	683.78	1520.99	2900	523.68	475.46
Cu-L2	3420	1615	1225	690	1529.32	2910	560	486.07
Cu-L3	3500	1620	1250	680	1500	2925	581.55	480.28
Cu-L4	3435	1611.	1244.11	685.71	1500	2830	530	480.28

For the synthesized Schiff base ligands (figure 9, 20, 21 and 22), the sharp peak at 1250-1267.23 cm^{-1} was assigned to be υ (C-O, phenolic) shifted to lower wave numbers in the Cu (II) complexes (figure 23, 24, 25 and 26), indicating the coordination of the phenolic oxygen atom to the metal ion (Rosu *et al.*, 2011). Furthermore, additional weak bands appear at regions of 532.68-581.55 cm^{-1} and 475.46-480.28 cm-1 in copper (II) complexes (figure 23, 24, 25 and 26) were attributed to υ (M-N) and υ (M-O), respectively. Hasan *et al*. (2024), observed similar results confirming the formation of the complex. This further shows that Schiff base ligands coordinated with Cu (II) ions through ‘’N’’ and ‘’O’’ atoms. This confirms that the synthesized Schiff base is a bidentate ligand of NO type. Lastly, the bands at the regions of 1500-1568.13 cm^{-1} are

attributed to υ (C=C) of the phenyl ring (Al-Fakeh *et al.*, 2024), while that at regions of 2950-2900 cm^{-1} was attributed to υ (C-H) (Kargar *et al.*, 2021).

4.2.2 Electronic Spectra Analysis

Figure 10 shows a representative UV-Vis absorption of Schiff base ligand L1: The electronic spectra of L_2-L_4 and Cu-L_1-Cu-L_4 complexes are shown in Appendix II. The λ Max (acetonitrile) nm of Schiff base ligands and their Cu (II) complexes are given as follows: **L_1** 340.5, 291 and 240.5: **L_2** 330, 288.5 and 248: **L_3** 335.5,259.5 and 226: **L_4** 340.5 and 284.5: **Cu-L_1** 297.5 and 243.5: **Cu-L_2** 330 and 250.5: **Cu-L_3** 334.5, 259 and 225.5: Cu-**L_4** 289.5 and 204.

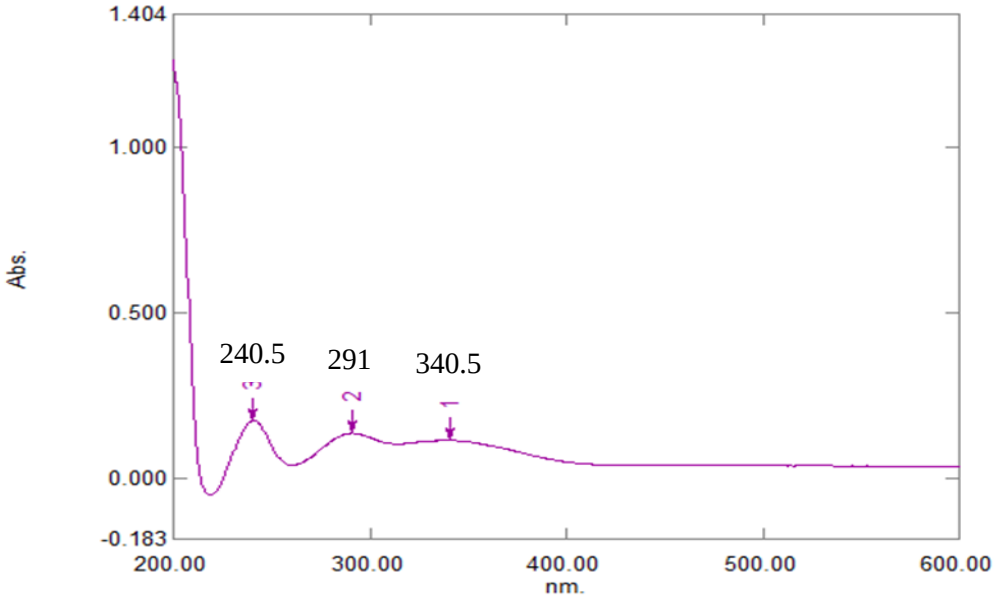

Figure 10: UV-Vis spectrum of ligand L_1 in acetonitrile

The Schiff base ligand, **L_1** (figure 10)**,** showed three significant peaks at (340.5nm) 29411.76cm^{-1}, (291nm) 33364.26cm^{-1} and (240.5nm) 41580.04cm^{-1} in Figure 10 above. L_1, L_2 and L_3 (figure 10, 27 and 28, respectively) show three peaks. The 226-248 nm peak was attributed to the $\pi \rightarrow \pi^*$ transitions of aromatic rings and was assigned to Intra-Ligand Charge Transfer (ILCT). The second peak at 259.5-291nm attributed to $n \rightarrow \pi^*$ is due to the transition, resulting from the non-bonding present in the azomethine group. The last band at 335.5-340 nm (Table 4.3) was assigned to be the phenolic group, which results in $n \rightarrow \pi^*$ transitions (Şahin *et al.*, 2013; Dhanaraj & Johnson, 2014).

Table 4.3: Assignment of the important λ max (nm) of the free ligands and Cu (II) complexes

Compound	λ Max (nm)	Transitions	Assignment	Geometry
L_1	340.5	$\pi \rightarrow \pi^*$	ILCT	
	291	$n \rightarrow \pi^*$	ILCT	-
	240.5	$n \rightarrow \pi^*$	ILCT	
L_2	330	$\pi \rightarrow \pi^*$	ILCT	
	288.5	$n \rightarrow \pi^*$	ILCT	-
	248	$n \rightarrow \pi^*$	ILCT	
L_3	335.5	$\pi \rightarrow \pi^*$	ILCT	
	259.5	$n \rightarrow \pi^*$	ILCT	-
	226	$n \rightarrow \pi^*$	ILCT	
L_4	340.5	$\pi \rightarrow \pi^*$	ILCT	
	284.5	$n \rightarrow \pi^*$	ILCT	-
Cu-L_1	297.5	$\pi \rightarrow \pi^*$	ILCT	Octahedral
	243.5	$\pi \rightarrow \pi^*$	ILCT	
Cu-L_2	330	$\pi^* \rightarrow d$	LMCT	
	250.5	$\pi \rightarrow \pi^*$	ILCT	Octahedral
	203.5	$n \rightarrow \pi^*$	ILCT	
Cu-L_3	334.5	$\pi^* \rightarrow d$	LMCT	
	259	$\pi \rightarrow \pi^*$	ILCT	Octahedral
	225.5	$\pi \rightarrow \pi^*$	ILCT	
Cu-L_4	289.5	$\pi \rightarrow \pi^*$	ILCT	Octahedral
	204	$n \rightarrow \pi^*$	ILCT	

Where ILCT=Intra-Ligand Charge Transfer; LMCT= Ligand-Metal Charge Transfer

The electronic spectra of Cu-L_1 and Cu-L_4 (figure 30 and 34) show two bands at 297.5-289.5 nm and 204-243.5 nm. The two bands were due to intra-ligand transitions within the organic moiety of the complexes (Nkungli *et al*., 2015). The λ_{max} of Cu-L_1 and Cu-L_4 (figure 30 and figure 33, respectively) were shifted to higher wavelengths relative to L_1 and L_4 (figure 10 and 29), which support the complexation of the metal ions with the ligands. The Cu-L_2 (figure 31) electronic spectra also show three bands at 203.5, 250.5 and 330 nm. The band at 330nm was attributed to O →Cu ligand- metal charge transfer, while the other bands at 250.5 and 203.5nm were due to intra-ligand transitions. Thus, this transition suggests octahedral geometry around Cu (II) ions (Ommenya *et al*., 2020).

The electronic spectra of Cu-L_3 (figure 32) show three bands at 225.5, 259 and 334.5nm. The band at 225.5-259 nm was due to intra-ligands transitions, while the band at 334.5

was attributed to O →Cu ligand- metal charge transfer. This transition also suggested octahedral geometry (Ommenya *et al*., 2020).

4.2.3 Molar Conductivity

The molar conductivity values of the synthesized Copper (II) complexes in DMSO 10^{-3} M were determined at room temperature (Table 4.4). The molar conductivity values of the synthesized compounds were below 50 S cm^2mol^{-1}, confirming their non-ionic nature (Musa *et al*., 2022). This revealed that they are non-electrolytes; thus, no ions were present outside the complexes' coordination sphere (Abd El-halim *et al*., 2011). Also, molar conductance revealed that two negatively charged anions doubly coordinate L_1, L_2, L_3 and L_4, indicating deprotonation of the two phenolic OH groups on coordination of Cu (II) ions (Keypour *et al*., 2012).

Table 4.4: Molar conductivity measurements of Cu (II) complexes

Compound	Λ_m (Scm^2mol^{-1})
L_1	8.46
L_2	12.58
L_3	6.21
L_4	4.86
Cu-L_1	17.32
Cu-L_2	22.08
Cu-L_3	16.67
Cu-L_4	13.34

4.2.4 NMR Spectra Analysis

Figure 11 shows a representative ^{1}H NMR spectrum of Ligand L_1, while those of L_2-L_4 and Cu-L_1 -Cu-L_4 complexes are shown in Appendix III. The chemical shifts (δ, ppm) and multiplicities (singlet, s; multiplet, m) of signals in the ^{1}H NMR spectra of Ligands **L_1-L_4** were: **L_1**: 3.87 ppm (s); 6.33-9.37 ppm (m) and 12.65 ppm (s); **L_2**: 3.88-3.87 ppm (m); 7.09-7.72 ppm (m) and 12.65 ppm (s); **L_3** 3.14 ppm (s); 6.67-8.45 ppm (s) and 11.81 ppm (s) **L_4**; 3.27-3.24 ppm (m), 7.04-6.33 ppm(m) and 12.30 ppm (s) and **Cu-L_1**; 2.92 ppm (s); 6.50 ppm (s) and 7.67-8.13 ppm (m); **Cu-L_2**; 1.81-1.98 ppm(m) and 6.68ppm (m) **Cu-L_3**; 2.215 ppm (s); 2.70-3.77 ppm(m) and 7.15-6.9 ppm (m) and **Cu-L_4** 3.22-3.30 ppm (m);5.96-6.03 ppm(m) 6.85-6.59 ppm (m).

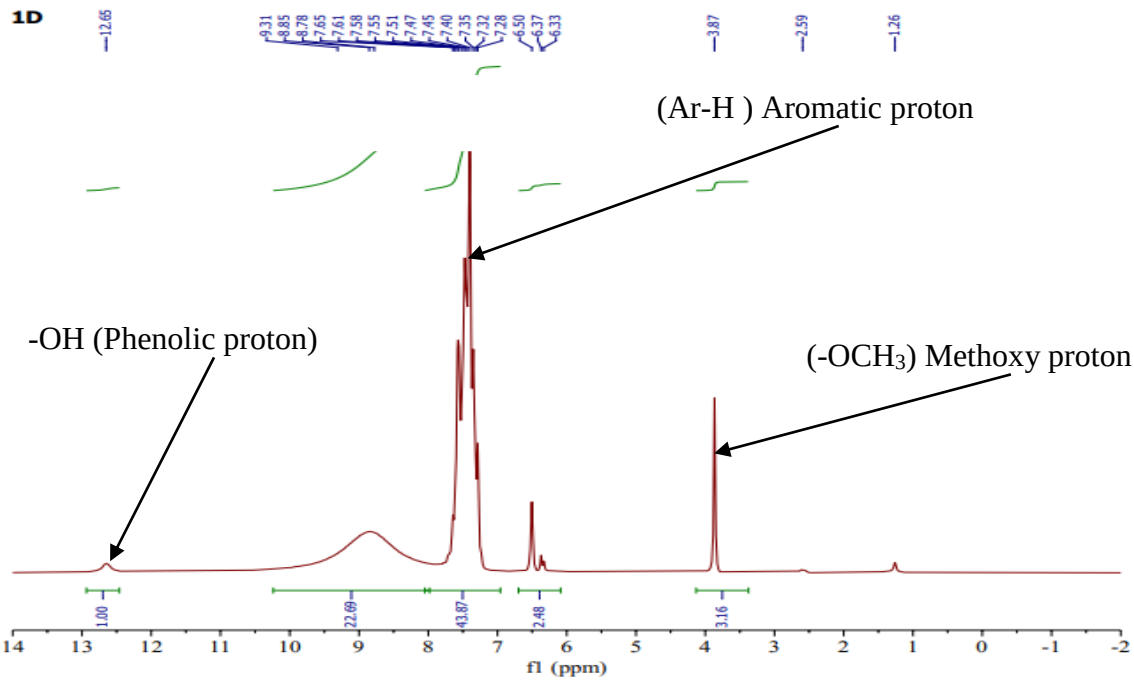

Figure 11: ^{1}H NMR spectrum of L_1

The ^{1}H NMR spectra of the four ligands (figure 11, 34, 35 and 36) showed a singlet signal at δ 11.81-12.65 ppm assigned to the proton of the OH group and this was in agreement with the reported values by Venkatesh *et al.* (2024). This peak disappears in the spectra of the four Copper (II) complexes (figure 37, 38, 39 and 40), thus confirming the deprotonation of the phenolic group and coordination of the negatively charged oxygen species to the Cu (II) ion (Abdel-Rahman *et al.*, 2023). All the ligands L_1-L_4 (figure 11, 34, 35 and 36) also displayed signals at δ 3.22-3.87 ppm, which attributed to the protons of the methoxy groups (Endale & Desalegn, 2018). Multiplet signals observed at δ 7.61-6.95 are due to aromatic protons in the Schiff base ligands (Rezaei *et al.*, 2023). L_2 (figure 34) shown a singlet signal at δ 2.34 which was due to protons of methyl group (Zafar *et al.*, 2015) while for L_4 (figure 36) also shown a singlet signal at δ 12.71 which was assigned due to proton of carboxyl group (Anacona *et al.*, 2014).

4.3 Antibacterial Data

The antibacterial activities of the test compounds were determined using disk diffusion (1000- 125 ppm). Antibacterial data was obtained by zones of bacterial growth inhibitions using the disk diffusion method, as tabulated in Table 4.5.

Table 4.5:Zones of growth inhibition recorded

		Zones of Bacterial Growth Inhibitions								
		E. coli			*P. aeruginosa*			*S. aureus*		
Test	Concentration	Replication			Replication			Replication		
Compounds	(ppm)	1	2	3	1	2	3	1	2	3
L_1	1000	7	8	7	9	9	6	9	8	8
	500	6.5	7.5	6	6	8	7	6	6.5	8
	250	6	7	6.5	6	6	8	6	6.5	6.5
	125	6	6.5	6	6	6	7	6	6	6
L_2	1000	11	12	11.5	10	11	12.5	9	9.5	9.5
	500	9	9	9.5	7	8	9	8	7	7
	250	7	6.5	6	8	7	6	6.5	6.5	6
	125	6	6.5	6	6	7	6	6	6	6
L_3	1000	10	9	9	11	11	10	10	12	13
	500	8	8	7	10	9	8	7	7	7
	250	7	7	6.5	7	8	9	6	7	6.5
	125	6	6.5	6	7	6	6	6	6	6
L_4	1000	9	9.5	11	10.5	10	10.5	12	12	10
	500	9	9.5	9	9	10	9	8	8	8.5
	250	8	7.5	8	6.5	6	6	7	7	7
	125	6.5	6.5	6	6	6	6	6	7	6
Cu-L_1	1000	12	12	12	15	14	13	12	12	10
	500	10	9.5	11	12	10	9	12	11	8
	250	8	8.5	9	10	11	8	10	10	7
	125	7	7	7	7	8	6	8	8	7
Cu-L_2	1000	15	15	12	12	11	13	14	15	15
	500	13	13	8	8	9	10	13	12	11
	250	10	10	8	8	8	9	11	11	8
	125	8	8	9	7	7	7	9	8	10
Cu-L_3	1000	13	13	12	12	12	13	14	13	12
	500	12	11	10	11	10	11	11	9	12
	250	10	8	9	8	7	10	10	10	10
	125	8	8	7	6	6	6	7	6	8
	1000	15	14	14	12	12	11	10	11	12
Cu-L_4	500	10	12	12	10	10	11	9	12	9
	250	8.5	9	10.5	8	10	9	7	7.5	8
	125	7	6	7	8	8	8	6	7	7
Amoxiclav		17	18	19	17	18	19	20	18	21
Gentamicin		20	21	22	19	20	21	19	24	18
DMSO		-	-	-	-	-	-	-	-	-

4.3.1 Antibacterial Activity of Compounds Against Various Bacteria *Staphylococcus aureus, Pseudomonas aeruginosa* and *Escherichia coli*

4.3.1.1 *Staphylococcus aureus*

At 1000 ppm, significant differences ($p < 0.05$) in zones of inhibition were observed among the various compounds against *Staphylococcus aureus* (Appendix IV). Gentamicin displayed the highest inhibition zone (20.333 mm), closely followed by Amoxiclav (19.667 mm), which was not significantly different from Gentamicin. Both antibiotics outperformed all test compounds, showcasing their superior antibacterial efficacy. Cu-L2 exhibited the highest inhibition zone among the test compounds at

14.667 mm. Additionally, Cu-L_1, L_4, and Cu-L_4 demonstrated similar inhibition zones around 11.000 mm, whereas L_2 and L_1 displayed lower zones of 9.333 mm and 8.333 mm, respectively (Table 4.6).

At 125 ppm, significant differences ($p < 0.05$) in inhibition zones were observed among the various compounds against *Staphylococcus aureus* (Appendix IV). Gentamicin displayed the highest inhibition zone (15.000 mm), closely followed by amoxiclav (14.667 mm). Both antibiotics significantly outperformed all test compounds. Among the test compounds, Cu-L_2 had the highest inhibition zone at 9.000 mm, followed by Cu-L_1 at 7.667 mm. Compounds L_4, L_3, L_1, and L_2 showed comparable inhibition zones around 6.333 mm to 6.000 mm. Additionally, DMSO exhibited no antibacterial activity, with a consistent zone of inhibition of 0.000 mm at all tested concentrations (Table 4. 6).

Table 4.6: Bioactivity of various compounds at different concentrations against *Staphylococcus aureus*

Concentration	Treatment	N	Inhibition Zones	CV (%)	LSD (α=0.05)	Mean (mm)
	Gentamicin	3	20.333[a]			
	Amoxiclav	3	19.667[a]			
	Cu-L2	3	14.667[b]			
	Cu-L3	3	13.000[bc]			
	L3	3	11.667[c]			
	Cu_L1	3	11.333[cd]	11.469	2.306	11.878
	L4	3	11.333[cd]			
1000ppm	Cu-L4	3	11.000[cd]			
	L2	3	9.333[de]			
	L1	3	8.333[e]			
	DMSO	3	0.000[f]			
	Gentamicin	3	18.667 [a]			
	Amoxiclav	3	18.333 [a]			
	Cu-L2	3	12.000 [b]			
	Cu-L3	3	10.667 [b]			
	Cu_L1	3	10.333 [bc]			
	Cu-L4	3	10.000 [bc]	11.469	2.306	11.878
	L4	3	8.167 [cd]			
500ppm	L2	3	7.333 [d]			
	L3	3	7.000 [d]			
	L1	3	6.833 [d]			
	DMSO	3	0.000 [e]			
	Amoxiclav	3	17.333[a]			
	Gentamicin	3	16.000[a]			
	Cu-L2	3	10.000[b]			
	Cu-L3	3	10.000[b]			
	Cu_L1	3	9.000[bc]			
	Cu-L4	3	7.500[cd]	15.450	2.283	8.727
	L4	3	7.000[cd]			
250ppm	L3	3	6.500[d]			
	L1	3	6.333[d]			
	L2	3	6.333[d]			
	DMSO	3	0.000[e]			
	Gentamicin	3	15.000 [a]			
	Amoxiclav	3	14.667 [a]			
	Cu-L2	3	9.0000 [b]			
	Cu_L1	3	7.667 [bc]			
	Cu-L3	3	7.000 [bc]			
	Cu-L4	3	6.667 [bc]	20.181	2.620	7.667
	L4	3	6.333[c]			
125ppm	L3	3	6.000[c]			
	L1	3	6.000[c]			
	L2	3	6.000[c]			
	DMSO	3	0.000 [d]			

Means followed by the same letter are not significantly different according to the LSD test at α=0.05.

4.3.1.2 *Pseudomonas aeruginosa*

At 1000 ppm, significant differences ($p < 0.05$) in inhibition zones were observed among various compounds against *Pseudomonas aeruginosa* (Appendix V). Gentamicin demonstrated the highest inhibition zone (20.000 mm), followed by

Amoxiclav (18.000 mm). Among the test compounds, Cu-L_1 exhibited a notable inhibition zone of 14.000 mm, followed by Cu-L3 (12.333 mm). Compound L_1 showed a lower inhibition zone of 8.000 mm (Table 4.7). At 500 ppm, significant differences ($p < 0.05$) in inhibition zones were observed among various compounds against *Pseudomonas aeruginosa* (Appendix V). Gentamicin exhibited the highest inhibition zone (18.000 mm), followed by Amoxiclav (16.667 mm). Among the test compounds, Cu-L_3 displayed an inhibition zone of 10.667 mm. The lowest inhibition zone was observed with compound L1 at 7.000 mm (Table 4.7). At 250 ppm, significant differences ($p < 0.05$) in inhibition zones were observed among various compounds against *Pseudomonas aeruginosa* (Appendix V). Gentamicin and Amoxiclav exhibited the highest inhibition zones, with mean diameters of 16.000 mm and 15.000 mm, respectively. Among the test compounds, Cu-L_1 displayed an inhibition zone of 9.667 mm, followed by Cu-L_4 with 9.000 mm. L_4 showed the lowest inhibition zone of 6.167 mm (Table 4.7). At 125 ppm, significant differences ($p < 0.05$) in inhibition zones were observed among various compounds against *Pseudomonas aeruginosa* (Appendix V).

Table 4.7: Bioactivity of various compounds at different concentrations against *Pseudomonas aeruginosa*

Concentration	Treatment	N	Inhibition Zones	CV (%)	LSD (α=0.05)	Mean (mm)
	Gentamicin	3	20.000[a]			
	Amoxiclav	3	18.000[b]			
	Cu_L1	3	14.000[c]			
	Cu-L3	3	12.333[d]			
	Cu-L2	3	12.000[de]			
	Cu-L4	3	11.667[def]	8.046	1.587	11.652
	L2	3	11.167[def]			
1000ppm	L3	3	10.667[ef]			
	L4	3	10.333[f]			
	L1	3	8.000[g]			
	DMSO	3	0.000[h]			
	Gentamicin	3	18.000[a]			
	Amoxiclav	3	16.667[a]			
	Cu-L3	3	10.667[b]			
	Cu-L4	3	10.333[bc]			
	Cu_L1	3	10.333[bc]			
	L4	3	9.333[bcd]	9.519	1.587	9.848
	Cu-L2	3	9.000[cd]			
500ppm	L3	3	9.000[cd]			
	L2	3	8.000[de]			
	L1	3	7.000[e]			
	DMSO	3	0.000[f]			
	Gentamicin	3	16.000[a]			
	Amoxiclav	3	15.000[a]			
	Cu_L1	3	9.667[b]			
	Cu-L4	3	9.000[b]			
	Cu-L2	3	8.333[bc]			
	Cu-L3	3	8.333[bc]	13.373	1.939	8.561
	L3	3	8.000[bcd]			
250ppm	L2	3	7.000[cd]			
	L1	3	6.667[cd]			
	L4	3	6.167[d]			
	DMSO	3	0.000[e]			
	Gentamicin	3	15.000 [a]			
	Amoxiclav	3	14.000 [a]			
	Cu_L1	3	8.000 [b]			
	Cu-L4	3	7.000 [bc]			
	Cu-L2	3	7.000 [bc]			
	Cu-L3	3	6.333 [bc]	14.583	1.841	7.454
	L3	3	6.333 [bc]			
125ppm	L2	3	6.333 [bc]			
	L1	3	6.000 [c]			
	L4	3	6.000 [c]			
	DMSO	3	0.0000 [d]			

Means followed by the same letter are not significantly different according to the LSD test at α=0.05.

Gentamicin exhibited the highest inhibition zone (15.000 mm), followed closely by Amoxiclav (14.000 mm). Among the test compounds, Cu-L1 exhibited an inhibition zone of 8.000 mm, followed by Cu-L4. L1 and L4 both exhibited inhibition zones of 6.000 mm each (Table 4.7).

4.3.1.3 *Escherichia coli*

At 1000 ppm, significant differences ($p < 0.05$) in inhibition zones were observed among various compounds against *Escherichia coli* (Appendix VI). Gentamicin demonstrated the highest inhibition zone (21.000 mm), followed by Amoxiclav (18.000 mm). Among the test compounds, Cu-L_4 exhibited a notable inhibition zone (14.333 mm), followed by Cu-L_2 (14.000 mm). Compounds L_3 and L_1 exhibited lower inhibition zones of 9.333 mm and 7.333 mm, respectively (Table 4.8). At 500 ppm, significant differences ($p < 0.05$) were also observed (Appendix VI). Gentamicin again demonstrated the highest inhibition zone (19.000 mm), followed by Amoxiclav (16.667 mm). Among the test compounds, Cu-L_2 and Cu-L_4 exhibited notable inhibition zones of 11.333 mm. Compound L_1 exhibited a lower inhibition zone of 6.667 mm (Table 4.8).

At 250 ppm, significant differences ($p < 0.05$) in inhibition zones were observed (Appendix VI). Gentamicin demonstrated the highest inhibition zone (17.667 mm), followed by Amoxiclav (13.667 mm). Among the test compounds, Cu-L_2 and Cu-L_4 exhibited inhibition zones of 9.333 mm, followed by Cu-L_3 (9.000 mm). Compounds L_3 and L_1 exhibited lower inhibition zones of 6.500 mm each (Table 4.8).

Table 4.8: Bioactivity of various compounds at different concentrations against *Escherichia coli*

Concentration	Treatment	N	Inhibition Zones	CV (%)	LSD (α=0.05)	Mean (mm)
	Gentamicin	3	21.000[a]			
	Amoxiclav	3	18.000[b]			
	Cu-L4	3	14.333[c]			
	Cu-L2	3	14.000[cd]			
	Cu-L3	3	12.667[de]			
	Cu_L1	3	12.000[de]	7.064	1.414	11.818
	L2	3	11.500[e]			
1000ppm	L4	3	9.833[f]			
	L3	3	9.333[f]			
	L1	3	7.333[g]			
	DMSO	3	0.000[h]			
	Gentamicin	3	19.000[a]			
	Amoxiclav	3	16.667[b]			
	Cu-L2	3	11.333[c]			
	Cu-L4	3	11.333[c]			
	Cu-L3	3	11.000[cd]			
	Cu_L1	3	10.167[cd]	11.703	2.021	10.196
	L2	3	9.167[de]			
500ppm	L4	3	9.167[de]			
	L3	3	7.667[ef]			
	L1	3	6.667[f]			
	DMSO	3	0.000[g]			
	Gentamicin	3	17.667[a]			
	Amoxiclav	3	13.667[b]			
	Cu-L2	3	9.333[c]			
	Cu-L4	3	9.333[c]			
	Cu-L3	3	9.000[c]			
	Cu_L1	3	8.500[cd]	14.497	2.021	8.651
	L2	3	7.833[cde]			
250ppm	L4	3	6.833[de]			
	L3	3	6.500[e]			
	L1	3	6.500[e]			
	DMSO	3	0.000[f]			
	Gentamicin	3	16.667[a]			
	Amoxiclav	3	12.667[b]			
	Cu-L2	3	8.333[c]			
	Cu-L3	3	7.667[c]			
	Cu_L1	3	7.000[c]			
	Cu-L4	3	6.667[c]	13.121	1.693	7.632
	L4	3	6.333[c]			
125ppm	L3	3	6.167[c]			
	L1	3	6.167[c]			
	L2	3	6.167[c]			
	DMSO	3	0.000[f]			

Means followed by the same letter are not significantly different according to the LSD test at α=0.05.

At 125 ppm, significant differences ($p < 0.05$) were observed (Appendix VI). Gentamicin demonstrated the highest inhibition zone (16.667 mm), followed by Amoxiclav (12.667 mm). Among the test compounds, Cu-L_2 exhibited a notable inhibition zone of 8.333 mm, while compound L2 showed a lower inhibition zone of 6.167 mm (Table 4.8).

4.3.1.4 Comparison of Bioactivity of Tested Compounds with Gentamicin and Amoxiclav

There was a significant ($p < 0.05$) difference in the bioactivity of Gentamicin, Amoxiclav, and compound L_1 against the three test organisms (*E. coli*, *P. aeruginosa*, and *S. aureus*) (Appendix VII). Higher bioactivity was observed with Gentamicin (21.0 mm for *E. coli*, 20.0 mm for *P. aeruginosa*, and 20.3 mm for *S. aureus*). Compound L_1 did not display significant bioactivity against the three test organisms (Figure 12).

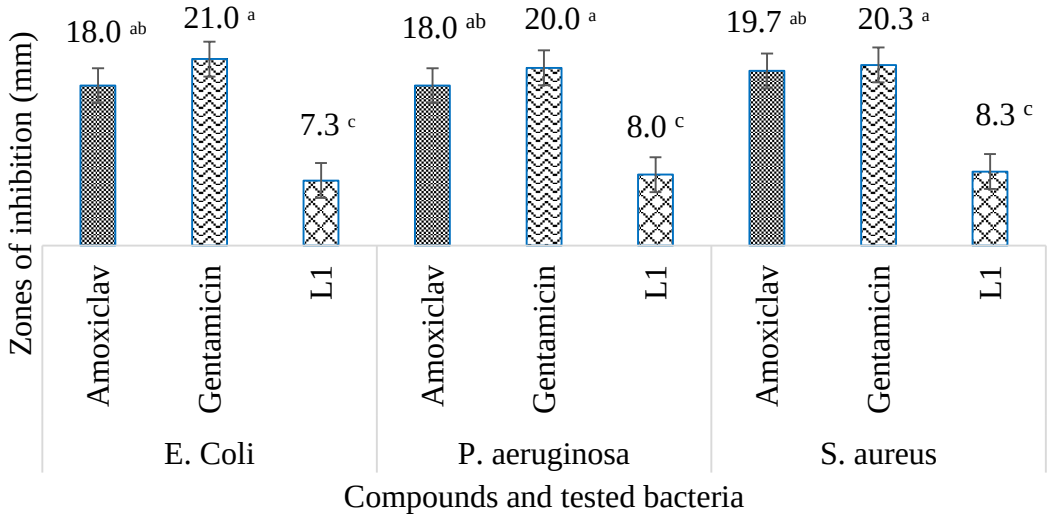

Figure 12: Bioactivity of L_1 against *E. Coli, P. aeruginosa*, and *S. aureus* compared to standard antibiotics (Amoxiclav and Gentamicin). Means followed by the same letter are not significantly different according to the LSD test at α=0.05

There was a significant ($p < 0.05$) difference in the bioactivity of Gentamicin, Amoxiclav, and compound L2 against the three test organisms [(*E. coli*, *P. aeruginosa*, and *S. aureus*) Appendix VIII]. Higher bioactivity was observed with Gentamicin, with zones of inhibition measuring 21.0 mm for *E. coli*, 20.0 mm for *P. aeruginosa*, and 20.3 mm for *S. aureus*.

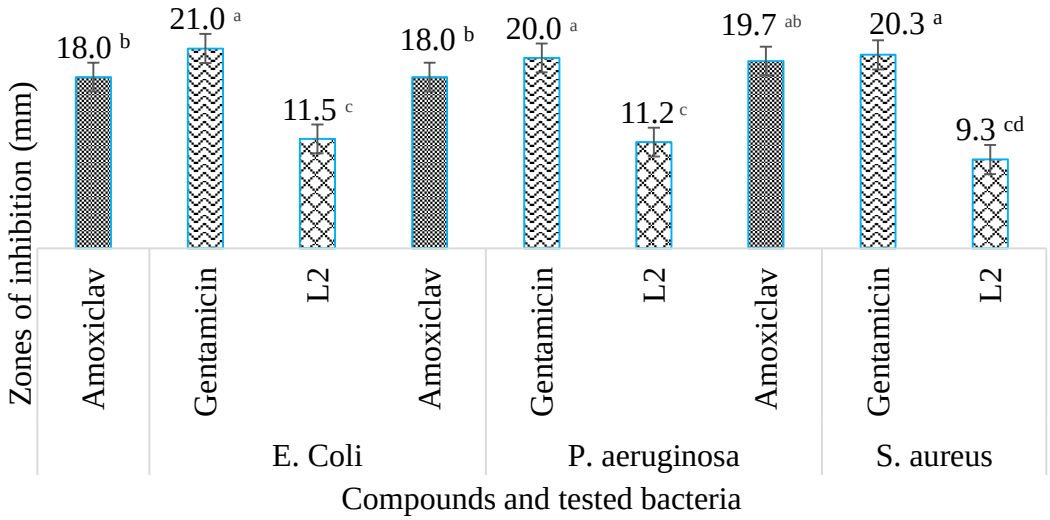

Figure 13: Bioactivity of L_2 against *E. Coli, P. aeruginosa, and S. aureus* compared to standard antibiotics (Amoxiclav and Gentamicin). Means followed by the same letter are not significantly different according to the LSD test at α=0.05.

Gentamicin had the largest zones of inhibition for all three bacteria, but its bioactivity was not significantly different from that of Amoxiclav. Compound L2 did not display significant bioactivity against the three test organisms (Figure 13).

There was a significant ($p < 0.05$) difference in the bioactivity of Gentamicin, Amoxiclav, and compound L3 against the three test organisms (*E. coli*, *P. aeruginosa*, and *S. aureus*) (Appendix IX). Higher bioactivity was observed with Gentamicin, with zones of inhibition measuring 21.0 mm for *E. coli*, 20.0 mm for *P. aeruginosa*, and 20.3 mm for *S. aureus*. Gentamicin had the largest zones of inhibition for all three bacteria, but its bioactivity was not significantly different from that of Amoxiclav. Compound L3 did not display significant bioactivity against the three test organisms (Figure 14).

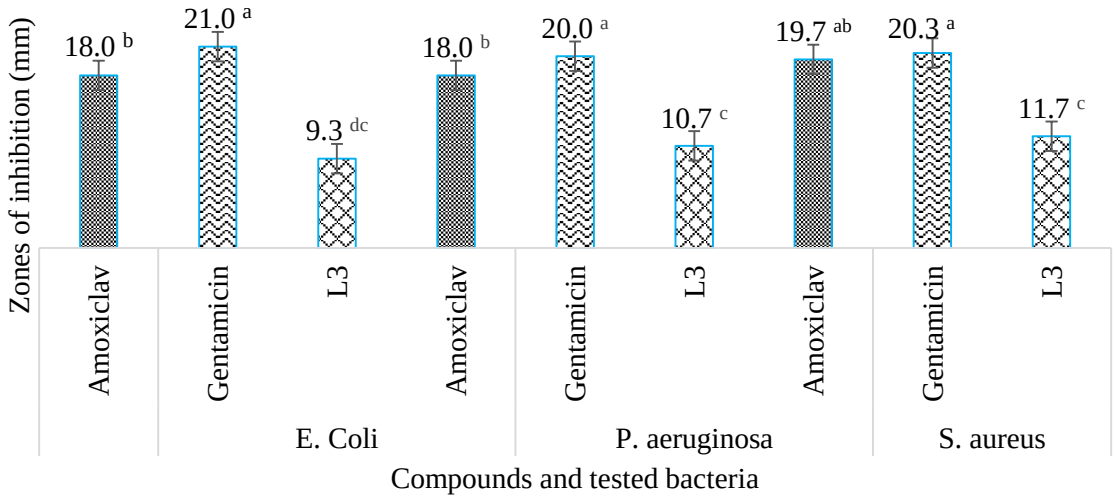

Figure 14: Bioactivity of L_3 against *E. Coli, P. aeruginosa, and S. aureus* compared to standard antibiotics (Amoxiclav and Gentamicin). Means followed by the same letter are not significantly different according to the LSD test at α=0.05.

There was a significant ($p < 0.05$) difference in the bioactivity of Gentamicin, Amoxiclav, and compound L4 against the three test organisms (*E. coli*, *P. aeruginosa*, and *S. aureus*) (Appendix X). Higher bioactivity was observed with Gentamicin, with zones of inhibition measuring 21.0 mm for *E. coli*, 20.0 mm for *P. aeruginosa*, and 20.3 mm for *S. aureus*. Gentamicin had the largest zones of inhibition for all three bacteria, but its bioactivity was not significantly different from that of Amoxiclav. Compound L4 did not display significantly different bioactivity against the three test organisms (Figure 15).

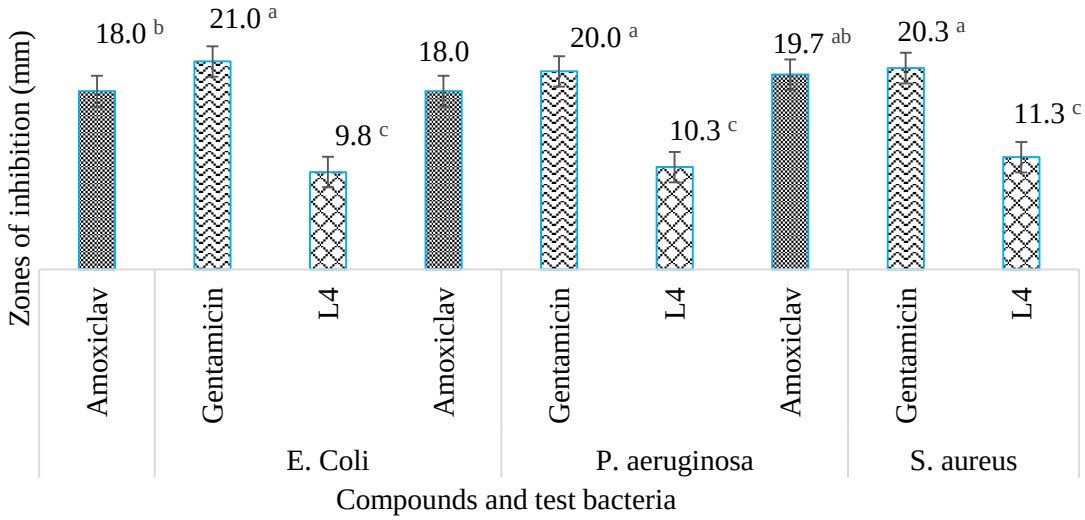

Figure 15: Bioactivity of L_4 against *E. Coli, P. aeruginosa, and S. aureus* compared to standard antibiotics (Amoxiclav and Gentamicin)

There was a significant ($p < 0.05$) difference in the bioactivity of Gentamicin, Amoxiclav, and compound Cu-L_1 against the three test organisms (*E. coli*, *P. aeruginosa*, and *S. aureus*) (Appendix XI). Higher bioactivity was observed with Gentamicin, with zones of inhibition measuring 21.0 mm for *E. coli*, 20.0 mm for *P. aeruginosa*, and 20.3 mm for *S. aureus*. Gentamicin had the largest zones of inhibition for all three bacteria, but its bioactivity was not significantly different from that of Amoxiclav. Compound Cu-L_1 exhibited a significantly larger inhibition zone against *S. aureus* (14.0 mm) than *E. coli* and *P. aeruginosa* (Figure 16).

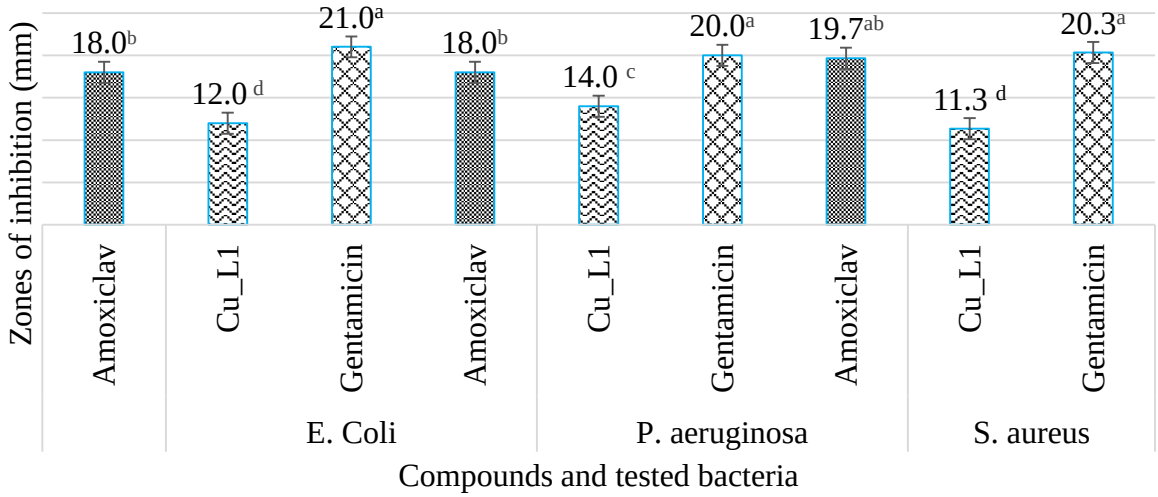

Figure 16: Bioactivity of Cu-L_1 against *E. Coli, P. aeruginosa, and S. aureus* compared to standard antibiotics (Amoxiclav and Gentamicin). Means followed by the same letter are not significantly different according to the LSD test at α=0.05.

There was a significant ($p < 0.05$) difference in the bioactivity of Gentamicin, Amoxiclav, and compound Cu-L2 against the three test organisms (*E. coli*, *P. aeruginosa*, and *S. aureus*) (Appendix XII). Higher bioactivity was observed with Gentamicin, with zones of inhibition measuring 21.0 mm for *E. coli*, 20.0 mm for *P. aeruginosa*, and 20.3 mm for *S. aureus*. Gentamicin had the largest zones of inhibition for all three bacteria, but its bioactivity was not significantly different from that of Amoxiclav. Compound Cu-L2 had significantly higher inhibition against *S. aureus* with a zone of 14.7 mm (Figure 17).

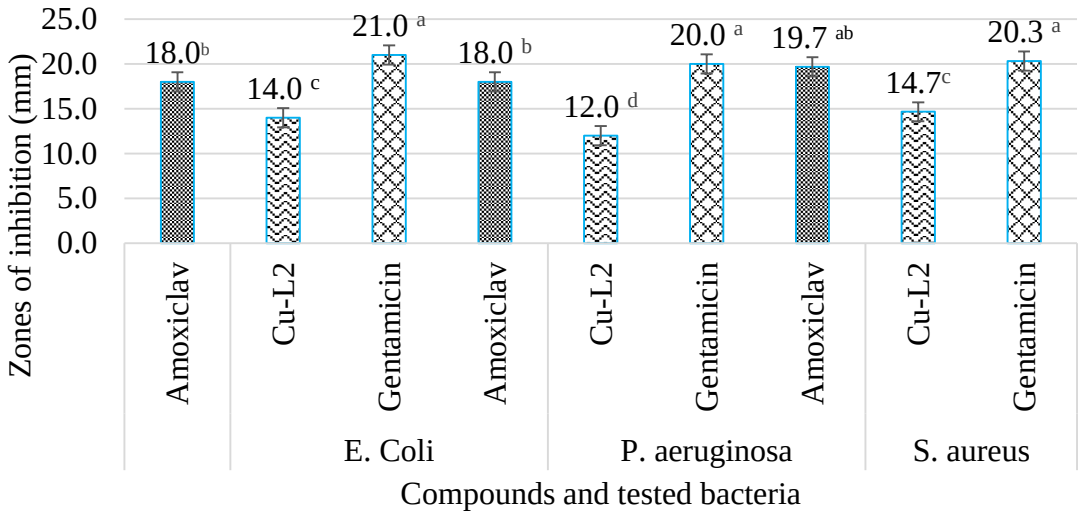

Figure 17: Bioactivity of Cu-L_2 against *E. Coli, P. aeruginosa, and S. aureus* compared to standard antibiotics (Amoxiclav and Gentamicin). Means followed by the same letter are not significantly different according to the LSD test at α=0.05.

There was a significant ($p < 0.05$) difference in the bioactivity of Gentamicin, Amoxiclav, and compound Cu-L_3 against the three test organisms (*E. coli*, *P. aeruginosa*, and *S. aureus*) (Appendix XIII). Higher bioactivity was observed with Gentamicin, with zones of inhibition measuring 21.0 mm for *E. coli*, 20.0 mm for *P. aeruginosa*, and 20.3 mm for *S. aureus*. Gentamicin had the largest zones of inhibition for all three bacteria, but its bioactivity was not significantly different from that of Amoxiclav. Compound Cu-L_3 did not exhibit significantly different bioactivity against these test bacteria (Figure 18).

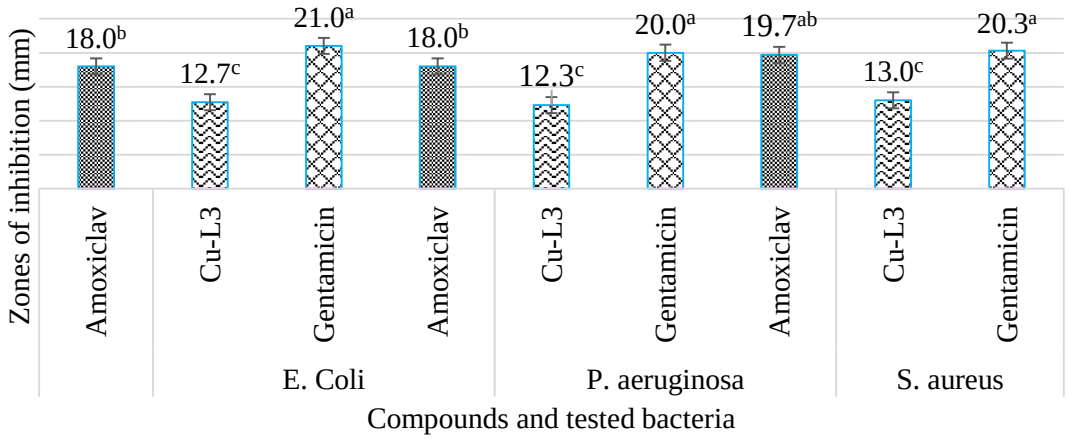

Figure 18: Bioactivity of Cu-L_3 against *E. Coli, P. aeruginosa, and S. aureus* compared to standard antibiotics (Amoxiclav and Gentamicin). Means followed by the same letter are not significantly different according to the LSD test at α=0.05.

There was a significant ($p < 0.05$) difference in the bioactivity of Gentamicin, Amoxiclav, and compound Cu-L_4 against the three test organisms (*E. coli*, *P. aeruginosa*, and *S. aureus*) (Appendix XIV). Gentamicin exhibited higher bioactivity, with zones of inhibition measuring 21.0 mm for *E. coli*, 20.0 mm for *P. aeruginosa*, and 20.3 mm for *S. aureus*. While Gentamicin had the largest zones of inhibition for all three bacteria, its bioactivity was not significantly different from that of Amoxiclav. Compound Cu-L_4 displayed a significantly larger inhibition zone against *E. coli* (14.3 mm) compared to *P. aeruginosa* and *S. aureus* (Figure 19).

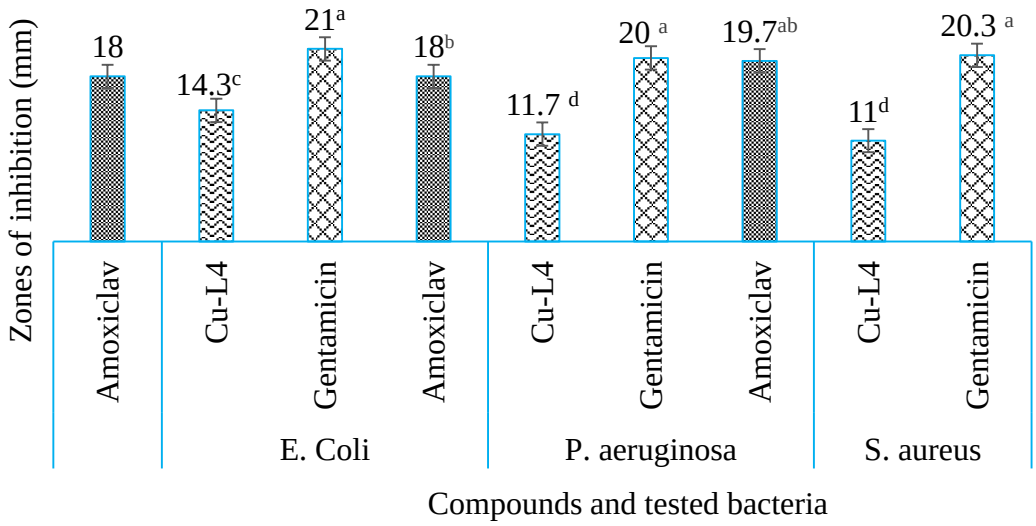

Figure 19: Bioactivity of Cu-L_4 against *E. Coli, P. aeruginosa, and S. aureus* compared to standard antibiotics (Amoxiclav and Gentamicin). Means followed by the same letter are not significantly different according to the LSD test at α=0.05.

4.3.1.5 Discussion of Antibacterial Activities Results

All synthesized Schiff base ligands and their Cu (II) complexes demonstrated antibacterial activities against selected bacteria strains (Rosu *et al.*, 2011); Kargar *et al.*, 2021). This could be due to the present azomethine bonds in synthesized Schiff base ligands and Cu (II) complexes responsible for their antibacterial activities. Results based on synthesized Schiff bases and corresponding metal complexes revealed (table 4.5) metal complexes showed higher antibacterial activities than the free ligands (Salehi *et al.*, 2016). Cu-L_2 showed the highest activity against S. *aureus* (Table 4.5), while Cu-L_4 and Cu-L_1 showed the maximum inhibition zone against *E. coli* and *P. aeruginosa* at 1000 ppm. Cu-L_1, Cu-L_2, Cu-L_3 and Cu-L_4 showed slightly higher activities (plate 4-6) than L_1, L_2, L_3 and L_4 against *E. coli*, *S. aureus* and *P. aeruginosa*. The synthesized

ligands L_1, L_2, L_3 and L_4 (Table 4.5) were mildly active against all selected bacteria strains due to the presence of azomethine and hydroxy groups, which led to the formation of hydrogen bonding in the active centres of the cells constituting cell membrane active centres and therefore the permeability was increased (Erturk, 2020; Kargar *et al*., 2021).

Ligand L_2 bears methyl group in phenyl ring show better activity against all the tested bacteria strains. This suggests that a methyl group has an essential contribution to the antibacterial activity of this compound (Bazzini & Wermuth, 2008). Usually, introducing a methyl group into the structure of a bioactive compound increases its lipophilicity, which improves cell membrane permeability (Bockus *et al*., 2015). Several publications have pointed out that incorporating the methyl group helps improve the antibacterial activities of compounds (Alterhoni *et al*., 2021). Ligand L_3 bears two nitro groups, one at the para position and the other at the ortho position. Incorporating two nitro groups improves the antibacterial activity of this compound (Noriega *et al*., 2022). Ligand L_4 bears -COOH group show better activity against *S. aureus*, moderate activity against *P. aeruginosa* and low activity against *E. coli*. This observation suggests that incorporating the carboxyl group improves the antibacterial activity of this compound (Kariuki and Njagi, 2018).

Transition metal ions have also been used to modify the antibacterial activities of Schiff base ligands. In most cases, metal complexes are bioactive compounds that have been found to demonstrate better activities than their corresponding free ligands (Kumar *et al*., 2023). In the present study, Cu (II) complexes of the Schiff base ligands have been synthesized and their antibacterial activities have been determined alongside free ligands (Sunitha *et al*., 2012).). The results of antibacterial activities are consistent with previous findings in recent publications that revealed that metal complexes of Schiff base ligands also possess antibacterial properties (Awolope *et al*., 2023). The copper (II) complex formed in a 2:1 (L: M) ratio, increasing bulkiness and activity. Thus, the action of nitrogen and oxygen donor atoms in the synthesized free ligands bound to metal ions creating chelates is responsible for the complexes' improved biological activity against the tested bacteria strains compared to the free Schiff base (Saritha & Metilda, 2021). The higher antibacterial activity of synthesized copper complexes

could be attributed to their solubility, particle fitness, metal ion size, and the inclusion of bulkier organic moieties. Other factors boosting synthesised compounds' activity are solubility, conductivity, dipole moment, cell permeability mechanism (influenced by metal ions), and bond length between the metal and ligand (Bennour *et al*., 2022). The mode of action of copper complexes involves the formation of hydrogen bonds with the azomethine group by the active sites, leading to interference with cell wall synthesis (Khan *et al.*, 2021; Zafar *et al.*, 2023). The increased antibacterial activity of the metal complexes can be explained using Overtone's cell permeability concept. Liposolubility is essential to antibacterial activity (Beyene *et al*., 2020). The polarity of the ligand orbital during chelation, together with the partial sharing of the metal ion's positive charge with donor groups, promotes the lipophilicity of the complex by increasing the delocalization of π-electrons throughout the entire chelates ring (Yousef *et al*., 2019). This increased lipophilicity enhances the penetration of the complexes into lipid membranes and blocks the metal binding sites on enzymes of microorganisms (Raman *et al*., 2020).

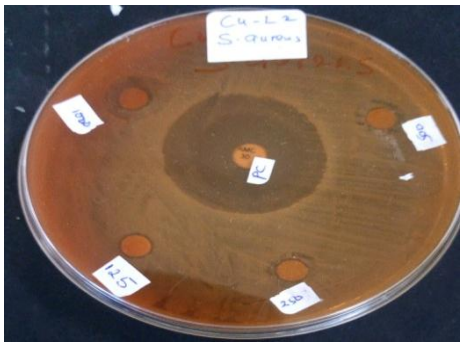

Plate 5: Zone of inhibition of Cu-L_2 complex against *Staphylococcus aureus*

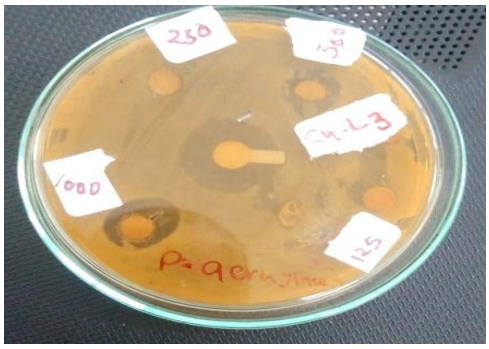

Plate 6: Zone of inhibition of Cu-L_3 complex against *Pseudomonas aeruginosa*

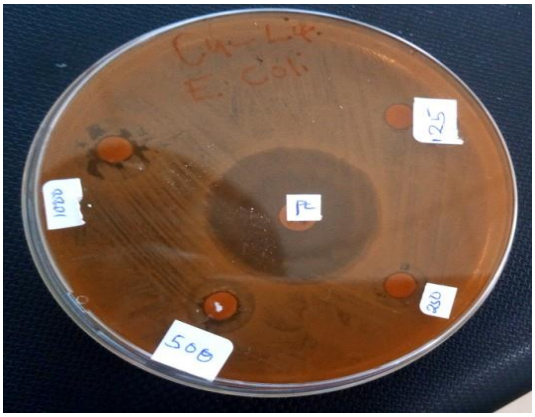

Plate 7: Zone of inhibition of Cu-L_4 complex against *Escherichia coli*

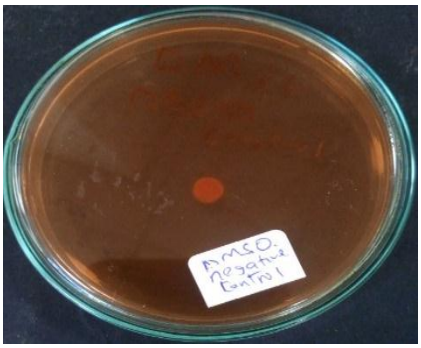

Plate 8: Zone of inhibition of DMSO against *Escherichia coli*

CHAPTER FIVE
CONCLUSION AND RECOMMENDATION

5.1 Summary

New Schiff base ligands and their Cu (II) complexes were successfully synthesized in the present work. Different analytical techniques were employed to elucidate these compounds' structural and physical properties. The techniques used included Fourier Transform Infrared (FT-IR) spectroscopy, ultra-violet /Visible (UV-vis) spectroscopy, proton nuclear magnetic resonance (^{1}H NMR) and molar conductivity measurements. The FT-IR and NMR data of the Schiff base ligands displayed the absence of NH_2 and C=O, confirming the formation of the azomethine group (-HC=N-). At the same time, those complexes showed the formation of Cu-O and Cu-N upon complexation of the Schiff base ligands. Thus, the synthesized Schiff base was suggested to be a bidentate ligand of NO type. Electronic spectra data of the Cu (II) complexes revealed the existence of ligand-metal charge transfer transitions. Molar conductivity data showed that the synthesized Schiff base ligands and their Cu (II) complexes were non-ionic.

The synthesized Schiff base ligands and their Cu (II) complexes were screened for antibacterial activities against gram-positive and gram-negative *Pseudomonas aeruginosa*, *Escherichia coli*, and one gram-positive *Staphylococcus aureus*. The inhibition zones were observed on all the test compounds in four concentrations. This revealed that all the synthesized compounds were active against the tested bacteria strains, but no test compound displayed better antibacterial activity than Gentamycin and Amoxiclav. *E. coli* showed the highest zones of inhibition among the three bacteria tested. This indicated that *Escherichia coli* is most susceptible to the synthesized compounds, followed by *Pseudomonas aeruginosa*, and *Staphylococcus aureus* is the least susceptible. This implies that these synthesized compounds can be the best antibacterial agents for gram-negative but less suitable for gram-positive bacteria. Cu (II) complexes displayed zones of inhibition close to that of gentamycin and Amoxiclav. This could be due to the presence of the methyl group, an electron-donating group in the ligand L_2, and nitro and Carboxylic, both electrons withdrawing groups in L_3 and L_4 structures. This reveals that introducing electron-donating and electron-withdrawing groups in the structure of Schiff base ligands increases the antibacterial

activity of both free ligands and their Cu (II) complexes. Lastly, Copper (II) complexes displayed higher antibacterial activity than the corresponding Schiff base.

5.2 Conclusion

It was that concluded as follows:

i. The Schiff base ligands and its Cu (II) complexes were successfully synthesized and characterized.
ii. The FT-IR, UV-vis, and ^{1}H NMR spectral studies showed that the Schiff base ligands coordinated to the Cu (II) ion via the azomethine nitrogen and phenolic oxygen.
iii. Octahedral structure has been suggested for the Cu (II) complexes.
iv. Based on molar conductance data, the synthesized Schiff base and their Cu (II) complexes are non-electrolytes.
v. The Cu (II) complexes exhibited enhanced antibacterial properties relative to the parent ligand under the same experimental conditions.
vi. Cu-L_4 complex was the most effective against the three tested bacteria while *S. aureus* was the most resistant bacterial strain.
vii. The inhibitory ability of the Schiff base ligands and their Cu (II) complexes towards selected bacterial strains increased with increasing concentration.

5.3 Recommendation of the Study

From this study the following were recommended for future studies:

i. Only the antibacterial activity of the synthesized Schiff base and their corresponding Cu (II) complexes were studied. Other biological properties of these compounds should be considered, such as antiviral, antifungal, antimalarial, antiproliferative, and anti-inflammatory properties.
ii. Catalytic and electrochemical activities of synthesized Cu (II) complexes should be investigated.
iii. It is also recommended that synthesized Schiff base ligands were only complex with Cu (II) ions; thus, there is a need to complex with other transitional metals such as Co (II), Zn (II), Ni (II) and Mn (II) ions to design more potent antibacterial agents for the treatment of some common diseases caused by *E. coli*, *P. aeruginosa* and *S. aureus.*

iv. 2-hydroxy-4-methoxybenzophenone can be condensed with other electron-withdrawing and donating groups to develop a better antibacterial compound.

REFERENCES

Abd El-halim, H. F., Omar, M. M., & Mohamed, G. G. (2011). Synthesis, structural, thermal studies and biological activity of a tridentate Schiff base ligand and their transition metal complexes. *Spectrochimica Acta Part A: Molecular and Biomolecular Spectroscopy*, *78*(1), 36-44.

Abdel- Rahman, L. H., AbuDief, A. M., Moustafa, H., & Hamdan, S. K. (2017). Ni (II) and Cu (II) complexes with ONNO asymmetric tetradentate Schiff base ligand: synthesis, spectroscopic characterization, theoretical calculations, DNA interaction and antimicrobial studies. *Applied Organometallic Chemistry*,*31*(2), e3555.

Abdel-Rahman, L. H., Basha, M. T., Al-Farhan, B. S., Alharbi, W., Shehata, M. R., Al Zamil, N. O., & Abou El-ezz, D. (2023). Synthesis, characterization, DFT studies of novel Cu (II), Zn (II), VO (II), Cr (III), and La (III) chloro-substituted Schiff base complexes: aspects of its antimicrobial, antioxidant, anti-inflammatory, and photodegradation of methylene blue. *Molecules*, *28*(12), 4777.

Abendrot, M., Chęcińska, L., Kusz, J., Lisowska, K., Zawadzka, K., Felczak, A., & Kalinowska-Lis, U. (2020). Zinc (II) complexes with amino acids for potential use in dermatology: Synthesis, crystal structures, and antibacterial activity. *Molecules*, *25*(4), 951.

Abousaty, A. I., Reda, F. M., Hassanin, W. A., Felifel, W. M., El-Shwiniy, W. H., Selim, H. M., & Bendary, M. M. (2024). Sorbate metal complexes as newer antibacterial, antibiofilm, and anticancer compounds. *BMC Microbiology*, *24*(1), 1-17.

Abuamer, K.M., Maihub, A.A., El-Ajaily, M.M., Etorki, A.M., Abou-Krisha, M.M. and Almagani, M.A. (2014) The Role of Aromatic Schiff Bases in the Dyes Techniques. *International Journal of Organic Chemistry*, 4, 7-15.

Abubakar, S., Shallangwa, G. A., & Ibrahim, A. (2024). Syntheses and determination of activities of some metal (II) complexes with derivatives of a novel vanillin–tryptophan Schiff base ligand. *Journal of Umm Al-Qura University for Applied Sciences*, 1-11.

Abu-Dief, A. M., El-dabea, T., El-Khatib, R. M., Abdou, A., & El-Remailya, M. A. E. A. A. A. (2024). Development of new mixed Cu (II) chelate based on 2-benzimidazolylguanidine and phenanthroline ligands: Structural elucidation, biological evaluation, DFT and docking approaches. *Sohag Journal of Sciences*, *9*(2), 174-185.

Abushaheen, M. A., Fatani, A. J., Alosaimi, M., Mansy, W., George, M., Acharya, S., & Jhugroo, P. (2020). Antimicrobial resistance, mechanisms and its clinical significance. *Disease-a-Month*, *66*(6), 100971.

Abu-Yamin, A. A., Abduh, M. S., Saghir, S. A. M., & Al-Gabri, N. (2022). Synthesis, characterization and biological activities of new Schiff base compound and its lanthanide complexes. *Pharmaceuticals*, *15*(4), 454.

Adeolu, M., Alnajar, S., Naushad, S., & S. Gupta, R. (2016). Genome-based phylogeny and taxonomy of the 'Enterobacteriales': proposal for Enterobacterales ord. Nov. divided into the families Enterobacteriaceae, Erwiniaceae fam. nov., Pectobacteriaceae fam. nov., Yersiniaceae fam. nov., Hafniaceae fam. nov., Morganellaceae fam. nov., and Budviciaceae fam. nov. *International Journal of Systematic and Evolutionary Microbiology*, *66*(12), 5575-5599.

Ahmad, F., Zhu, D., & Sun, J. (2021). Environmental fate of tetracycline antibiotics: degradation pathway mechanisms, challenges, and perspectives. *Environmental Sciences Europe*, *33*(1), 64.

Al-Fakeh, M. S., Alsikhan, M. A., Alnawmasi, J. S., Alluhayb, A. H., & Al-Wahibi, M. S. (2024). New Nanosized V (III), Fe (III), and Ni (II) complexes comprising Schiff base and 2- amino- 4- methyl pyrimidine: Synthesis, properties, and biological activity. *International Journal of Biomaterials*, *2024*(1), 9198129.

Ali M. F., & Yunus, V. M. (2014). Microwave synthesis & antimicrobial activity of some Cu (II), Co (II), Ni (II) & Cr (III) complexes with Schiff base 2, 6-pyridinedicarboxaldehyde thiosemicabazone. *Oriental Journal of Chemistry*, *30*(1), 111-117.

Ali, I., Wani, W. A., & Saleem, K. (2013). Empirical formulae to molecular structures of metal complexes by molar conductance. *Synthesis and Reactivity in Inorganic, Metal-organic, and Nano-metal Chemistry*, *43*(9), 1162-1170.

Ali, M. A., Musthafa, S. A., Munuswamy-Ramanujam, G., & Jaisankar, V. (2022). 3-Formylindole-based chitosan Schiff base polymer: Antioxidant and *in vitro* cytotoxicity studies on THP-1 cells. *Carbohydrate Polymers*, *290*, 119501.

Almáši, M., Vilková, M., & Bednarčík, J. (2021). Synthesis, characterization and spectral properties of novel azo-azomethine-tetracarboxylic Schiff base ligand and its Co (II), Ni (II), Cu (II) and Pd (II) complexes. *Inorganica Chimica Acta*, *515*, 120064.

Alpert, N. L., Keiser, W. E., & Szymanski, H. A. (2012). *IR: Theory and Practice of Infrared Spectroscopy*. Springer Science & Business Media.

Al-Qahtani, S. D., Alsoliemy, A., Almehmadi, S. J., Alkhamis, K., Alrefaei, A. F., Zaky, R., & El-Metwaly, N. (2021). Green synthesis for new Co (II), Ni (II), Cu (II) and Cd (II) hydrazone-based complexes; characterization, biological activity and electrical conductance of nano-sized copper sulphate. *Journal of Molecular Structure*, *1244*, 131238.

Al-Radadi, N. S., Zayed, E. M., Mohamed, G. G., & Abd El Salam, H. A. (2020). Synthesis, spectroscopic characterization, molecular docking, and evaluation of antibacterial potential of transition metal complexes obtained using triazole chelating ligand. *Journal of Chemistry*, *2020*(1), 1548641.

Alshaheri, A. A., Tahir, M. I. M., Rahman, M. B. A., Begum, T., & Saleh, T. A. (2017). Synthesis, characterisation and catalytic activity of dithiocarbazate Schiff base complexes in oxidation of cyclohexane. *Journal of Molecular Liquids*, *240*, 486-496.

Alterhoni, E., Tavman, A., Hacioglu, M., Şahin, O., & Tan, A. S. B. (2021). Synthesis, structural characterization and antimicrobial activity of Schiff bases and benzimidazole derivatives and their complexes with $CoCl_2$, $PdCl_2$, $CuCl_2$ and $ZnCl_2$. *Journal of Molecular Structure*, *1229*, 129498.

Amer, S., El-Wakiel, N., & El-Ghamry, H. (2013). Synthesis, spectral, antitumor and antimicrobial studies on Cu (II) complexes of purine and triazole Schiff base derivatives. *Journal of Molecular Structure*, *1049*, 326-335.

Anacona, J. R., Rodriguez, J. L., & Camus, J. (2014). Synthesis, characterization and antibacterial activity of a Schiff base derived from cephalexin and sulphathiazole and its transition metal complexes. *Spectrochimica Acta Part A: Molecular and Biomolecular Spectroscopy*, *129*, 96-102.

Arendsen, L. P., Thakar, R., & Sultan, A. H. (2019). The use of copper as an antimicrobial agent in health care, including obstetrics and gynecology. *Clinical Microbiology Reviews*, *32*(4), 10-1128.

Armbruster, C. E., Mobley, H. L., & Pearson, M. M. (2018). Pathogenesis of *Proteus mirabilis* infection. *EcoSal Plus*, *8*(1), 10-1128.

Arshi, N., Mohd, S., Arikatla, V. R., Daya, S. S. and Nawal, K. S. (2009). Synthesis of Schiff bases via environmentally benign and energy-efficient greener methodologies. *E-Journal of Chemistry*, 6, S75-S78.

Ashish, B., Neeti, K., & Himanshu, K. (2013). Copper toxicity: a comprehensive study. *Research Journal Recent Science*, *2*(ISC-2012), 58-67.

Ashraf, M. A., Mahmood, K., Wajid, A., Maah, M. J., & Yusoff, I. (2011). Synthesis, characterization and biological activity of Schiff bases. *IPCBEE*, *10*(1), 185.

Atkins, P., Overton, T., Rourke, J., Rourke, J., Weller, M., Armstrong, F., Hagerman, M. (2010). 'Shriver and Atkins' Inorganic Chemistry, 5th Ed. Oxford University Press, London.pp. 246-247

Awolope, R. O., Ejidike, I. P., & Clayton, H. S. (2023). Schiff base metal complexes as a dual antioxidant and antimicrobial agents. *Journal of Applied Pharmaceutical Science*, *13*(3), 132-140.

Bafana, A., Devi, S. S., & Chakrabarti, T. (2011). Azo dyes: past, present and the future. *Environmental Reviews*, *19*(NA), 350-371.

Ballatore, C., Huryn, D. M., & Smith III, A. B. (2013). Carboxylic acid (bio) isosteres in drug design. *ChemMedChem*, *8*(3), 385-395.

Balouiri, M., Sadiki, M., & Ibnsouda, S. K. (2016). Methods for *in vitro* evaluating antimicrobial activity: A review. *Journal of Pharmaceutical Analysis*, *6*(2), 71-79.

Banerjee, M., Panjikar, P. C., Das, D., Iyer, S., Bhosle, A. A., & Chatterjee, A. (2022). Grindstone chemistry: A "green" approach for the synthesis and derivatization of heterocycles. *Tetrahedron*, *112*, 132753.

Bash, M., Alghanmi, R., and Shehata, M 2019). Synthesis, structural characterization, DFT calculation, biological investigation, molecular docking and DNA binding of Co (II), Ni (II) and Cu (II) nanosized Schiff base complexes bearing pyrimidine moiety. *Journal of Molecular Biology*,1183,298-310

Bazzini, P., & Wermuth, C. G. (2008). Substituent groups. *In*: C. G. Wermuth (Ed.). *The Practice of Medicinal Chemistry* (pp. 429-463). Academic Press.

Bersuker, I. B. (2010). *Electronic structure and properties of transition metal compounds: Introduction to the Theory*. John Wiley & Sons.

Beyene, B. B., Mihirteu, A. M., Ayana, M. T., & Yibeltal, A. W. (2020). Synthesis, characterization and antibacterial activity of metalloporphyrins: Role of central metal ion. *Results in Chemistry*, *2*, 100073.

Bhagat, S., Sharma, N., & Chundawat, T. S. (2013). Synthesis of some salicylaldehyde- based Schiff bases in aqueous media. *Journal of Chemistry*, *2013*(1), 909217.

Bharadishettar, N., Bhat K, U., & Bhat Panemangalore, D. (2021). Coating technologies for copper based antimicrobial active surfaces: A perspective review. *Metals*, *11*(5), 711.

Bockus, A. T., Lexa, K. W., Pye, C. R., Kalgutkar, A. S., Gardner, J. W., Hund, K. C., & Lokey, R. S. (2015). Probing the physicochemical boundaries of cell permeability and oral bioavailability in lipophilic macrocycles inspired by natural products. *Journal of Medicinal Chemistry*, *58*(11), 4581-4589.

Bourne, C. R. (2014). Utility of the biosynthetic folate pathway for targets in antimicrobial discovery. *Antibiotics*, *3*(1), 1-28.

Boyanova, L., Gergova, G., Nikolov, R., Derejian, S., Lazarova, E., Katsarov, N., ... & Krastev, Z. (2005). Activity of Bulgarian propolis against 94 Helicobacter pylori strains in vitro by agar-well diffusion, agar dilution and disc diffusion methods. *Journal of Medical Microbiology*, *54*(5), 481-483.

Bredael, K., Geurs, S., Clarisse, D., De Bosscher, K., & D'hooghe, M. (2022). Carboxylic acid bioisosteres in medicinal chemistry: Synthesis and properties. *Journal of Chemistry*, *2022*, 1-21.

Bu, S., Jiang, G., Jiang, G., Liu, J., Lin, X., Shen, J., ... & Liao, X. (2020). Antibacterial activity of ruthenium polypyridyl complexes against *Staphylococcus aureus* and biofilms. *JBIC Journal of Biological Inorganic Chemistry*, *25*, 747-757.

Bysewski, O., Sittig, M., Winter, A., Dietzek-Ivanšić, B., & Schubert, U. S. (2024). Photobasic transition-metal complexes. *Coordination Chemistry Reviews*, *498*, 215441.

Chang, J., Lee, R. E., & Lee, W. (2020). A pursuit of *Staphylococcus aureus* continues: a role of persister cells. *Archives of Pharmacal Research*, *43*, 630-638.

Chiu, C. T., Lai, C. H., Huang, Y. H., Yang, C. H., & Lin, J. N. (2021). Comparative analysis of gradient diffusion and disk diffusion with agar dilution for susceptibility testing of Elizabethkingia anophelis. *Antibiotics*, *10*(4), 450.

Chohan, Z. H., Supuran, C. T., & Scozzafava, A. (2004). Metalloantibiotics: synthesis and antibacterial activity of cobalt (II), copper (II), nickel (II) and zinc (II) complexes of kefzol. *Journal of Enzyme Inhibition and Medicinal Chemistry*, *19*(1), 79-84.

Chopra, I., & Roberts, M. (2001). Tetracycline antibiotics: mode of action, applications, molecular biology, and epidemiology of bacterial resistance. *Microbiology and Molecular Biology Reviews*, *65*(2), 232-260.

Claudel, M., Schwarte, J. V., & Fromm, K. M. (2020). New antimicrobial strategies based on metal complexes. *Chemistry*, *2*(4), 849-899.

CLSI (2017). Performance standards for antimicrobial susceptibility testing. *CLSI supplement M100*, 106-112.

Collins, J. A., & Osheroff, N. (2024). Gyrase and Topoisomerase IV: Recycling Old Targets for New Antibacterials to Combat Fluoroquinolone Resistance. *ACS Infectious Diseases*, *10*(4), 1097-1115.

Crone, S., Vives- Flórez, M., Kvich, L., Saunders, A. M., Malone, M., Nicolaisen, M. H., ... & Bjarnsholt, T. (2020). The environmental occurrence of *Pseudomonas aeruginosa*. *Apmis*, *128*(3), 220-231.

Daravath, S., Rambabu, A., Ganji, N., Ramesh, G., & Lakshmi, P. A. (2022). Spectroscopic, quantum chemical calculations, antioxidant, anticancer, antimicrobial, DNA binding and photo physical properties of bioactive Cu (II) complexes obtained from trifluoromethoxy aniline Schiff bases. *Journal of Molecular Structure*, *1249*, 131601.

De Angelis, G., Del Giacomo, P., Posteraro, B., Sanguinetti, M., & Tumbarello, M. (2020). Molecular mechanisms, epidemiology, and clinical importance of β-lactam resistance in Enterobacteriaceae. *International Journal of Molecular ciences*, *21*(14), 5090.

de Fátima, Â., de Paula Pereira, C., Olímpio, C. R. S. D. G., de Freitas Oliveira, B. G., Franco, L. L., & da Silva, P. H. C. (2018). Schiff bases and their metal complexes as urease inhibitors–a brief review. *Journal of Advanced Research*, *13*, 113-126.

Deeth, R. J., Anastasi, A., Diedrich, C., & Randell, K. (2009). Molecular modelling for transition metal complexes: Dealing with d-electron effects. *Coordination Chemistry Reviews*, *253*(5-6), 795-816.

Dehghanpour, S., & Mahmoudi, A. (2007). Synthesis, structure, and redox properties of copper (I) complexes with phenylpyridin-2-ylmethyleneamine derivatives. *Main Group Chemistry*, *6*(2), 121-130.

Dhanaraj, C. J., & Johnson, J. (2014). Synthesis, characterization, electrochemical and biological studies on some metal (II) Schiff base complexes containing quinoxaline moiety. *Spectrochimica Acta Part A: Molecular and Biomolecular Spectroscopy*, *118*, 624-631.

Diekema, D. J., & Jones, R. N. (2001). Oxazolidinone antibiotics. *The Lancet*, *358*(9297), 1975-1982.

Dinku, D., Demissie, T. B., Beas, I. N., Eswaramoorthy, R., Abdi, B., & Desalegn, T. (2024). Antimicrobial activities and docking studies of new Schiff base ligand and its Cu (II), Zn (II) and Ni (II) Complexes: Synthesis and Characterization. *Inorganic Chemistry Communications*, *160*, 111903.

Dorenbos, P. (2017). Charge transfer bands in optical materials and related defect level location. *Optical Materials*, *69*, 8-22.

Dorn, J. M., Alpern, M., McNulty, C., & Volcheck, G. W. (2018). Sulfonamide drug allergy. *Current Allergy and Asthma Reports*, *18*, 1-10.

Dowling, P. M. (2013). Aminoglycosides and aminocyclitols. *Antimicrobial Therapy in Veterinary Medicine*, 233-255.

Dubreuil, L. J. (2024). Fifty years devoted to anaerobes: historical, lessons, and highlights. *European Journal of Clinical Microbiology & Infectious Diseases*, *43*(1), 1-15.

Elangovan, N., Gangadharappa, B., Thomas, R., & Irfan, A. (2022). Synthesis of a versatile Schiff base 4-((2-hydroxy-3, 5-diiodobenzylidene) amino) benzenesulfonamide from 3, 5-diiodosalicylaldehyde and sulfanilamide, structure, electronic properties, biological activity prediction and experimental antimicrobial properties. *Journal of Molecular Structure*, *1250*, 131700.

El-Asmy, A. A., & Al-Hazmi, G. A. A. (2009). Synthesis and spectral feature of benzophenone-substituted thiosemicarbazones and their Ni (II) and Cu (II) complexes. *Spectrochimica Acta Part A: Molecular and Biomolecular Spectroscopy*, *71*(5), 1885-1890.

El-Gammal, O. A., Mohamed, F. S., Rezk, G. N., & El-Bindary, A. A. (2021). Synthesis, characterization, catalytic, DNA binding and antibacterial activities of Co (II), Ni (II) and Cu (II) complexes with new Schiff base ligand. *Journal of Molecular Liquids*, *326*, 115223.

Endale, A. T. M., & Desalegn, T. (2018). Synthesis, characterization and antibacterial activity of copper (II) and cobalt (II) vanillin-aniline Schiff base complexes. *Synthesis*, *10*(2), 2018.

Erturk, A. G. (2020). Synthesis, structural identifications of bioactive two novel Schiff bases. *Journal of Molecular Structure*, *1202*, 127299.

Es-Sounni, B., Harboul, K., Mouhib, A., Alanazi, A. S., Hefnawy, M., Bakhouch, M., ... & Fahim, M. (2024). Ruthenium (II) Complex-Based Tetradentate Schiff Bases: Synthesis, Spectroscopic, Antioxidant, and Antibacterial Investigations. *International Journal of Molecular Sciences*, *25*(14), 7879.

Es-Sounni, B., Nakkabi, A., Bouymajane, A., Elaaraj, I., Bakhouch, M., Filali, F. R., ... & Fahim, M. (2023). Synthesis, characterization, antioxidant and antibacterial activities of six metal complexes based tetradentate salen type bis-Schiff base. *Biointerface Research. Application. Chemistry*, *13*(4), 333.

Evans, A., & Kavanagh, K. A. (2021). Evaluation of metal-based antimicrobial compounds for the treatment of bacterial pathogens. *Journal of Medical Microbiology*, *70*(5), 001363.

Fadeeva, V. P., Tikhova, V. D., & Nikulicheva, O. N. (2008). Elemental analysis of organic compounds with the use of automated CHNS analyzers. *Journal of Analytical Chemistry*, *63*, 1094-1106.

Faruque, S. M., Balakrish Nair, G., & Mekalanos, J. J. (2004). Genetics of stress adaptation and virulence in toxigenic *Vibrio cholerae*. *DNA and Cell Biology*, *23*(11), 723-741.

Ferraz, C. A., Tintino, S. R., Teixeira, A. M., Bandeira, P. N., Santos, H. S., Cruz, B. G., & Coutinho, H. D. (2020). Potentiation of antibiotic activity by chalcone (E)-1-(4′-aminophenyl)-3-(furan-2-yl)-prop-2-en-1-one against gram-positive and gram-negative MDR strains. *Microbial Pathogenesis*, *148*, 104453.

Fonkui, T. Y., Ikhile, M. I., Njobeh, P. B., & Ndinteh, D. T. (2019). Benzimidazole Schiff base derivatives: Synthesis, characterization and antimicrobial activity. *BMC Chemistry*, *13*(1), 1-11.

Frei, A. (2020). Metal complexes, an untapped source of antibiotic potential? *Antibiotics*, *9*(2), 90.

Fukuzumi, S., Lee, Y. M., & Nam, W. (2019). Structure and reactivity of the first-row d-block metal-superoxo complexes. *Dalton Transactions*, *48*(26), 9469-9489.

Gabbaï, F. P., Chirik, P. J., Fogg, D. E., Meyer, K., Mindiola, D. J., Schafer, L. L., & You, S. L. (2016). An editorial about elemental analysis. *Organometallics*, *35*(19), 3255-3256.

Ghanghas, P., & Poonia, K. (2024). Synthesis, characterization and biological activities of novel Schiff base ligand and its Co (II) and Mn (II) complexes. *Results in Chemistry*, *7*, 101221.

Ghanghas, P., Choudhary, A., Kumar, D., & Poonia, K. (2021). Coordination metal complexes with Schiff bases: Useful pharmacophores with comprehensive biological applications. *Inorganic Chemistry Communications*, *130*, 108710.

Gupta, K. C., & Sutar, A. K. (2008). Catalytic activities of Schiff base transition metal complexes. *Coordination Chemistry Reviews*, *252*(12-14), 1420-1450.

Gupta, S., Prakash, A., Savita, S., Hashmi, K., Mishra, P., Veg, E., ... & Joshi, S. (2024). Studies of some mixed ligand-metal complexes of 4-((2-(phenylcarbamothioyl) hydrazinylidene) methyl) benzoic acid in search of potential antimicrobial activity. *Journal of Molecular Structure*, 139319.

Hameed, A., Al-Rashida, M., Uroos, M., Abid Ali, S., & Khan, K. M. (2017). Schiff bases in medicinal chemistry: a patent review (2010-2015). *Expert Opinion on Therapeutic Patents*, *27*(1), 63-79.

Hamid, S. J., & Salih, T. (2022). Design, synthesis, and anti-inflammatory activity of some coumarin Schiff base derivatives: *In silico* and *in vitro* study. *Drug Design, Development and Therapy*, 2275-2288.

Harrison, C. J., & Bratcher, D. (2008). Cephalosporins: a review. *Pediatrics in Review*, *29*(8), 264-273.

Hasan, H. A., Mahdi, S. M., & Ali, H. A. (2024). Tetradentate azo Schiff base Ni (II), Pd (II) and Pt (II) complexes: Synthesis, spectral properties, antibacterial activity, cytotoxicity and docking studies. *Bulletin of the Chemical Society of Ethiopia*, *38*(1), 99-111.

Hemalatha, S., Dharmaraja, J., Shobana, S., Subbaraj, P., Esakkidurai, T., & Raman, N. (2020). Chemical and pharmacological aspects of novel hetero MLB complexes derived from NO_2 type Schiff base and N_2 type 1, 10-phenanthroline ligands. *Journal of Saudi Chemical Society*, *24*(1), 61-80.

Hoffman, R. E. (2006). Standardization of chemical shifts of TMS and solvent signals in NMR solvents. *Magnetic Resonance in Chemistry*, *44*(6), 606-616.

Hooper, D. C., & Jacoby, G. A. (2015). Mechanisms of drug resistance: quinolone resistance. *Annals of the New York academy of sciences*, *1354*(1), 12-31.

Hore, P. J. (2015). *Nuclear Magnetic Resonance*. Oxford University Press, USA.

Ibrahim, F. M., & Abdalhadi, S. M. (2021). Performance of Schiff bases metal complexes and their ligand in biological activity: a review. *Al-Nahrain Journal of Science*, *24*(1), 1-10.

Iftikhar, B., Javed, K., Khan, M. S. U., Akhter, Z., Mirza, B., & Mckee, V. (2018). Synthesis, characterization and biological assay of Salicylaldehyde Schiff base Cu (II) complexes and their precursors. *Journal of Molecular Structure*, *1155*, 337-348.

Iraji, M., Salehi, M., Malekshah, R. E., Khaleghian, A., & Shamsi, F. (2022). Liposomal formulation of new arsenic Schiff base complex as drug delivery agent in the treatment of acute promyelocytic leukemia and quantum chemical and docking calculations. *Journal of Drug Delivery Science and Technology*, *75*, 103600.

Jang, J., Hur, H. G., Sadowsky, M. J., Byappanahalli, M. N., Yan, T., & Ishii, S. (2017). Environmental Escherichia coli: ecology and public health implications a review. *Journal of Applied Microbiology*, *123*(3), 570-581.

Jorgensen, J. H., & Turnidge, J. D. (2015). Susceptibility test methods: dilution and disk diffusion methods. *Manual of Clinical Microbiology*, 1253-1273.

Jose, E. S., Philip, J. E., Shanty, A. A., Kurup, M. R. P., & Mohanan, P. V. (2018). Novel class of mononuclear 2-methoxy-4-chromanones ligated Cu (II), Zn (II), Ni (II) complexes: synthesis, characterization and biological studies. *Inorganica Chimica Acta*, *478*, 155-165.

Judd, B. R. (1988). The Theory of the Jahn-Teller Effect. *In*: C. D. Flint (Ed.). *Vibronic Processes in Inorganic Chemistry* (pp. 79-101). Springer Dordrecht

Kakanejadifard, A., Esna-ashari, F., Hashemi, P., & Zabardasti, A. (2013). Synthesis and characterization of an azo dibenzoic acid Schiff base and its Ni (II), Pb (II), Zn (II) and Cd (II) complexes. *Spectrochimica Acta Part A: Molecular and Biomolecular Spectroscopy*, *106*, 80-85.

Kanwal, A., Parveen, B., Ashraf, R., Haider, N., & Ali, K. G. (2022). A review on synthesis and applications of some selected Schiff bases with their transition metal complexes. *Journal of Coordination Chemistry*, *75*(19-24), 2533-2556.

Karam, G., Chastre, J., Wilcox, M. H., & Vincent, J. L. (2016). Antibiotic strategies in the era of multidrug resistance. *Critical Care*, *20*(1), 1-9.

Kargar, H., Ardakani, A. A., Tahir, M. N., Ashfaq, M., & Munawar, K. S. (2021). Synthesis, spectral characterization, crystal structure determination and antimicrobial activity of Ni (II), Cu (II) and Zn (II) complexes with the Schiff base ligand derived from 3, 5-dibromosalicylaldehyde. *Journal of Molecular Structure*, *1229*, 129842.

Kariuki, A.F. & Njagi, E. C. (2018). Synthesis, characterization and antimicrobial activities of hydroxytriazenes and their copper (II) complexes. *Journal of Environmental Sustainability Advancement Research*, *4*, 151-160

Kasare, M. S., Dhavan, P. P., Jadhav, B. L., & Pawar, S. D. (2019). Synthesis of Azo Schiff Base Ligands and Their Ni (II), Cu (II) and Zn (II) Metal Complexes as Highly- Active Antibacterial Agents. *Chemistry Select*, *4*(36), 10792-10797.

Kazemnejadi, M., Dehno Khalaji, A., & Mighani, H. (2017). Synthesis and characterization of Schiff-base polymer derived from 2, 5-dichloroaniline and 2-hydroxybenzaldehyde. *Iranian Chemical Communication*, *5*(3),237-363.

Keeler, J. (2010). *Understanding NMR spectroscopy*. John Wiley & Sons.

Keypour, H., Shayesteh, M., Golbedaghi, R., Chehregani, A., & Blackman, A. G. (2012). Synthesis, characterization, and X-ray crystal structures of metal complexes with new Schiff-base ligands and their antibacterial activities. *Journal of Coordination Chemistry*, *65*(6), 1004-1016.

Khan, E., Hanif, M., & Akhtar, M. S. (2022). Schiff bases and their metal complexes with biologically compatible metal ions; biological importance, recent trends and future hopes. *Reviews in Inorganic Chemistry*, *42*(4), 307-325.

Khan, M. W., Mishra, R. P., Patel, B., Patel, S., Gupta, S., & Sen, S. (2021). Synthesis, Characterization, Swiss ADME and Antimicrobial Activity of Copper (II) Complex with 2-Sulfanilamidopyrimidine: Through DFT Spectroscopic with Profound Biological Implications. *Asian Journal Application Chemistry Research.*, *9*, 16-32.

Khan, S. A., Khan, S. B., Khan, L. U., Farooq, A., Akhtar, K., & Asiri, A. M. (2018). Fourier transform infrared spectroscopy: fundamentals and application in functional groups and nanomaterials characterization. *Handbook of Materials Characterization*, 317-344.

Khan, S. N., & Khan, A. U. (2016). Breaking the spell: combating multidrug resistant 'superbugs'. *Frontiers in microbiology*, *7*, 174.

Kim, D., Kim, S., Kwon, Y., Kim, Y., Park, H., Kwak, K., ... & Kang, L. W. (2023). Structural insights for β-lactam antibiotics. *Biomolecules & Therapeutics*, *31*(2), 141.

Kohanski, M. A., Dwyer, D. J., & Collins, J. J. (2010). How antibiotics kill bacteria: from targets to networks. *Nature Reviews Microbiology*, *8*(6), 423-435.

Kovács, O., & Jakab, E. (2020). *Pseudomonas aeruginosa* at the dawn of a post-antibiotic era: clinical significance, resistance mechanisms, novel antibiotics and alternative treatments. *Studia Universitatis Babeș-Bolyai Biologia*, 31-67.

Kulshrestha, A., & Baluja, S. (2010). Microwave promoted synthesis of some Schiff bases. *Archives of Applied Science Research*, *2*(3), 221-224.

Kumar, R., Singh, A. A., Kumar, U., Jain, P., Sharma, A. K., Kant, C., & Faizi, M. S. H. (2023). Recent advances in synthesis of heterocyclic Schiff base transition metal complexes and their antimicrobial activities especially antibacterial and antifungal. *Journal of Molecular Structure*, *1294*, 136346.

Lalitha, M. K. (2004). Manual on antimicrobial susceptibility testing. *Performance standards for antimicrobial testing: Twelfth Informational Supplement, 56238*, 454-456.

Lambert, J. B., Mazzola, E. P., & Ridge, C. D. (2019). *Nuclear magnetic resonance spectroscopy: An Introduction to Principles, Applications, and Experimental Methods*. John Wiley & Sons.

Lei, C., Yang, W., Lin, Z., Tao, Y., Ye, R., Jiang, Y., ... & Zhou, B. (2024). Synthesis and bioactivity investigation of benzophenone and its derivatives. *RSC Advances*, *14*(28), 20339-20350.

Liang, J., Sun, D., Yang, Y., Li, M., Li, H., & Chen, L. (2021). Discovery of metal-based complexes as promising antimicrobial agents. *European Journal of Medicinal Chemistry*, *224*, 113696.

Liang, X., Luan, S., Yin, Z., He, M., He, C., Yin, L., & Zhang, W. (2018). Recent advances in the medical use of silver complex. *European Journal of Medicinal Chemistry*, *157*, 62-80.

Lima, L. M., da Silva, B. N. M., Barbosa, G., & Barreiro, E. J. (2020). β-lactam antibiotics: An overview from a medicinal chemistry perspective. *European Journal of Medicinal Chemistry*, *208*, 112829.

López-Malo, A., Mani-López, E., Davidson, P. M., & Palou, E. (2020). Methods for activity assay and evaluation of results. *In*: P. M. Davidson, T. M. Taylor and J. R. D. David (Eds.). *Antimicrobials in Food* (pp. 13-40). CRC Press.

Love, B. E., & Ren, J. (1993). Synthesis of sterically hindered imines. *The Journal of Organic Chemistry*, *58*(20), 5556-5557.

Lu, Y., Ma, X., Chang, X., Liang, Z., Lv, L., Shan, M., ... & Liu, W. (2022). Recent development of gold (I) and gold (III) complexes as therapeutic agents for cancer diseases. *Chemical Society Reviews*, *51*(13), 5518-5556.

Luzzaro, F., Perilli, M., Amicosante, G., Lombardi, G., Belloni, R., Zollo, A., ... & Toniolo, A. (2001). Properties of multidrug-resistant, ESBL-producing *Proteus mirabilis* isolates and possible role of β-lactam/β-lactamase inhibitor combinations. *International Journal of Antimicrobial Agents*, *17*(2), 131-135.

Maddela, S., Venugopal, M., Maddela, R., & Ajitha, M. (2015). Design and synthesis of new N'-substituted-2-methylquinoline-3-carbohydrazides with antioxidant and antimicrobial activity. *Indian Journal of Chemistry*; 54:930-935.

Maher, K. A., & Mohammed, S. R. (2015). Metal complexes of Schiff base derived from salicylaldehyde-A review. *International Journal of Current Research and Review*, *7*(2), 6.

Mahmood, A. A. (2022). Green synthesis of Schiff bases: a review study. *Iraqi Journal of Pharmacy*, *18*(2), 180-193.

Marinov, T., Kokanova-Nedialkova, Z., & Nedialkov, P. T. (2023). Naturally occurring simple oxygenated benzophenones: Structural diversity, distribution, and biological properties. *Diversity*, *15*(10), 1030.

Martin, R. M., & Bachman, M. A. (2018). Colonization, infection, and the accessory genome of *Klebsiella pneumoniae*. *Frontiers in Cellular and Infection Microbiology*, *8*, 4.

Mehta, D., & Sharma, A. K. (2016). Cephalosporins: A review on imperative class of antibiotics. *Inventi Rapid: Molecular Pharmacology*, *1*(3), 1-6.

Missoun, F., de los Ríos, A. P., Ortiz-Martínez, V., Salar-García, M. J., Hernández-Fernández, J., & Hernández-Fernández, F. J. (2020). Discovering low toxicity ionic liquids for Saccharomyces cerevisiae by using the agar well diffusion test. *Processes*, *8*(9), 1163.

Mitchell, J., Webber, J. B. W., & Strange, J. H. (2008). Nuclear magnetic resonance cryoporometry. *Physics Reports*, *461*(1), 1-36.

Mohamed, G. G., Omar, M. M., & Ibrahim, A. A. (2009). Biological activity studies on metal complexes of novel tridentate Schiff base ligand. Spectroscopic and thermal characterization. *European Journal of Medicinal Chemistry*, *44*(12), 4801-4812.

Mondal, K., & Mistri, S. (2023). Schiff base based metal complexes: A review of their catalytic activity on aldol and henry reaction. *Comments on Inorganic Chemistry*, *43*(2), 77-105.

More, M. S., Joshi, P. G., Mishra, Y. K., & Khanna, P. K. (2019). Metal complexes driven from Schiff bases and semicarbazones for biomedical and allied applications: a review. *Materials Today Chemistry*, *14*, 100195.

Moreno, D., Daier, V., Palopoli, C., Tuchagues, J. P., & Signorella, S. (2010). Synthesis, characterization and antioxidant activity of water-soluble Mn (III) complexes of sulphonato-substituted Schiff base ligands. *Journal of Inorganic Biochemistry*, *104*(5), 496-502.

Mounika, K., Pragathi, A., & Gyanakumari, C. (2010). Synthesis characterization and biological activity of a Schiff base derived from 3-ethoxy salicylaldehyde and 2-amino benzoic acid and its transition metal complexes. *Journal of Scientific Research*, *2*(3), 513.

Musa, A., Suraj, I. T., & Sanusi, S. (2022). Synthesis, characterization and antimicrobial studies on Schiff base derived from 4-amino-2-hydroxybenzoic acid and 2-hyroxybenzaldehyde and its cobalt (II) and nickel (II) complexes. *IRESPUB Journal of Natural & Applied Sciences*, *2*, 1-7.

Naganagowda, G., Meijboom, R., & Petsom, A. (2014). Synthesis and antimicrobial activity of new Schiff base compounds containing 2-hydroxy-4-pentadecylbenzaldehyde moiety. *Advance Chemistry*, 1-9.

Nasiri Sovari, S., & Zobi, F. (2020). Recent studies on the antimicrobial activity of transition metal complexes of groups 6–12. *Chemistry*, *2*(2), 418-452.

Nassar, A. F. (2022). Drug design strategies: Role of structural modifications of drug candidates to improve pk parameters of new drugs. *Drug Metabolism Handbook: Concepts and Applications in Cancer Research*, *1*, 323-343.

Nath, B. D., Islam, M. M., Karim, M. R., Rahman, S., Shaikh, M. A. A., Georghiou, P. E., & Menelaou, M. (2022). Recent progress in metal- incorporated acyclic Schiff- base derivatives: Biological aspects. *Chemistry Select*, *7*(14), e202104290.

Nkungli, N. K., Ghogomu, J. N., Nogheu, L. N., & Gadre, S. R. (2015). DFT and TD-DFT study of bis [2-(5-amino-[1, 3, 4]-oxadiazol-2-yl) phenol](diaqua) M (II) complexes [M= Cu, Ni and Zn]: Electronic structures, properties and analyses. *Computational Chemistry*, *3*(3), 29-44.

Noriega, S., Cardoso-Ortiz, J., López-Luna, A., Cuevas-Flores, M. D. R., & Flores De La Torre, J. A. (2022). The diverse biological activity of recently synthesized nitro compounds. *Pharmaceuticals*, *15*(6), 717.

Okoh, A. I., & Igbinosa, E. O. (2010). Antibiotic susceptibility profiles of some Vibrio strains isolated from wastewater final effluents in a rural community of the Eastern Cape Province of South Africa. *BMC Microbiology*, *10*, 1-6.

Oliphant, C. M., & Green, G. M. (2002). Quinolones: a comprehensive review. *American Family Physician*, *65*(3), 455-465.

Ommenya, F. K., Nyawade, E. A., Andala, D. M., & Kinyua, J. (2020). Synthesis, characterization and antibacterial activity of Schiff base, 4-Chloro-2-{(E)-[(4-fluorophenyl) imino] methyl} phenol metal (II) complexes. *Journal of Chemistry*, *2020*, 1-8.

Omoruyi, G. l., Sadimenko, A.P.& Hosten, E. (2016). Metal complexes of new bioactive pyrazolone phenylhyrazone; crystal structure of 4-Acetyl-3-methyl-1-phenyl-2-pyrazoline-5-one phenylhydrazone Ampp-ph. *International Journal of Molecular Science* ,17(2016), 687-687

Osterman, I. A., Dontsova, O. A., & Sergiev, P. V. (2020). rRNA methylation and antibiotic resistance. *Biochemistry (Moscow)*, *85*, 1335-1349.

Pang, X., Li, D., Zhu, J., Cheng, J., & Liu, G. (2020). Beyond antibiotics: photo/sonodynamic approaches for bacterial theranostics. *Nano-Micro Letters*, *12*, 1-23.

Parekh, N. M., Mistry, B. M., Pandurangan, M., Shinde, S. K., & Patel, R. V. (2017). Investigation of anticancer potencies of newly generated Schiff base imidazolylphenylheterocyclic-2-ylmethylenethiazole-2-amines. *Chinese Chemical Letters*, *28*(3), 602-606.

Pashanova, K. I., Ershova, I. V., Trofimova, O. Y., Rumyantsev, R. V., Fukin, G. K., Bogomyakov, A. S., ... & Piskunov, A. V. (2022). Charge transfer chromophores derived from 3d-row transition metal complexes. *Molecules*, *27*(23), 8175.

Paul, M., Carrara, E., Retamar, P., Tängdén, T., Bitterman, R., Bonomo, R. A., ... & Rodríguez-Baño, J. (2022). European Society of Clinical Microbiology and Infectious Diseases (ESCMID) guidelines for the treatment of infections caused by multidrug-resistant Gram-negative bacilli (endorsed by European society of intensive care medicine). *Clinical Microbiology and Infection*, *28*(4), 521-547.

Perkampus, H. H. (2013). *UV-VIS Spectroscopy and its Applications*. Springer Science & Business Media.

Persch, E., Dumele, O., & Diederich, F. (2015). Molecular recognition in chemical and biological systems. *Angewandte Chemie International Edition*, *54*(11), 3290-3327.

Plata, K., Rosato, A., & Węgrzyn, G. (2009). *Staphylococcus aureus* as an infectious agent: overview of biochemistry and molecular genetics of its pathogenicity. *Acta Biochimica Polonica*, *56*(4), 597-612.

Power, P. P. (2012). Stable two-coordinate, open-shell (d_1–d_9) transition metal complexes. *Chemical Reviews*, *112*(6), 3482-3507.

Qin, W., Long, S., Panunzio, M., & Biondi, S. (2013). Schiff bases: A short survey on an evergreen chemistry tool. *Molecules*, *18*(10), 12264-12289.

Quist, D. A., Diaz, D. E., Liu, J. J., & Karlin, K. D. (2017). Activation of dioxygen by copper metalloproteins and insights from model complexes. *JBIC Journal of Biological Inorganic Chemistry*, *22*, 253-288.

Raczuk, E., Dmochowska, B., Samaszko-Fiertek, J., & Madaj, J. (2022). Different Schiff bases—structure, importance and classification. *Molecules*, *27*(3), 787.

Rafique, S., Idrees, M., Nasim, A., Akbar, H., & Athar, A. (2010). Transition metal complexes as potential therapeutic agents. *Biotechnology and Molecular Biology Reviews*, *5*(2), 38-45.

Rahmani, F., Fooladi, A., Marashi, S., & Nourani, M. (2012). Drug resistance in Vibrio cholerae strains isolated from clinical specimens. *Acta Microbiologica et Immunologica Hungarica*, *59*(1), 77-84.

Raju, S. K., Settu, A., Thiyagarajan, A., Rama, D., Sekar, P., & Kumar, S. (2022). Biological applications of Schiff bases: An overview. *GSC Biological and Pharmaceutical Sciences*, *21*(3), 203-215.

Rao, V. K., Reddy, S. S., Krishna, B. S., Naidu, K. R. M., Raju, C. N., & Ghosh, S. K. (2010). Synthesis of Schiff's bases in aqueous medium: a green alternative approach with effective mass yield and high reaction rates. *Green Chemistry Letters and Reviews*, *3*(3), 217-223.

Reddy, S. L., Endo, T., & Reddy, G. S. (2012). Electronic (absorption) spectra of 3d transition metal complexes. *Advanced Aspects of Spectroscopy*, 3-48.

Rezaei, M. T., Keypour, H., Hajari, S., Farida, S. H. M., Saadati, M., & Gable, R. W. (2023). Theoretical and solid-state structures of three new macroacyclic Schiff base complexes and the investigation of their anticancer, antioxidant and antibacterial properties. *RSC Advances*, *13*(14), 9418-9427.

Richards, S. A., & Hollerton, J. C. (2023). *Essential practical NMR for organic chemistry*. John Wiley & Sons.

Riwu, K. H. P., Effendi, M. H., & Rantam, F. A. (2020). A Review of Extended Spectrum β-Lactamase (ESBL) Producing *Klebsiella pneumoniae* and Multidrug Resistant (MDR) on Companion Animals. *Systematic Reviews in Pharmacy*, *11*(7).

Rocha, F. S., Gomes, A. J., Lunardi, C. N., Kaliaguine, S., & Patience, G. S. (2018). Experimental methods in chemical engineering: Ultraviolet visible spectroscopy—UV- Vis. *The Canadian Journal of Chemical Engineering*, *96*(12), 2512-2517.

Rosu, T., Pahontu, E., Maxim, C., Georgescu, R., Stanica, N., & Gulea, A. (2011). Some new Cu (II) complexes containing an ON donor Schiff base: Synthesis, characterization and antibacterial activity. *Polyhedron*, *30*(1), 154-162.

Sachdeva, H., Saroj, R., Khaturia, S., & Dwivedi, D. (2012). Operationally simple green synthesis of some Schiff bases using grinding chemistry technique and evaluation of antimicrobial activities. *Green Processing and Synthesis*, *1*(5), 469-477.

Saeed, A. M., AlNeyadi, S. S., & Abdou, I. M. (2020). Anticancer activity of novel Schiff bases and azo dyes derived from 3-amino-4-hydroxy-2H-pyrano [3, 2-c] quinoline-2, 5 (6H)-dione. *Heterocyclic Communications*, *26*(1), 192-205.

Şahin, M., Koçak, N., Erdenay, D., & Arslan, U. (2013). Zn (II), Ni (II), Cu (II) and Pb (II) complexes of tridentate asymmetrical Schiff base ligands: Synthesis, characterization, properties and biological activity. *Spectrochimica Acta Part A: Molecular and Biomolecular Spectroscopy*, *103*, 400-408.

Saikumari, N. (2021). Synthesis and characterization of amino acid Schiff base and its copper (II) complex and its antimicrobial studies. *Materials Today: Proceedings*, *47*, 1777-1781.

Saito, R., Okugawa, S., Kumita, W., Sato, K., Chida, T., Okamura, N., ... & Koike, K. (2007). Clinical epidemiology of ciprofloxacin- resistant Proteus mirabilis isolated from urine samples of hospitalised patients. *Clinical Microbiology and Infection*, *13*(12), 1204-1206.

Salehi, M., Ghasemi, F., Kubicki, M., Asadi, A., Behzad, M., Ghasemi, M. H., & Gholizadeh, A. (2016). Synthesis, characterization, structural study and antibacterial activity of the Schiff bases derived from sulfanilamides and related copper (II) complexes. *Inorganica Chimica Acta*, *453*, 238-246.

Saritha, T. J., & Metilda, P. (2021). Synthesis, spectroscopic characterization and biological applications of some novel Schiff base transition metal (II) complexes derived from curcumin moiety. *Journal of Saudi Chemical Society*, *25*(6), 101245.

Schroeder, M. R., & Stephens, D. S. (2016). Macrolide resistance in *Streptococcus pneumonia*e. *Frontiers in Cellular and Infection Microbiology*, *6*, 98.

Shi, L., Ge, H. M., Tan, S. H., Li, H. Q., Song, Y. C., Zhu, H. L., & Tan, R. X. (2007). Synthesis and antimicrobial activities of Schiff bases derived from 5-chloro-salicylaldehyde. *European Journal of Medicinal Chemistry*, *42*(4), 558-564.

Shntaif, A. H., & Rashid, Z. M. (2016). The Synthesis of Schiff bases under microwave Irradiation: Review. *Journal of Chemical and Pharmaceutical Science*, *9*(3), 1066-1068.

Silverman, R. B., & Holladay, M. W. (2014). *The organic chemistry of drug design and drug action*. Academic press.

Singh, D. P., Deivedi, S. K., Hashim, S. R., & Singhal, R. G. (2010). Synthesis and antimicrobial activity of some new quinoxaline derivatives. *Pharmaceuticals*, *3*(8), 2416-2425.

Singha, N. R., Chattopadhyay, P. K., Dutta, A., Mahapatra, M., & Deb, M. (2019). Review on additives-based structure-property alterations in dyeing of collagenic matrices. *Journal of Molecular Liquids*, *293*, 111470.

Sinicropi, M. S., Ceramella, J., Iacopetta, D., Catalano, A., Mariconda, A., Rosano, C., ... & Longo, P. (2022). Metal complexes with Schiff bases: Data collection and recent studies on biological activities. *International Journal of Molecular Sciences*, *23*(23), 14840.

Sohn, K. M., Kang, C. I., Joo, E. J., Ha, Y. E., Chung, D. R., Peck, K. R., ... & Song, J. H. (2011). Epidemiology of ciprofloxacin resistance and its relationship to extended-spectrum β-lactamase production in *Proteus mirabilis* bacteremia. *The Korean Journal of Internal Medicine*, *26*(1), 89.

Solankee, A., Kapadia, K., Ćirić, A., Soković, M., Doytchinova, I., & Geronikaki, A. (2010). Synthesis of some new S-triazine based chalcones and their derivatives as potent antimicrobial agents. *European Journal of Medicinal Chemistry*, *45*(2), 510-518.

Solomon, E. I., & Bell III, C. B. (2010). *Inorganic and Bioinorganic Spectroscopy* (p. 6). Wiley: New Jersey, USA.

Somily, A. M., Absar, M. M., Arshad, M. Z., Al Aska, A. I., Shakoor, Z. A., Fatani, A. J., ... & Murray, T. S. (2012). Antimicrobial susceptibility patterns of multidrug-resistant *Pseudomonas aeruginosa* and *Acinetobacter baumannii* against carbapenems, colistin, and tigecycline. *Saudi Medical Journal*, *33*(7), 750-5.

Sora, V. M., Meroni, G., Martino, P. A., Soggiu, A., Bonizzi, L., & Zecconi, A. (2021). Extraintestinal pathogenic *Escherichia coli*: Virulence factors and antibiotic resistance. *Pathogens, 10*(11), 1355.

Sousa, S. A., Feliciano, J. R., Pita, T., Soeiro, C. F., Mendes, B. L., Alves, L. G., & Leitao, J. H. (2021). Bacterial nosocomial infections: multidrug resistance as a trigger for the development of novel antimicrobials. *Antibiotics, 10*(8), 942.

Spinu, C., Pleniceanu, M., & Tigae, C. (2008). Biologically active new Fe (II), Co (II), Ni (II), Cu (II), Zn (II) and Cd (II) complexes of N-(2-thienylmethylene) methanamine. *Journal of the Serbian Chemical Society*, *73*(4), 415-421.

Stavropoulou, E., Voidarou, C., Rozos, G., Vaou, N., Bardanis, M., Konstantinidis, T., & Tsakris, A. (2022). Antimicrobial evaluation of various honey types against carbapenemase-producing Gram-negative clinical isolates. *Antibiotics*, *11*(3), 422.

Stratton, C. W. (2002). Chloramphenicol. *Antimicrobics and Infectious Diseases Newsletter*, *18*(12), 89-91.

Stuart, B. H. (2004). *Infrared Spectroscopy: fundamentals and applications*. John Wiley & Sons

Sujarani, S., & Ramu, A. (2013). Synthesis, characterization, antimicrobial and DNA interaction studies of benzophenone–ethanamine Schiff base with transition metal (II) [Cu (II), Co (II), Mn (II) and Ni (II)] complexes. *Journal of Chemical and Pharmaceutical Research, 5*(4), 347-358.

Sunitha, M., Jogi, P., Ushaiah, B., & Kumari, C. G. (2012). Synthesis, characterization and antimicrobial activity of transition metal complexes of Schiff base ligand derived from 3-ethoxy salicylaldehyde and 2-(2-Aminophenyl) 1-H-benzimidazole. *E-Journal of Chemistry*, *9*(4), 2516-2523.

Tasumi, M. (Ed.). (2014). *Introduction to Experimental Infrared Spectroscopy: Fundamentals and Practical Methods*. John Wiley & Sons.

Teng, J., Imani, S., Zhou, A., Zhao, Y., Du, L., Deng, S., & Wang, Q. (2023). Combatting resistance: understanding multi-drug resistant pathogens in intensive care units. *Biomedicine & Pharmacotherapy*, *167*, 115564.

Tenson, T., Lovmar, M., & Ehrenberg, M. (2003). The mechanism of action of macrolides, lincosamides and streptogramin B reveals the nascent peptide exit path in the ribosome. *Journal of Molecular Biology*, *330*(5), 1005-1014.

Tomar, R. S., Sharma, P., Sharma, A., & Mishra, R. (2015). Assessment and evaluation of methods used for antimicrobial activity assay: an overview. *WJPR*, *4*(5), 907-934.

Trylska, J., & Kulik, M. (2016). Interactions of aminoglycoside antibiotics with rRNA. *Biochemical Society Transactions*, *44*(4), 987-993.

Uddin, M. N., Ahmed, S. S., & Alam, S. R. (2020). Biomedical applications of Schiff base metal complexes. *Journal of Coordination Chemistry*, *73*(23), 3109-3149.

Urban-Chmiel, R., Marek, A., Stępień-Pyśniak, D., Wieczorek, K., Dec, M., Nowaczek, A., & Osek, J. (2022). Antibiotic resistance in bacteria—A review. *Antibiotics*, *11*(8), 1079.

Urgancı, N. N., Yılmaz, N., Alaşalvar, G. K., & Yıldırım, Z. (2022). Pseudomonas aeruginosa and its pathogenicity. *Turkish Journal of Agriculture-Food Science and Technology*, *10*(4), 726-738.

Varkey, A. J. (2010). Antibacterial properties of some metals and alloys in combating coliforms in contaminated water. *Scientific Research and Essays*, *5*(24), 3834-3839.

Vassallo, J., Besinis, A., Boden, R., & Handy, R. D. (2018). The minimum inhibitory concentration (MIC) assay with *Escherichia coli*: an early tier in the environmental hazard assessment of nanomaterials? *Ecotoxicology and Environmental Safety*, *162*, 633-646.

Vázquez-Laslop, N., & Mankin, A. S. (2018). How macrolide antibiotics work. *Trends in Biochemical Sciences*, *43*(9), 668-684.

Venkatesh, G., Vennila, P., Kaya, S., Ahmed, S. B., Sumathi, P., Siva, V., ... & Kamal, C. (2024). Synthesis and spectroscopic characterization of schiff base metal complexes, biological activity, and molecular docking studies. *ACS omega*, *9*(7), 8123-8138.

Verma, R., Lamba, N. P., Dandia, A., Srivastava, A., Modi, K., Chauhan, M. S., & Prasad, J. (2022). Synthesis of N-Benzylideneaniline by Schiff base reaction using Kinnow peel powder as green catalyst and comparative study of derivatives through ANOVA techniques. *Scientific Reports*, *12*(1), 9636.

Vila, J., & Pal, T. (2010). Update on antibacterial resistance in low-income countries: factors favoring the emergence of resistance. *Open Infectious Diseases Journal*, *4*(1), 38-54.

Waclaw, B. (2016). Evolution of drug resistance in bacteria. *Biophysics of Infection*, 49-67.

Wai, S. N., Mizunoe, Y., & Yoshida, S. I. (1999). How *Vibrio cholerae* survive during starvation. *FEMS Microbiology Letters*, *180*(2), 123-131.

Wei, L., Zhang, J., Tan, W., Wang, G., Li, Q., Dong, F., & Guo, Z. (2021). Antifungal activity of double Schiff bases of chitosan derivatives bearing active halogeno-benzenes. *International Journal of Biological Macromolecules*, *179*, 292-298.

Westheimer, F. H., & Taguchi, K. (1971). Catalysis by molecular sieves in the preparation of ketimines and enamines. *The Journal of Organic Chemistry*, *36*(11), 1570-1572.

World Health Organization. (2014). *Antimicrobial Resistance: Global Report on Surveillance*. World Health Organization.

Worthington, R. J., & Melander, C. (2013). Combination approaches to combat multidrug-resistant bacteria. *Trends in Biotechnology*, *31*(3), 177-184.

Xu, J., Liu, Y., & Hsu, S. H. (2019). Hydrogels based on Schiff base linkages for biomedical applications. *Molecules*, *24*(16), 3005.

Yadav, L. D. S. (2013). *Organic Spectroscopy*. Springer Science & Business Media.

Yalew, S. T. (2020). Review on antibiotic resistance: resistance mechanisms, methods of detection and its controlling strategies. *Biomedical Journal of Scientific & Technical Research*, *24*(5), 18651-18657.

Yaseen, A. A., Al-Tikrity, E. T., Al-Mashhadani, M. H., Salih, N., & Yousif, E. (2021). An Overview: Using Different Approaches to Synthesis New Schiff Bases Materials. *Journal of University of Anbar for Pure Science*, *15*(2), 53-59.

Yimer, A. M. (2014). Chemical synthesis, spectral characterization and antimicrobial studies on complexes of Ni (II), Cu (II) and Zn (II) with N, N-di (o-hydroxybenzenoylmethylene) ethylenediamine. *American Journal of Bioscience*, *2*(6-1), 22-34.

Yousef, T. A., El-Reash, G. A., Al-Zahab, M. A., & Safaan, M. A. A. (2019). Physicochemical investigations, biological studies of the Cr (III), Mn (II), Fe (III), Co (II), Ni (II), Cu (II), Zn (II), Cd (II), Hg (II) and UO2 (VI) complexes of picolinic acid hydrazide derivative: A combined experimental and computational approach. *Journal of Molecular Structure*, *1197*, 564-575.

Yuan, S., Shen, D. D., Bai, Y. R., Zhang, M., Zhou, T., Sun, C., ... & Liu, H. M. (2023). Oxazolidinone: A promising scaffold for the development of antibacterial drugs. *European Journal of Medicinal Chemistry*, *250*, 115239.

Zaera, F. (2022). Designing sites in heterogeneous catalysis: are we reaching selectivities competitive with those of homogeneous catalysts?. *Chemical Reviews*, *122*(9), 8594-8757.

Zafar, H., Ahmad, A., Khan, A. U., & Khan, T. A. (2015). Synthesis, characterization and antimicrobial studies of Schiff base complexes. *Journal of Molecular Structure*, *1097*, 129-135.

Zafar, W., Ashfaq, M., & Sumrra, S. H. (2023). A review on the antimicrobial assessment of triazole-azomethine functionalized frameworks incorporating transition metals. *Journal of Molecular Structure*, 135744.

Zafar, W., Sumrra, S. H., & Chohan, Z. H. (2021). A review: Pharmacological aspects of metal based 1, 2, 4-triazole derived Schiff bases. *European Journal of Medicinal Chemistry*, *222*, 113602.

Zarei, M., & Jarrahpour, A. (2011). Green and efficient synthesis of azo Schiff bases. *Iranian Journal of Science and Technology 35*(3), 235-242.

Zhao, Z., Dai, X., Li, C., Wang, X., Tian, J., Feng, Y., ... & Zheng, X. (2020). Pyrazolone structural motif in medicinal chemistry: Retrospect and prospect. *European Journal of Medicinal Chemistry*, *186*, 111893.

APPENDICES

Appendix I: The FT-IR Spectra of Schiff base Ligands and their Cu (II) Complexes

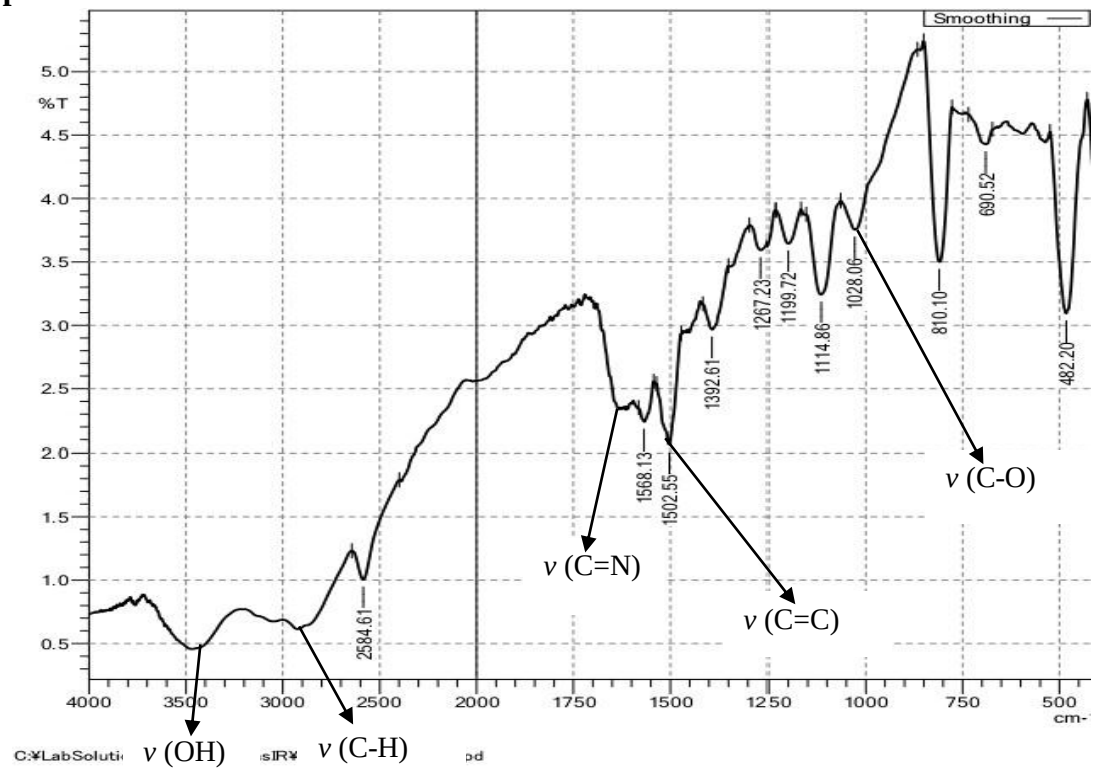

Figure 20:FT-IR spectrum of ligand L_2

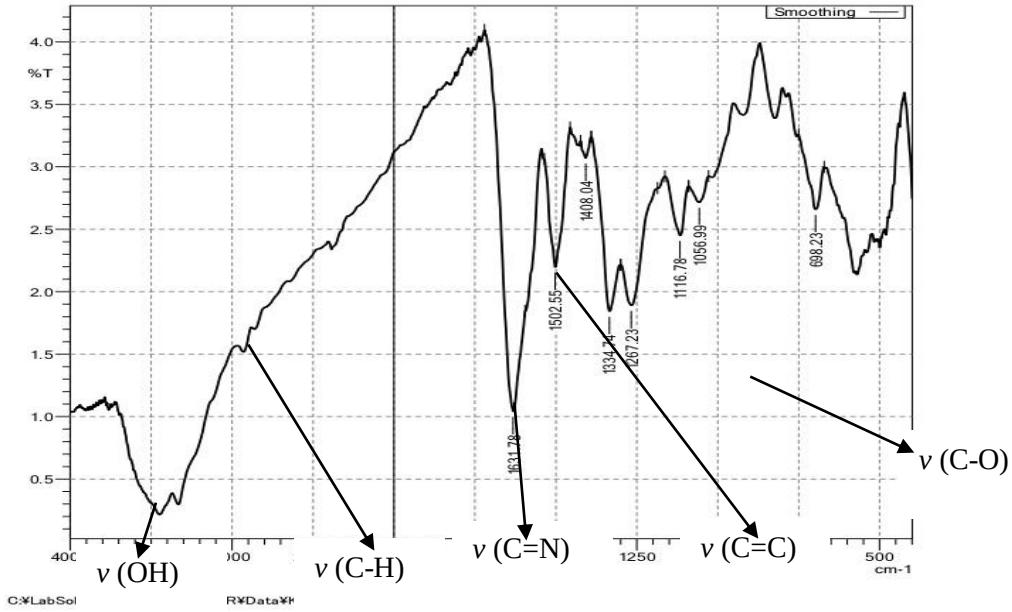

Figure 21:FT-IR spectrum of ligand L_3

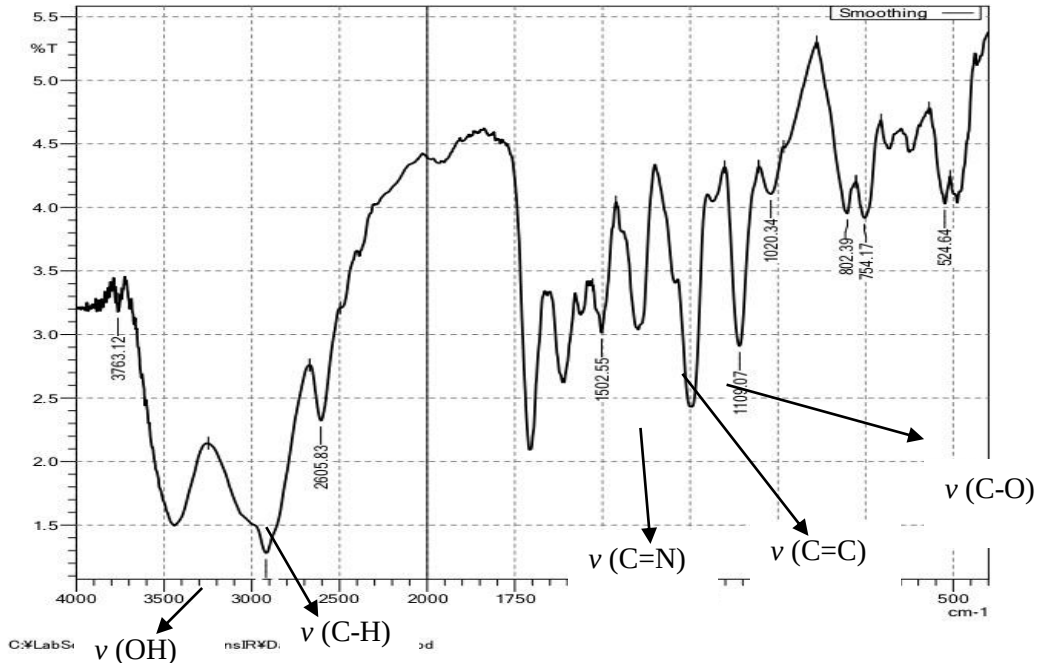

Figure 22:FT-IR spectrum of ligands L_4

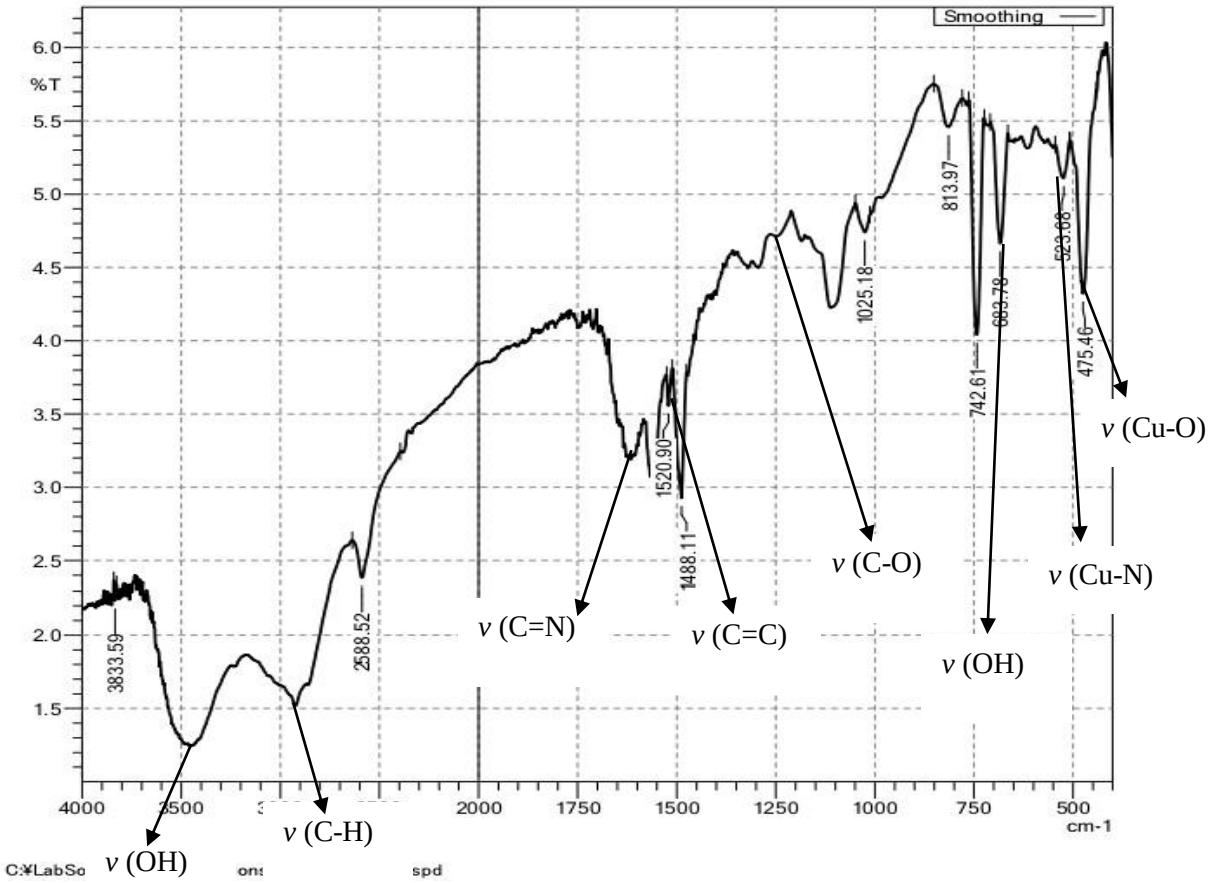

Figure 23:FT-IR spectrum of complex Cu-L_1

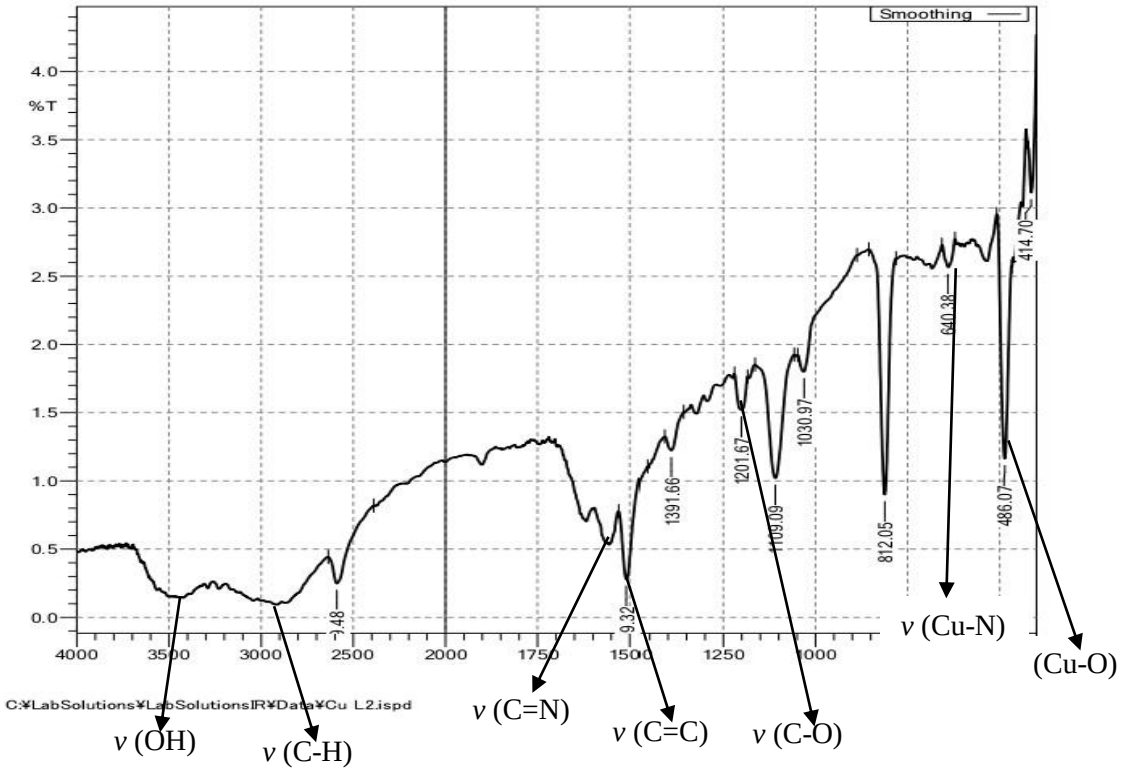

Figure 24:FT-IR spectrum oı complex Cu-L_2

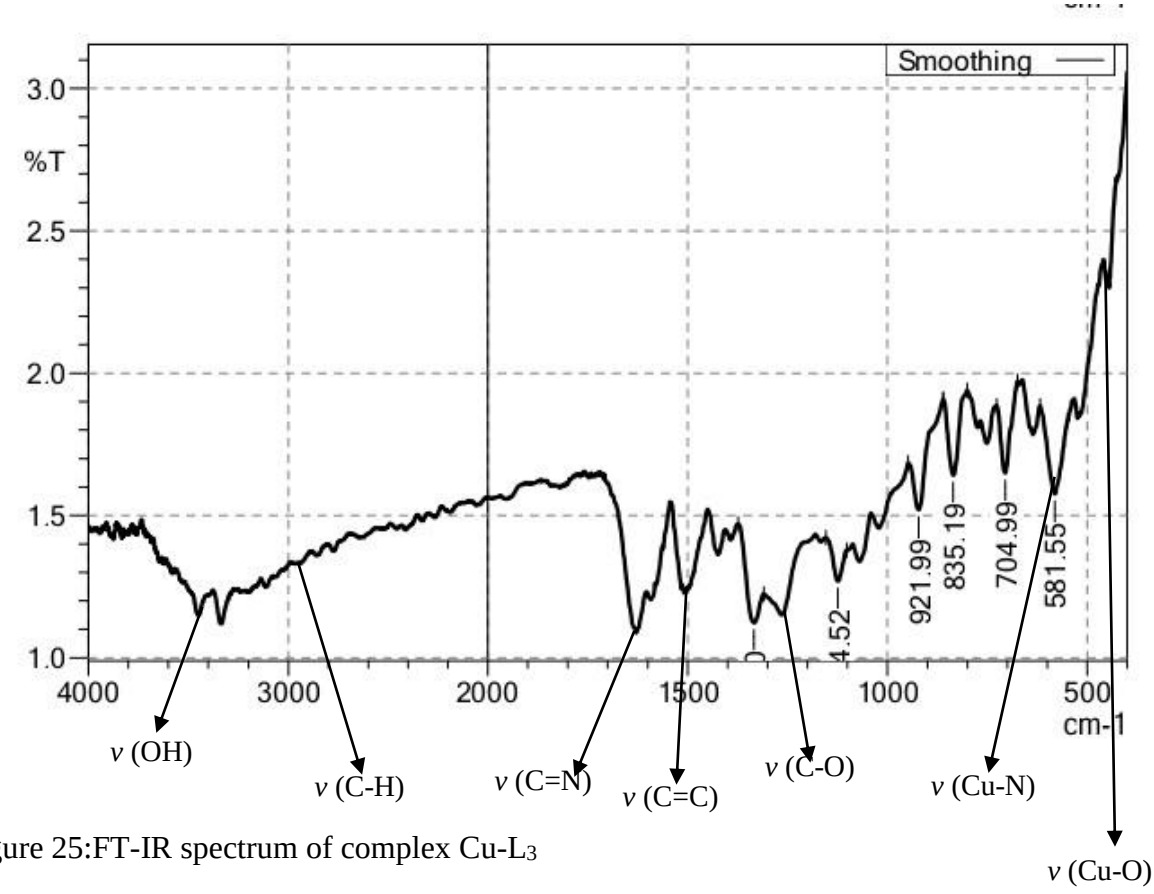

Figure 25:FT-IR spectrum of complex Cu-L_3

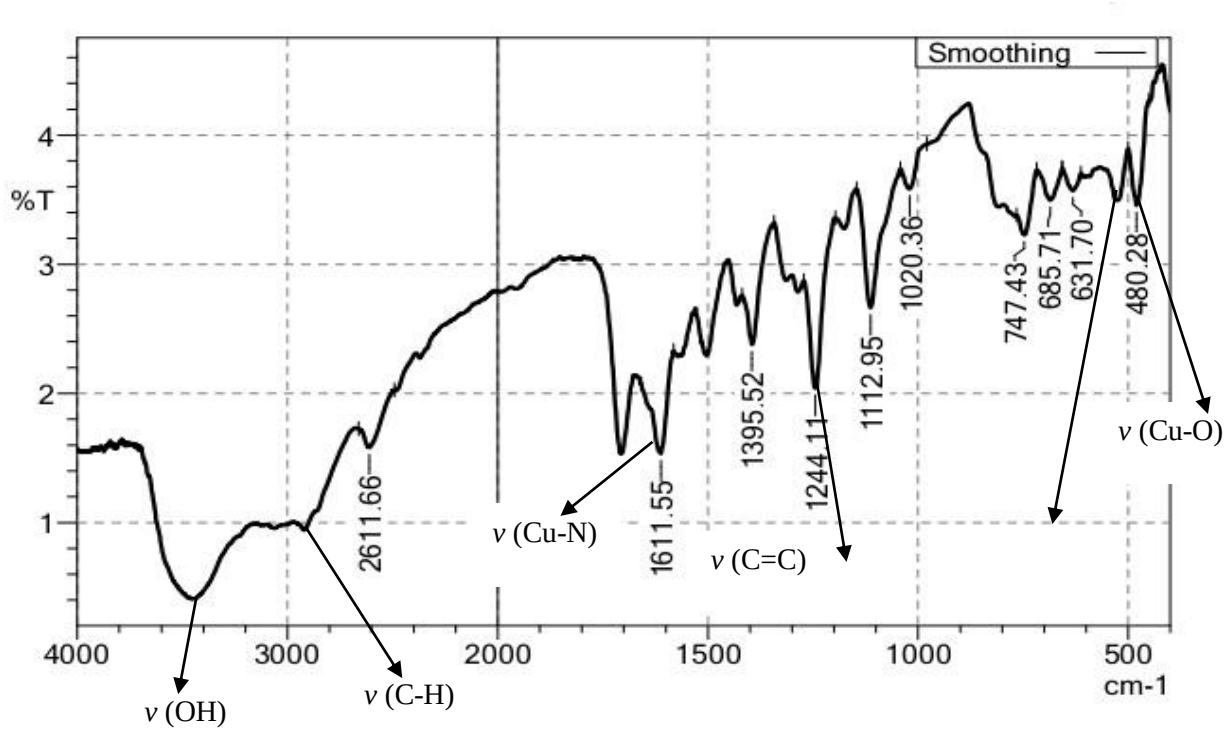

Figure 26:FT-IR spectrum of Cu-L_4 complex

Appendix II: Electronic Spectra of Schiff Base Ligands and their Cu (II) Complexes

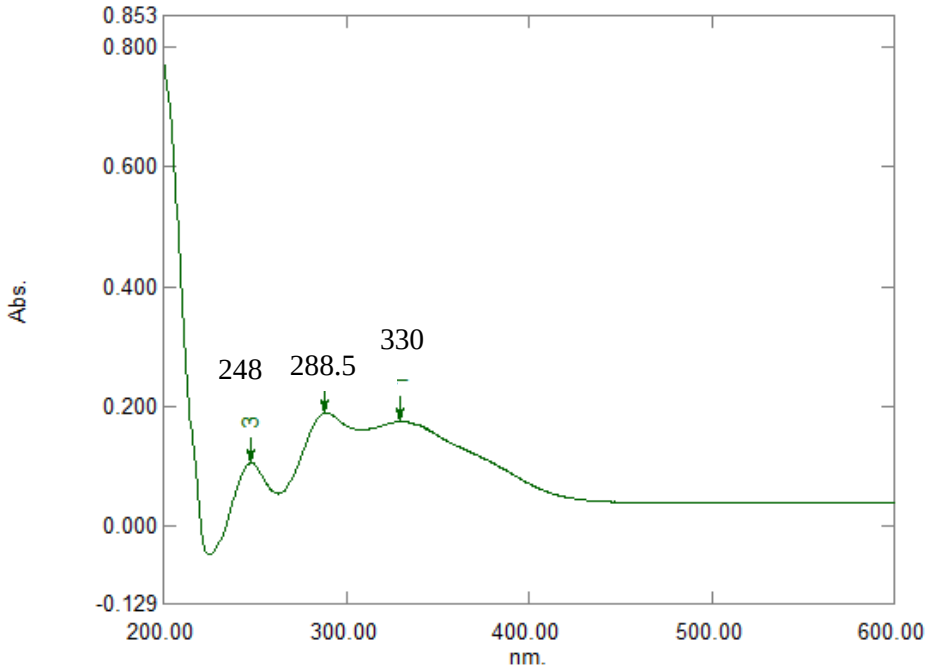

Figure 27:UV-Vis spectrum of ligand L_2 in acetonitrile

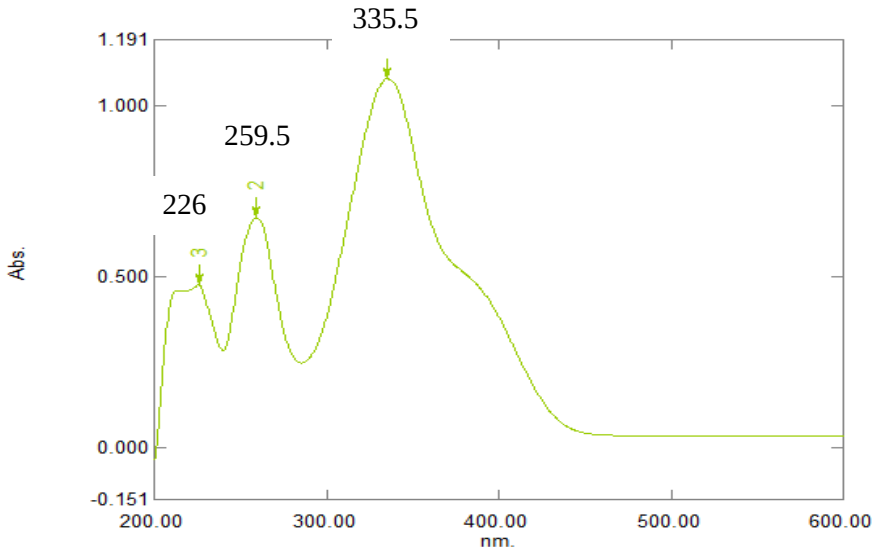

Figure 28:UV-Vis spectrum of ligand L_3 in acetonitrile

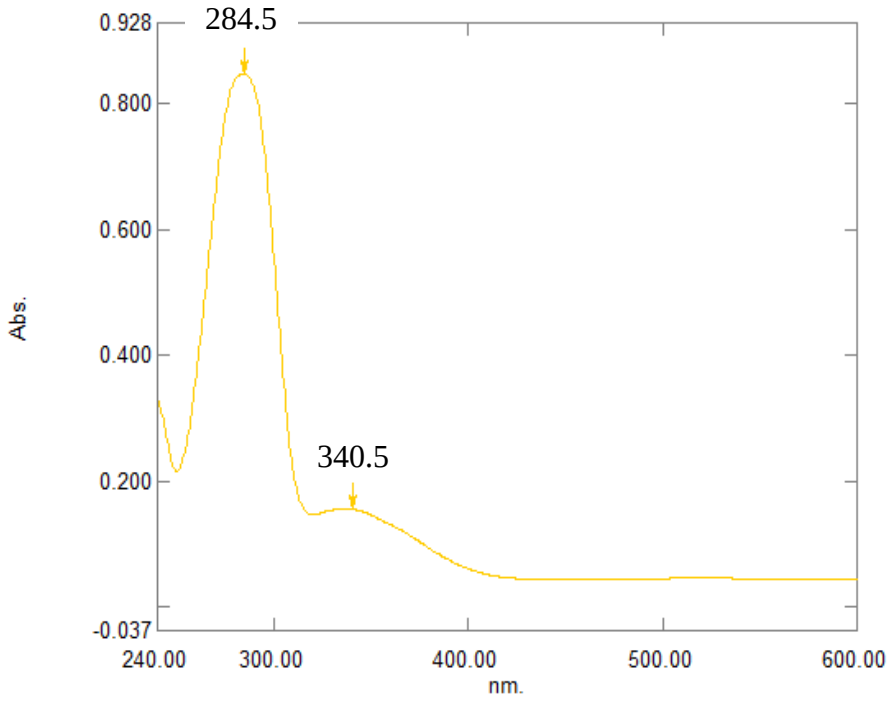

Figure 29:UV -vis spectrum of L_4 in in acetonitrile

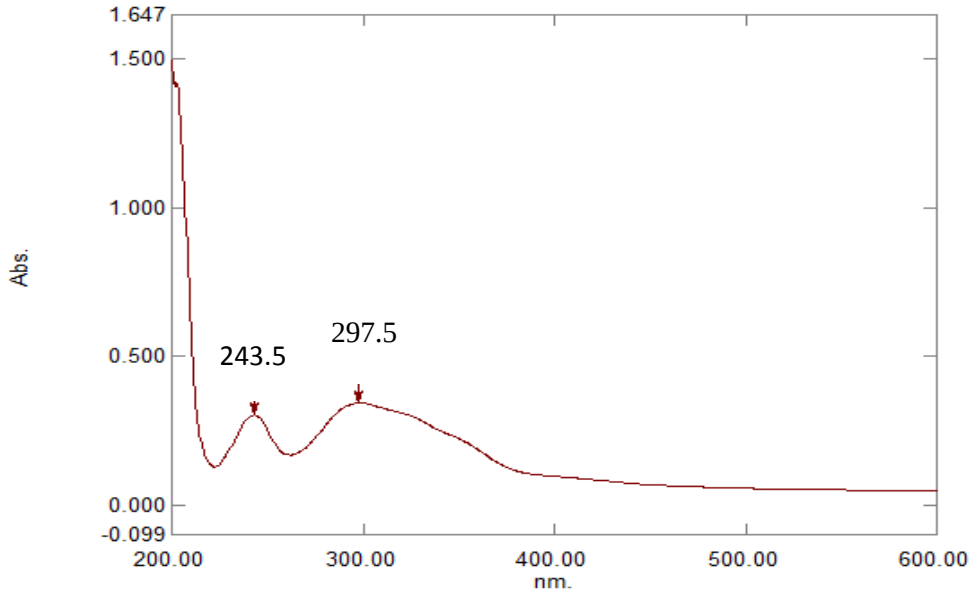

Figure 30: UV-vis of ligand Cu-L_1 in acetonitrile

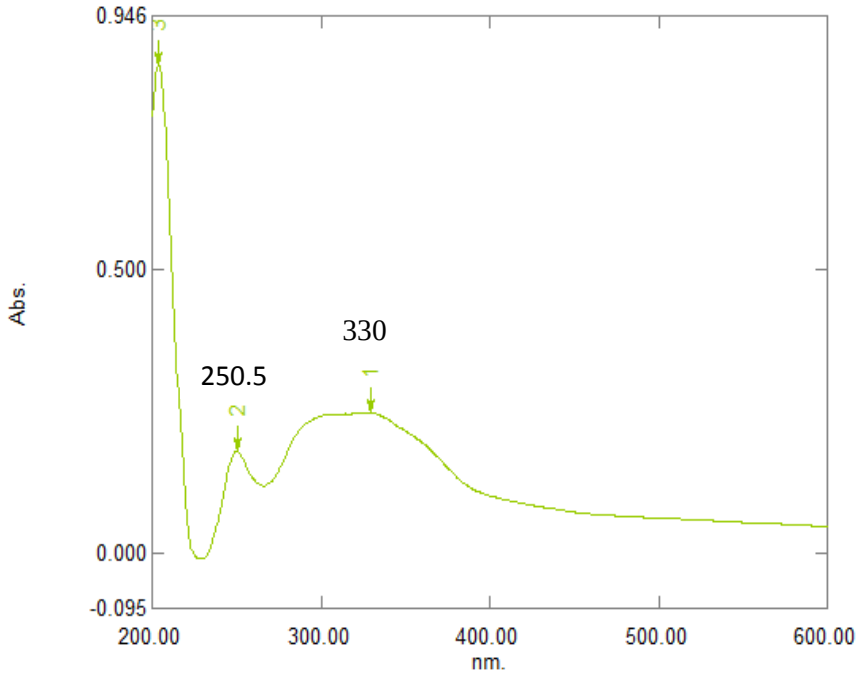

Figure 31:UV-Vis spectrum of Cu-L2 in acetonitrile

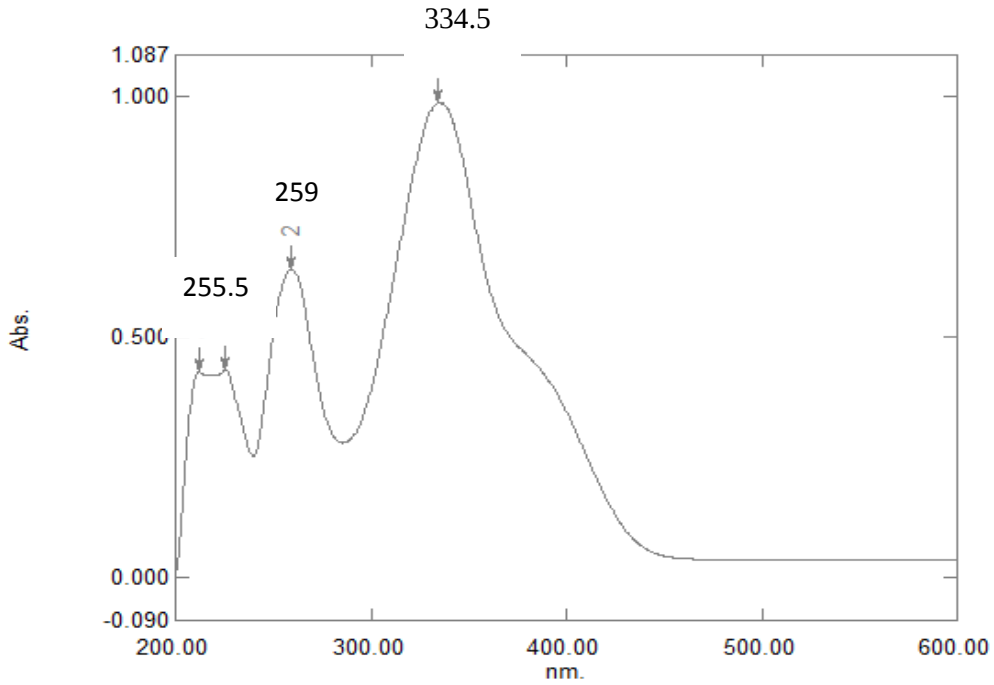

Figure 32:UV-Vis spectrum of Cu-L_3 in acetonitrile

289.5

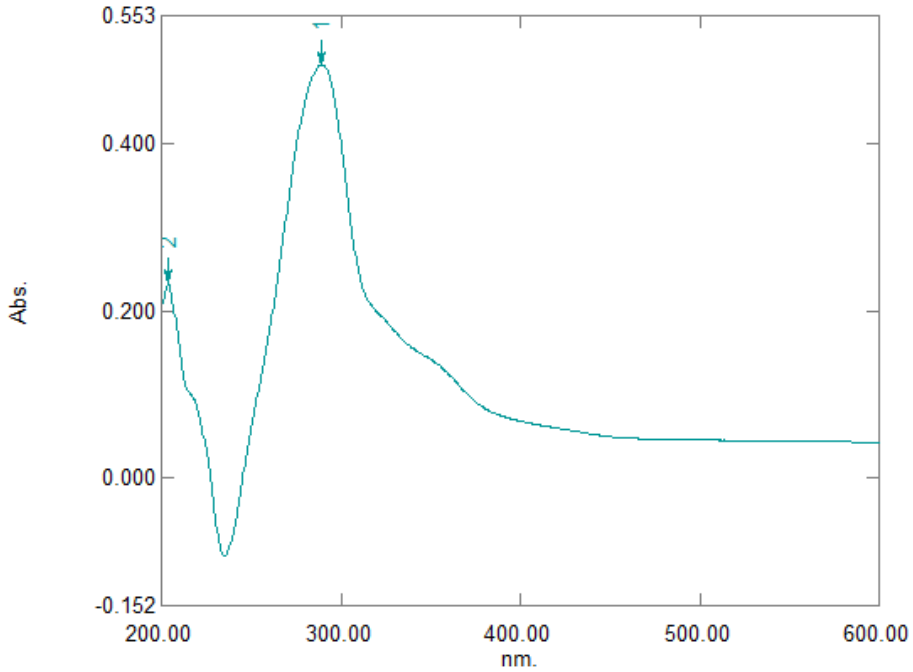

Figure 33:UV-Vis spectrum of Cu-L_4 in acetonitrile

Appendix III: The ^{1}H NMR Spectra of Schiff Base Ligands and Their Cu (II) Complexes

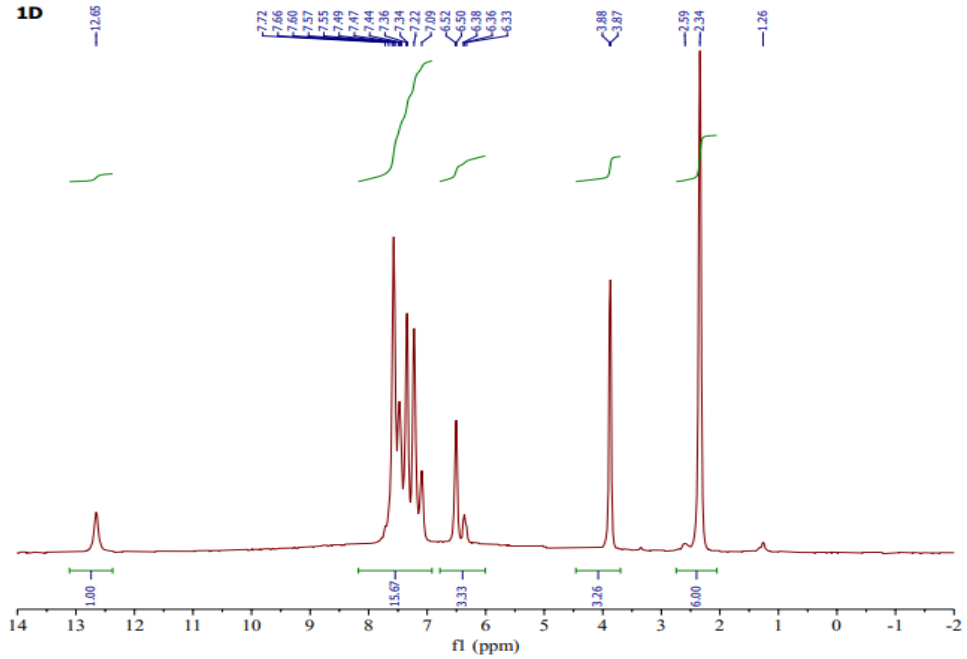

Figure 34: ^{1}H NMR spectrum of Ligand L_2

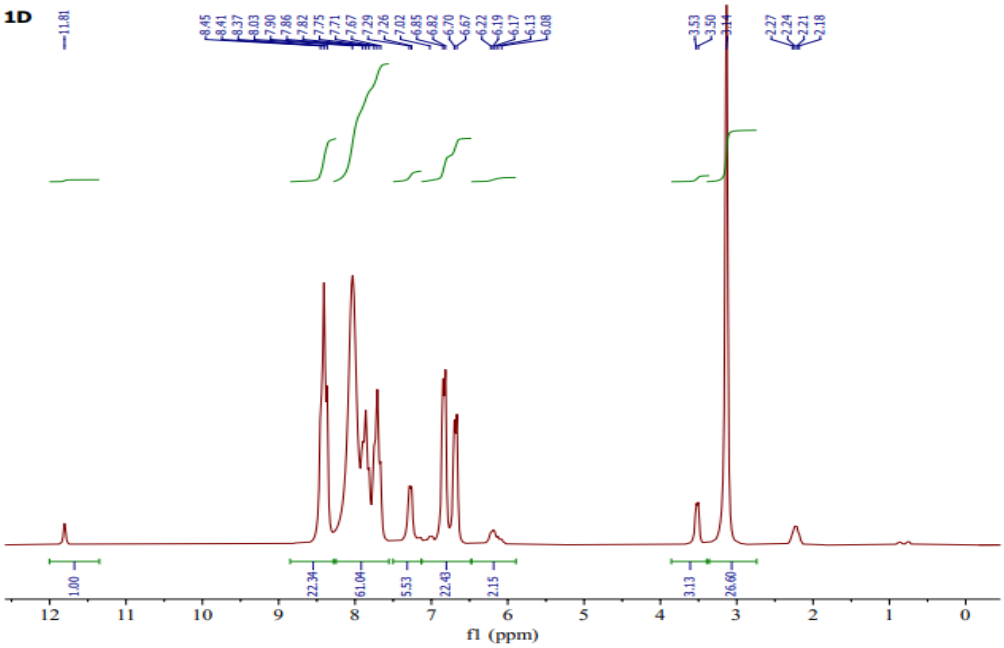

Figure 35: ^{1}H NMR spectrum of Ligand L_3

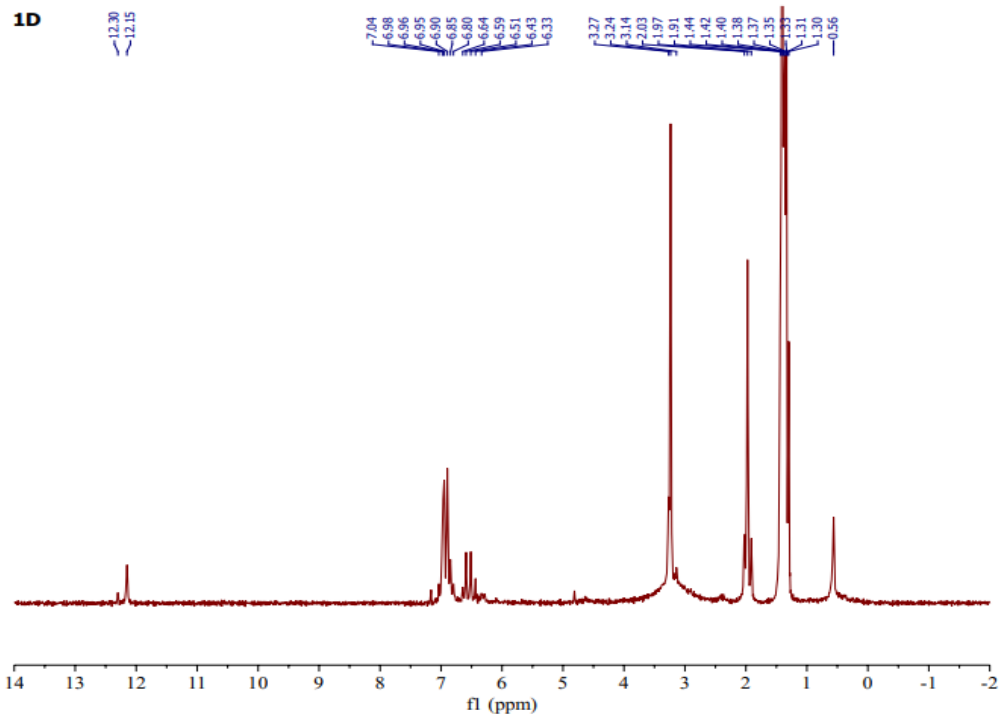

Figure 36: 1H NMR spectrum of Ligand L4

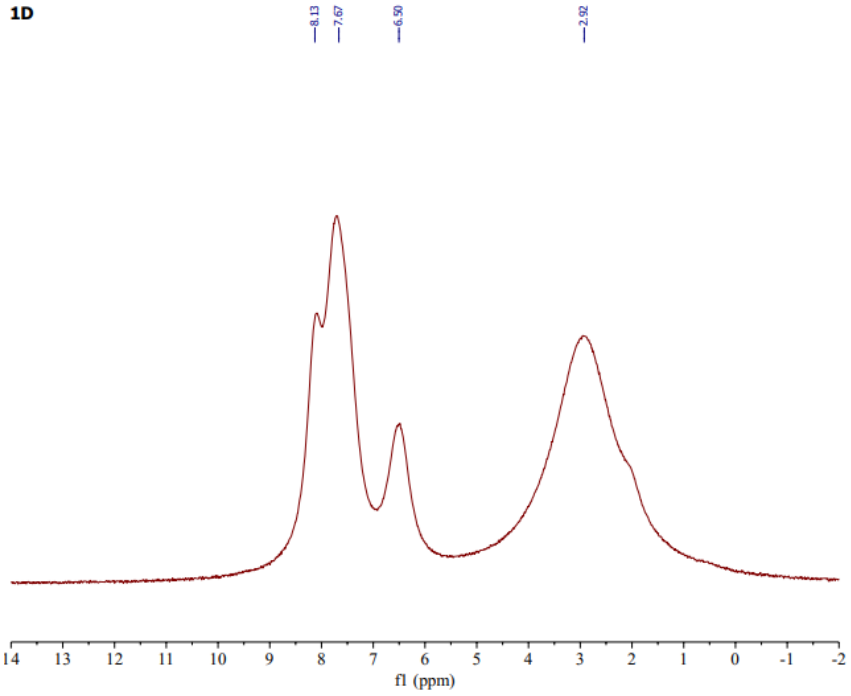

Figure 37: ^{1}H NMR spectrum of Cu-L_1 complex

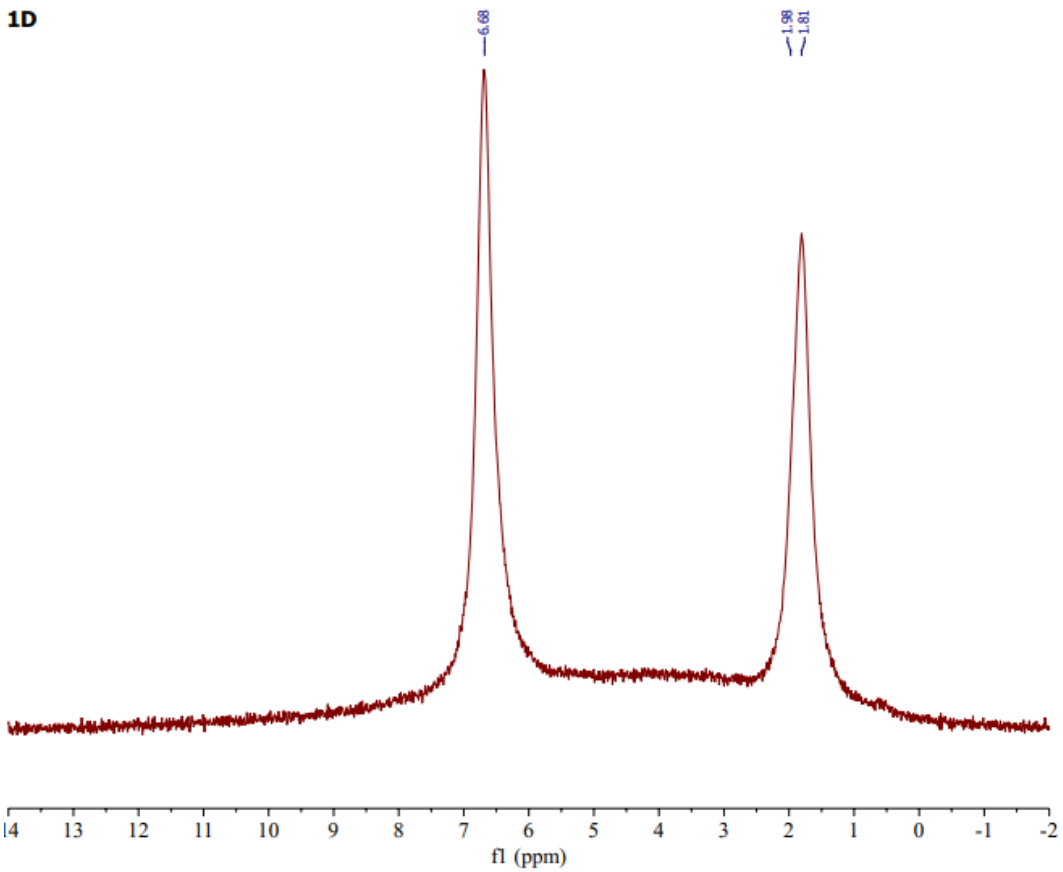

Figure 38: ^{1}H NMR spectrum of Cu-L_2 complex

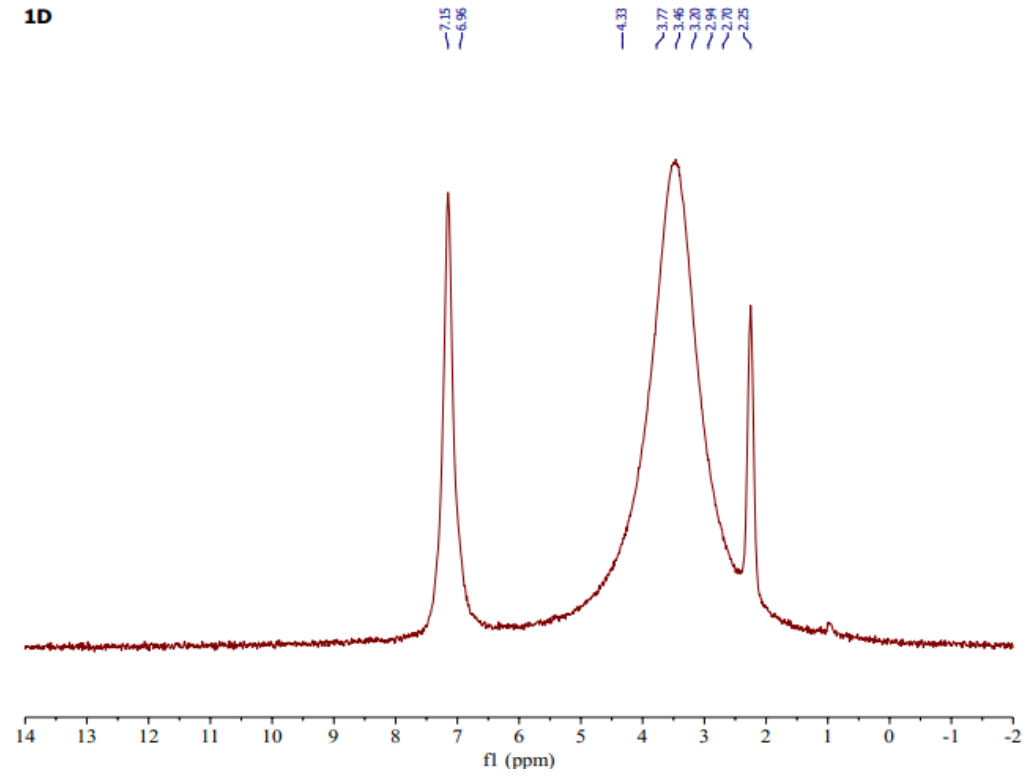

Figure 39: ^{1}H NMR spectrum of Cu-L_3 complex

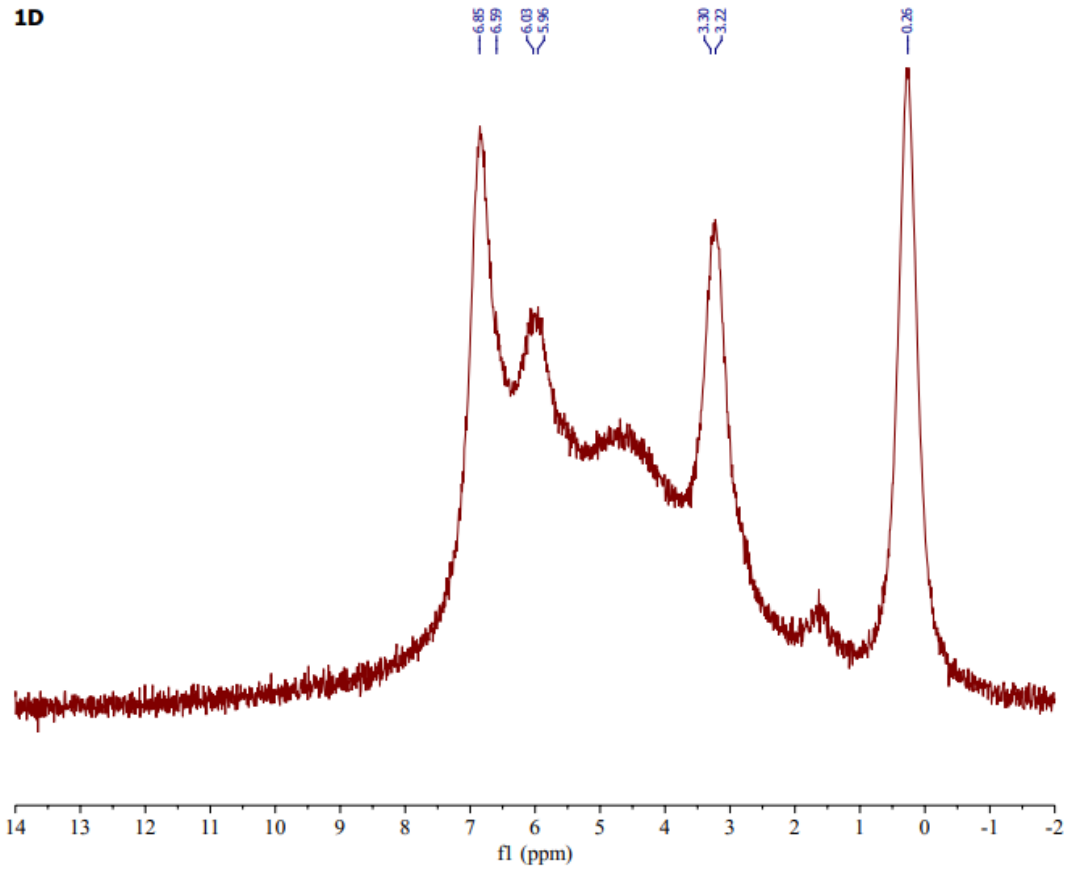

Figure 40: ^{1}H NMR spectrum of Cu-L_4 complex

Appendix IV: ANOVA Tables for *S. Aureus* AT Different Concentration

ANOVA TABLES FOR *S. AUREUS* AT 1000PPM

Source	DF	Sum of Squares	Mean Square	F Value	Pr > F
Model	10	908.1818182	90.8181818	48.93	<.0001
Error	22	40.8333333	1.8560606		
Corrected Total	32	949.0151515			

R-Square	Coeff Var	Root MSE	ZIH Mean
0.956973	11.46896	1.362373	11.87879

Source	DF	Type III SS	Mean Square	F Value	Pr > F
Treatment	10	908.1818182	90.8181818	48.93	<.0001

ANOVA TABLES FOR S. AUREUS AT 500PPM

Source	DF	Sum of Squares	Mean Square	F Value	Pr > F
Model	10	835.7121212	83.5712121	40.26	<.0001
Error	22	45.6666667	2.0757576		
Corrected Total	32	881.3787879			

Source	DF	Type I SS	Mean Square	F Value	Pr > F
Treatment	10	835.7121212	83.5712121	40.26	<.0001

Source	DF	Type III SS	Mean Square	F Value	Pr > F
Treatment	10	835.7121212	83.5712121	40.26	<.0001

ANOVA TABLES FOR S. AUREUS AT 250PPM

Source	DF	Sum of Squares	Mean Square	F Value	Pr > F
Model	10	835.7121212	83.5712121	40.26	<.0001
Error	22	45.6666667	2.0757576		
Corrected Total	32	881.3787879			

Source	DF	Type III SS	Mean Square	F Value	Pr > F
Treatment	10	835.7121212	83.5712121	40.26	<.0001

ANOVA TABLES FOR S. AUREUS AT 125PPM

Appendix V: ANOVA Tables for at *P. Aeruginosa* Different Concentration

ANOVA TABLES *P. aeruginosa* at 1000ppm

Source	DF	Sum of Squares	Mean Square	F Value	Pr > F
Model	10	804.4090909	80.4409091	91.54	<.0001
Error	22	19.3333333	0.8787879		
Corrected Total	32	823.7424242			

R-Square	Coeff Var	Root MSE	ZIH Mean
0.976530	8.045622	0.937437	11.65152

Source	DF	Type III SS	Mean Square	F Value	Pr > F
Treatment	10	804.4090909	80.4409091	91.54	<.0001

ANOVA table *P. aeruginosa* at 500ppm

Source	DF	Sum of Squares	Mean Square	F Value	Pr > F
Model	10	672.9090909	67.2909091	76.57	<.0001
Error	22	19.3333333	0.8787879		
Corrected Total	32	692.2424242			

R-Square	Coeff Var	Root MSE	ZIH Mean
0.972071	9.518590	0.937437	9.848485

Source	DF	Type I SS	Mean Square	F Value	Pr > F

Source	DF	Type III SS	Mean Square	F Value	Pr > F
Treatment	10	672.9090909	67.2909091	76.57	<.0001

At 250

Source	DF	Sum of Squares	Mean Square	F Value	Pr > F
Model	10	551.0454545	55.1045455	42.05	<.0001
Error	22	28.8333333	1.3106061		
Corrected Total	32	579.8787879			

R-Square	Coeff Var	Root MSE	ZIH Mean
0.950277	13.37308	1.144817	8.560606

Source	DF	Type III SS	Mean Square	F Value	Pr > F
Treatment	10	551.0454545	55.1045455	42.05	<.0001

125ppm

R-Square	Coeff Var	Root MSE	ZIH Mean
0.949825	14.58324	1.087115	7.454545

Source	DF	Type III SS	Mean Square	F Value	Pr > F
Treatment	10	492.1818182	49.2181818	41.65	<.0001

Appendix VI: ANOVA Tables for at E. Coli Different Concentration

ANOVA TABLES *E. COLI* at 1000ppm

Source	DF	Sum of Squares	Mean Square	F Value	Pr > F
Model	10	913.0757576	91.3075758	131.01	<.0001
Error	22	15.3333333	0.6969697		
Corrected Total	32	928.4090909			

R-Square	Coeff Var	Root MSE	ZIH Mean
0.983484	7.064091	0.834847	11.81818

Source	DF	Type III SS	Mean Square	F Value	Pr > F
Treatment	10	913.0757576	91.3075758	131.01	<.0001

500ppm

Source	DF	Sum of Squares	Mean Square	F Value	Pr > F
Model	10	742.6363636	74.2636364	52.14	<.0001
Error	22	31.3333333	1.4242424		
Corrected Total	32	773.9696970			

R-Square	Coeff Var	Root MSE	ZIH Mean
0.959516	11.70364	1.193416	10.19697

Source	DF	Type III SS	Mean Square	F Value	Pr > F
Treatment	10	742.6363636	74.2636364	52.14	<.0001

250 ppm

Source	DF	Sum of Squares	Mean Square	F Value	Pr > F
Model	10	586.7424242	58.6742424	43.03	<.0001
Error	22	30.0000000	1.3636364		
Corrected Total	32	616.7424242			

R-Square	Coeff Var	Root MSE	ZIH Mean
0.951357	13.49762	1.167748	8.651515

Source	DF	Type III SS	Mean Square	F Value	Pr > F
Treatment	10	586.7424242	58.6742424	43.03	<.0001

125ppm

Source	DF	Sum of Squares	Mean Square	F Value	Pr > F
Model	10	525.5151515	52.5515152	52.55	<.0001
Error	22	22.0000000	1.0000000		
Corrected Total	32	547.5151515			

R-Square	Coeff Var	Root MSE	ZIH Mean
0.959818	13.12127	1.00000	7.621212

Source	DF	Type III SS	Mean Square	F Value	Pr > F
Treatment	10	525.5151515	52.5515152	52.55	<.0001

Appendix VII: Bioactivity of Compound L_1 Against the three Test Organisms as Compared to Gentamycin and Amoxiclav

Source	DF	Sum of Squares	Mean Square	F Value	Pr > F
Model	8	833.6296296	104.2037037	46.12	<.0001
Error	18	40.6666667	2.2592593		
Corrected Total	26	874.2962963			

R-Square	Coeff Var	Root MSE	ZIH Mean
0.953486	9.616883	1.503083	15.62963

Source	DF	Type III SS	Mean Square	F Value	Pr > F
Treatment	2	824.9629630	412.4814815	182.57	<.0001

Organism	2	3.1851852	1.5925926	0.70	0.5073
Organism*Treatment	4	5.4814815	1.3703704	0.61	0.6630

Appendix VIII: Bioactivity of Compound L_2 against the Three Test Organisms as Compared to Gentamycin and Amoxiclav

Source	**DF**	**Sum of Squares**	**Mean Square**	**F Value**	**Pr > F**
Model	8	499.5000000	62.4375000	30.24	<.0001
Error	18	37.1666667	2.0648148		
Corrected Total	26	536.6666667			

R-Square	**Coeff Var**	**Root MSE**	**ZIH Mean**
0.930745	8.679542	1.436946	16.55556

Source	**DF**	**Type III SS**	**Mean Square**	**F Value**	**Pr > F**
Treatment	2	484.2222222	242.1111111	117.26	<.0001
Organism	2	1.0555556	0.5277778	0.26	0.7772
Organism*Treatment	4	14.2222222	3.5555556	1.72	0.1890

Appendix IX: Bioactivity of Compound L_3 against the Three Test Organisms as Compared to Gentamycin and Amoxiclav

Source	**DF**	**Sum of Squares**	**Mean Square**	**F Value**	**Pr > F**
Model	8	511.4074074	63.9259259	29.25	<.0001
Error	18	39.3333333	2.1851852		
Corrected Total	26	550.7407407			

R-Square	**Coeff Var**	**Root MSE**	**ZIH Mean**
0.928581	8.948970	1.478237	16.51852

Source	**DF**	**Type III SS**	**Mean Square**	**F Value**	**Pr > F**
Treatment	2	496.0740741	248.0370370	113.51	<.0001
Organism	2	6.7407407	3.3703704	1.54	0.2408
Organism*Treatment	4	8.5925926	2.1481481	0.98	0.4415

Appendix X: Bioactivity of Compound L_4 against the Three Test Organisms as compared to Gentamycin and Amoxiclav

Source	**DF**	**Sum of Squares**	**Mean Square**	**F Value**	**Pr > F**
Model	8	512.6666667	64.0833333	30.09	<.0001
Error	18	38.3333333	2.1296296		
Corrected Total	26	551.0000000			

R-Square	**Coeff Var**	**Root MSE**	**ZIH Mean**
0.930430	8.844394	1.459325	16.50000

Source	**DF**	**Type III SS**	**Mean Square**	**F Value**	**Pr > F**
Treatment	2	502.0555556	251.0277778	117.87	<.0001
Organism	2	5.1666667	2.5833333	1.21	0.3205
Organism*Treatment	4	5.4444444	1.3611111	0.64	0.6414

Appendix XI: Bioactivity of Compound Cu-L1 against the Three Test Organisms as Compared to Gentamycin and Amoxiclav

Source	**DF**	**Sum of Squares**	**Mean Square**	**F Value**	**Pr > F**
Model	8	333.4074074	41.6759259	19.74	<.0001
Error	18	38.0000000	2.1111111		
Corrected Total	26	371.4074074			

R-Square	**Coeff Var**	**Root MSE**	**ZIH Mean**

0.897686	8.473022	1.452966	17.14815

Source	DF	Type III SS	Mean Square	F Value	Pr > F
Treatment	2	314.7407407	157.3703704	74.54	<.0001
Organism	2	0.5185185	0.2592593	0.12	0.8852
Organism*Treatment	4	18.1481481	4.5370370	2.15	0.1164

Appendix XII: Bioactivity of Compound Cu-L2 against the Three Test Organisms as Compared to Gentamycin and Amoxiclav

Source	DF	Sum of Squares	Mean Square	F Value	Pr > F
Model	8	246.7407407	30.8425926	13.22	<.0001
Error	18	42.0000000	2.3333333		
Corrected Total	26	288.7407407			

R-Square	Coeff Var	Root MSE	ZIH Mean
0.854541	8.719489	1.527525	17.51852

Source	DF	Type III SS	Mean Square	F Value	Pr > F
Treatment	2	228.0740741	114.0370370	48.87	<.0001
Organism	2	11.1851852	5.5925926	2.40	0.1194
Organism*Treatment	4	7.4814815	1.8703704	0.80	0.5399

Appendix XIII: Bioactivity of Compound Cu-L3 against the Three Test Organisms as Compared to Gentamycin and Amoxiclav

The GLM Procedure

Class Level Information		
Class	Levels	Values
Organism	3	E_Coli P_aeruginosa S_aureus
Treatment	3	Amoxiclav Cu-L3 Gentamicin
Rep	3	1 2 3
Number of Observations Read		27
Number of Observations Used		27

Appendix XIV: Bioactivity of Compound Cu-L4 against the Three Test Organisms as Compared to Gentamycin and Amoxiclav

The GLM Procedure

Dependent Variable: ZIH

Source	DF	Sum of Squares	Mean Square	F Value	Pr > F
Model	8	304.0000000	38.0000000	18.65	<.0001
Error	18	36.6666667	2.0370370		
Corrected Total	26	340.6666667			

R-Square	Coeff Var	Root MSE	ZIH Mean
0.892368	8.287247	1.427248	17.22222

Source	DF	Type III SS	Mean Square	F Value	Pr > F
Treatment	2	296.2222222	148.1111111	72.71	<.0001
Organism	2	3.5555556	1.7777778	0.87	0.4348
Organism*Treatment	4	4.2222222	1.0555556	0.52	0.7234

Appendix XV: Research Authorization

REPUBLIC OF KENYA

NATIONAL COMMISSION FOR SCIENCE,TECHNOLOGY & INNOVATION

Ref No: 593977

Date of Issue: 26/February/2024

RESEARCH LICENSE

This is to Certify that Mr.. FESTUS KIMUTAI KOSGEI of Chuka University, has been licensed to conduct research as per the provision of the Science, Technology and Innovation Act, 2013 (Rev.2014) in Nairobi, Tharaka-Nithi on the topic: SYNTHESIS, CHARACTERIZATION ANF ANTIBACTERIAL PROPERTIES OF COPPER (II) COMPLEXES OF SCHIFF BASE DERIVED FROM BENZOPHENONE DERIVATIVES AND SELECTED ANILINES for the period ending : 26/February/2025.

License No: **NACOSTI/P/24/33409**

593977

Applicant Identification Number

Director General
NATIONAL COMMISSION FOR SCIENCE,TECHNOLOGY & INNOVATION

Verification QR Code

NOTE: This is a computer generated License. To verify the authenticity of this document, Scan the QR Code using QR scanner application.

See overleaf for conditions